MATHEMATICAL MODELING OF A SMALL-SCALE HELICOPTER AND MRAC DESIGN WITH TIME BASED UNCERTAINTY PARAMETRIZATIONS

A THESIS SUBMITTED TO
THE GRADUATE SCHOOL OF NATURAL AND APPLIED SCIENCES
OF
MIDDLE EAST TECHNICAL UNIVERSITY

BY

MUSTAFA GÜRLER

IN PARTIAL FULFILLMENT OF THE REQUIREMENTS
FOR
THE DEGREE OF MASTER OF SCIENCE
IN
AEROSPACE ENGINEERING

NOVEMBER 2018

Approval of the thesis:

MATHEMATICAL MODELING OF A SMALL-SCALE HELICOPTER AND MRAC DESIGN WITH TIME BASED UNCERTAINTY PARAMETRIZATIONS

submitted by **MUSTAFA GÜRLER** in partial fulfillment of the requirements for the degree of **Master of Science in Aerospace Engineering Department, Middle East Technical University** by,

Prof. Dr. Halil Kalıpçılar
Dean, Graduate School of **Natural and Applied Sciences** _____

Prof. Dr. Ozan Tekinalp
Head of Department, **Aerospace Engineering** _____

Assist. Prof. Dr. Ali Türker Kutay
Supervisor, **Aerospace Engineering, METU** _____

Examining Committee Members:

Prof. Dr. Ozan Tekinalp
Aerospace Engineering, METU _____

Assist. Prof. Dr. Ali Türker Kutay
Aerospace Engineering, METU _____

Assoc. Prof. Dr. İlkay Yavrucuk
Aerospace Engineering, METU _____

Assist. Prof. Dr. Volkan Nalbantoğlu
School of Civil Aviation, Atılım University _____

Prof. Dr. Metin Uymaz Salamcı
Mechanical Engineering, Gazi University _____

Date: 23.11.2018

I hereby declare that all information in this document has been obtained and presented in accordance with academic rules and ethical conduct. I also declare that, as required by these rules and conduct, I have fully cited and referenced all material and results that are not original to this work.

Name, Surname: Mustafa Gürler

Signature:

ABSTRACT

MATHEMATICAL MODELING OF A SMALL-SCALE HELICOPTER AND MRAC DESIGN WITH TIME BASED UNCERTAINTY PARAMETRIZATIONS

Gürler, Mustafa
Master of Science, Aerospace Engineering
Supervisor: Assist. Prof. Dr. Ali Türker Kutay

November 2018, 137 pages

In this thesis, nonlinear mathematical modeling of a small scale model helicopter is presented. In addition, problems in uncertainty parametrization component of Model Reference Adaptive Control (MRAC) is investigated and external uncertainty on the system is parametrized using universal approximators such as Fourier Series and Chebyshev Polynomials in time dependent form. Advantages of using times based universal approximators in MRAC design of MIMO systems are presented.

Proposed controller is tested on the model helicopter using derived mathematical model. Considering special capabilities of the model helicopters, hovering is the most problematic case in terms of stability issues and pilot workload. Therefore, simulations and case studies are performed at hover condition. Moreover, procedure of the MRAC design for a multi input multi output (MIMO) system is given and controller performance is evaluated with and without external disturbance. Adaptive law design and uncertainty parametrization method are the key parts of MRAC design. While the use of e-modification and projection operator in adaptive law improves the controller performance and provide adaptive weights boundedness, proper uncertainty parametrization method selection is important for estimating true adaptive weights..

Keywords: Helicopter Dynamics, Helicopter Modeling, Model Reference Adaptive Control, Uncertainty Parametrization, Fourier Series, Chebyshev Polynomials

ÖZ

KÜÇÜK BOYUTLU HELİKOPTERLER İÇİN MATEMATİK MODEL GELİŞTİRME VE ZAMANA BAĞLI BELİRSİZLİK PARAMETRİZE ETME YÖNTEMİ İLE MRAC TASARIMI

Gürler, Mustafa
Yüksek Lisans, Havacılık ve Uzay Mühendisliği
Tez Danışmanı: Dr. Öğr. Üyesi Ali Türker Kutay

Kasım 2018, 137 sayfa

Bu tezde, küçük ölçekli bir model helikopterin doğrusal olmayan matematiksel modellemesi sunulmuştur. Buna ek olarak, Model Referans Adaptif Kontrol'deki (MRAC) belirsizlik parametrizasyon bileşenindeki sorunlar araştırılmıştır ve dış kaynaklı belirsizlikler Fourier Serileri ve Chebyshev Polinomları gibi evrensel kestirimciler kullanılarak zamana bağlı formda parametrize edilmiştir. Zamana bağlı evrensel kestirimcilerin çok girişli ve çok çıkışlı (MIMO) sistemler için MRAC tasarımında sağladığı avantajlar sunulmuştur.

Önerilen kontrolcü, türetilmiş matematiksel modeli kullanarak model helikopter üzerinde test edilmiştir. Model helikopterlerin özel kabiliyetleri düşünüldüğünde, havada asılı kalma koşulu kararlılık ve pilot iş yükü açısından en problemli durumdur. Bu nedenle, simülasyon ve yapılan analiz çalışmaları havada asılı kalma durumunda gerçekleştirilmiştir. Ayrıca, MIMO sistemler için MRAC tasarım prosedürü anlatılmıştır ve kontrolcü performansı dış bozucular mevcutken ve mevcut değilken değerlendirilmiştir. Adaptif kontrol yasası tasarımı ve belirsizlik parametrizasyon yöntemi MRAC tasarımın önemli parçalarıdır. Adaptif kontrol yasasında kullanılan e-modifikasyon ve projeksiyon operatörü kontrolcü performansını geliştirip adaptif

ağırlıkları kısıtlarken, doğru adaptif ağırlıkları tahmin etmek için uygun belirsizlik parametrizasyon yöntemi seçimi önemlidir.

Anahtar Kelimeler: Helikopter Dinamiği, Helikopter Modelleme, Model Referans Adaptif Kontrol, Belirsizlik Paremetrize Etme, Fourier Serileri, Chebyshev Polinomları

To my parents…

ACKNOWLEDGMENTS

I would like to express the deepest gratitude to my thesis supervisor Dr. Ali Türker Kutay for his feedbacks and patience. His support, guidance and energy helped me to complete this work.

I would also like to thank my thesis committee members, Prof. Dr. Ozan Tekinalp, Dr. İlkay Yavrucuk, Prof. Dr. Metin U. Salamcı and Dr. Volkan Nalbantoğlu.

I am grateful to Sinan Özcan, İsmail Hakkı Şahin and Selahattin Burak Sarsılmaz for their contributions to this thesis work. I wish to state my appreciation to all my colleagues for their patience when I have troubles times in studying and writing this thesis.

I would also like to thank Ali Karakaya and Kadircan Kopşa for our brainstorming sessions and enjoyable friendships.

Last but not the least important, I owe more than thanks to my family. To my mother Mürüvet Gürler, especially for her patience in waking me up in the mornings after difficult and tiring nights. To my father Halil İbrahim Gürler, for his guidance and support whenever I need. To my sisters Tuba Arıcı and Ümmühan Gürler, for their love and invaluable friendship.

TABLE OF CONTENTS

LIST OF TABLES

TABLES

LIST OF FIGURES

FIGURES

CHAPTER 1

INTRODUCTION

Helicopters are rotary wing aircrafts with different unique qualities that make them special aerial vehicles. The main advantage of rotary wing aircrafts is to provide lift force without the need of forward flight. This lift force ensure the helicopter the ability of hover and vertical takeoff/landing which fixed wing aircrafts could not perform. Due to these abilities, helicopters are preferred for low speed tasks such as search and rescue, firefighting and transportation applications. Rather than full sized helicopters, unmanned small scale helicopters are widely used for performing these special tasks and their popularity have also been increasing as a new field of interest in literature for the last three decades [1].

Since rotary wing aircraft dynamics is highly nonlinear and coupled, piloting is not an easy task especially under some unstable flight conditions. Two basic flight conditions exist for helicopters; hovering and forward flight. Hovering is the most challenging case for a helicopter and pilot workload is high relative to forward flight condition. A great number of studies have been done by designing different types of controller in order to facilitate pilot tasks in hovering [46, 26, 24].

Since the development and production of the first helicopter, control systems have become compulsory part of the design. Most of the control systems lean on mathematical model of the systems and physical relations. Yet, in real world applications, perfect models representing the real system exactly do not exist and all physical systems may not be modeled easily. Moreover, in aerospace applications, describing system dynamics for all flight regime with one model is not possible and generally expose a nonlinear and coupled mathematical model. Since plant dynamics is nonlinear, control system needs to be nonlinear and robust to uncertainties. Robust control is

one of the most used approach for systems with uncertainties. In this approach, worst case is considered and excessive inputs may occur in control process. In other words, robust controllers are conservative by their nature and they may result in performance degrade. However, adaptive controllers try to cancel out uncertainties online and they generate required control input to overcome undesired effects on the system. Adaptive controllers can be classified into two main groups; direct and indirect. Direct adaptive controllers try to adapt controller variables without trying to estimate unknown parameters of the plant. Unlike direct adaptive controllers, indirect ones try to estimate unknown system parameters to use them in estimating controller variables. While indirect adaptive controllers provide long term learning, short term learning exists and controller response is fast in direct adaptive controllers. In other words, direct adaptive controllers focus on suppressing tracking error rather than estimating uncertainty itself.

Model Reference Adaptive Controllers (MRAC) are the most commonly used direct adaptive controllers in the latest years. Numerous subjects have been studied with MRAC such as aerospace vehicles, automobiles, medical processes and robotics. The goal of MRAC is to generate adaptive control law such that plant states track the predefined reference model. In order to achieve this, MRAC requires three major elements; reference model, uncertainty parametrization and weight update law. These three elements affect the controller tracking performance and it will be focused on uncertainty parametrization methods particularly in this thesis.

1.1 Literature Search

Unmanned helicopters are mostly used in surveillance and transportation applications in past decades. High lift-to-weight ratios, capability of aerobatic maneuvers and ease of piloting make such vehicles special relative to full-sized helicopters. These specifications result in high angular rates and fast dynamics to perform special tasks. The fastest and the most dominant motion for a miniature helicopter is flapping motion and most of the moments are produced by the main rotor around the main rotor hub. This relieves the use of higher fidelity mathematical models including secondary effects and dynamics generally used for full-sized helicopters in literature [12].

There are two common techniques for obtaining a helicopter model used in literature. These are system identification and simple physics and mathematical based modeling methods. For the modeling of the small scale helicopters, system identification in frequency domain was used in previously developed models. Mettler, Tischler and Kanade developed a small scale helicopter model based on frequency domain system identification and they verified the model with a time domain model [25]. In addition, Civita, Messner and Kanade presented a novel modeling technique based on global optimization in frequency domain for Yamaha R-50 type autonomous helicopter [8]. Although these frequency domain based models provide lower order linear models, accuracy is not good when there is a feedback [21] which is mendatory for helicopters as their open loop systems are mostly nonlinear. Although accuracy of high frequency modes is satisfactory, low frequency modes lack of accuracy and need flight test data which cannot be performed every case.

Other technique is physics and mathematical based modeling in literature [6, 50, 51, 16, 28, 39, 5]. Although a high number of mathematical models are developed in literature, Chen and Heffley have played a key role behind the main idea of developing mathematical model for a helicopter. Even though Chen presented flapping dynamics, non-teetering configurations, pitch-flap couplings and hinge restraints to the literature, mathematical models were not accurate in all flight regimes due to model assumptions [6]. Lastly, in 1986, Heffley and Mnich published a paper at NASA Annes Research Center. They developed a mathematical model based simulation model which can be used in all flight regimes with very low calculations, known as minimum complexity model [16].

Classical adaptive theory started with gain scheduling methods and self tuning control techniques. Gain scheduling is the control method where controller gains are calculated for specific flight conditions and changed as flight regime changes. Examples of gain scheduling can be found in literature [27, 49, 3, 42]. Another technique used in classical adaptive control is self tuning control. The main idea of self tuning control is to identify system parameters using parameter identification and to find a analytical relation with controller gains. Examples of such controller are presented in [17, 4, 22, 45].

Modern adaptive control theory can be classified as direct and indirect adaptive controllers. Indirect adaptive controllers use an estimating algorithm to approximate the uncertain system parameters and to use these parameters in estimating controller gains. On the other hand, direct adaptive controllers use instantaneous tracking error to directly estimate controller gains without requiring to estimate system parameters. The most known and widely used direct adaptive control technique is Model Reference Adaptive Control (MRAC). Examples of MRAC can be found in literature [54, 4, 30, 52].

The main idea of MRAC is to make the plant states track the predefined and desired reference model. MRAC can be considered as combination of three fundamental elements. The first one is the reference model. It is the desired response and characteristics that plant should follow. Although reference model can be selected as any proper desired dynamics, it can also be designed by and control methods by using open loop plant dynamics. The second element of MRAC is the weight update law. It is based on Lyapunov Stability and first studies with Lyapunov based MRAC are done in [44] and [37]. There are some modifications applied on the weight update law in literature. e-modification [29], σ-modification [15], dead-zone modification [38], K-modification [18], Kalman-modification [55], Q-modification [53], multi-objective control modification [31] and optimal control modification [33] are the some modifications presented in literature. Projection operator is another modification for ensuring adaptive weights in a compact set [20]. The last fundamental element of MRAC is uncertainty parametrization. The common way to parametrize the uncertainty is to use basis functions in terms of system states for structured uncertainties. Wing-rock motion [47] is widely studied subject in this manner and used in control literature [23, 48]. Another frequently used method to parametrize uncertainty is to use universal appproximators. Neural networks using Radial Basis Functions or Sigmoidal Functions are the most general technique used in literature [19, 7]. Fourier Series Expansion and Chebyshev Polynomials are the other universal approximators used in MRAC literature [13, 34]. Fourier Series is separated from others in terms of using time variable in uncertainty parametrization instead of system state variables.

1.2 Motivation

Motivation of this thesis is to develop a mathematical model for small scaled model helicopters and gain insight and expertise on one of the most popular modern control techniques. The goal of choosing a model helicopter as the plant is that helicopters are highly nonlinear and coupled systems and unmanned rotary wing aircrafts have become popular in industry especially for surveillance applications.

Nonlinearities and couplings in the nature of helicopter dynamics exposes to design a nonlinear and MIMO controller. Popularity in the last decades, allowing the use of a baseline controller with any techniques and simplicity in design put forward MRAC in other modern nonlinear control techniques. Robustness to external disturbances and unmodeled dynamics also encourage to use MRAC controller for model helicopters even if we do not have a high fidelity mathematical model.

1.3 Contributions

Beside developing a mathematical model for a nonlinear helicopter model, another goal of this thesis is to improve tracking performance of MRAC controllers by focusing uncertainty parametrization component. Apart from Fourier Series, in literature, all uncertainty parametrization methods are in terms of system states or outputs. Since defining the uncertainty as state dependent may not be an easy task for nonlinear and coupled high order MIMO systems, a necessity of time based universal approximators usage is appeared. Beside Fourier Series Expansion, Chebyshev Polynomials are defined in terms of time by using trigonometric relations and these time based uncertainty methods are used in MRAC uncertainty parametrization.

1.4 Thesis Outline

In this thesis, there are five chapters: Introduction, Mathematical Model Derivation, Model Reference Adaptive Control, Results and Discussion and Conclusion.

The first chapter is introduction to the thesis which contains overview of the helicopter

dynamics and control. Literature survey in helicopter mathematical modelling and MRAC theory and applications are presented in this chapter. Lastly, thesis motivation and structure are given.

Chapter 2 contains derivation of the nonlinear mathematical model. Sub-components of the helicopter are mathematically modeled separately and combined to create a built up model. Nonlinear helicopter model is analyzed by trying with a sample model helicopter parameters. Considering control purpose, trimming, linearization and model order reductions are also presented in this chapter. Lastly, model verification is done by comparing results in literature and sub-component testing.

In Chapter 3, MIMO adaptive control design and modifications are presented. First, MRAC components are described and all fundamental elements are formulated and designed. Design part starts with the reference model to be tracked. After decided reference model, standard MRAC formulation and MIMO design procedures are presented. In the following parts of this section, MRAC adaptive law modifications and uncertainty parametrization methods are given.

Chapter 4 presents implementation of the controllers, designed controllers results on the helicopter model, modifications on the controller design and discussions. First, linear and nonlinear helicopter model responses with baseline controller are given and reason for needing an adaptive controller is presented. After, modifications in MRAC are applied to the controller and their results and effects are discussed considering tracking performance of reference model. Lastly, robustness of the proposed controller is evaluated.

The last chapter is conclusion of the thesis. This chapter contains a thesis summary and future work considerations.

CHAPTER 2

MATHEMATICAL MODEL DERIVATION

In this chapter, mathematical model derivation procedure for a helicopter is described. The main aim of the deriving mathematical model is that it is required for designing control laws. Stepwise refinement is the main method to be considered in modeling. In other words, it is started with describing general functions and then they are broken down into more details until whole system is fully covered. In this manner, firstly, reference frames used in derivation is determined. Then, starting with rigid body and main rotor dynamics, all forces and moments acting on the helicopter is defined. Blade Element Theory [40] is the main method used in main rotor dynamics. Constant inflow is assumed and calculated according to Momentum Theory [16]. Other components are modeled based on basic aerodynamics facts.

After deriving all components, nonlinear simulation model is developed using mathematical model. After trimming and linearizing around hover condition, linear and nonlinear models are ready for control design and simulation purposes.

2.1 Mathematical Model Overview and Structure

Mathematical model consists of some main blocks which are responsible for different tasks from each other. These subblocks can be seen in Figure 2.1. This mathematical model describes the motion from pilot inputs (u_{lon}, u_{lat}, u_{coll}, u_{ped}) to helicopter attitudes and motions. It has four primary and one auxiliary blocks and detailed explanations of them are given below:

- **Rotary Wing Dynamics**: This block consists of main rotor and stabilizer bar dynamics. It is responsible for deriving flapping dynamics which is the most dominant motion for helicopter behaviour. Outputs of Rotary Wing Dynamics block are used in determining forces and moments generated by the main rotor. This block uses swash plate inputs and helicopter model states to compute flapping angles (β_0, β_{1s}, β_{1c}) and main rotor inflow (V_i).

- **Forces and Moments Generation**: This block consists of five different sources which create forces and moments. The first one is Main Rotor Forces and Moments which calculates main rotor forces and moments at main rotor hub. The second one is Tail Rotor Forces and Moments. Other force and moments sources are Horizontal Stabilizer, Vertical Fin and Fuselage Drag. This block uses flapping angles, swash plate inputs, pedal input (u_{ped}), main rotor inflow (v_i) and helicopter model states to calculate all forces and moments generated on the helicopter.

- **Forces and Moments Summation**: This block basically transform all generated forces and moments of subparts of the helicopter to CG position. Then, it sums all forces and moments in order to use them in Newtonian Mechanics. This block uses main rotor, tail rotor, horizontal stabilizer, vertical fin and fuselage forces and moments and calculates total force and total moment in BF.

- **Rigid Body Dynamics**: This block consists of differential equations of six degree of freedom dynamics. It uses total force and total moments at CG position and calculates helicopter attitudes, translational velocities and rotational velocities in BF.

- **Atmosphere Model**: This block basically uses American National Standard Guide to Reference and Standard Atmosphere Models [2] to calculate density of the air as the altitude changes in flight.

- **Velocity and Position Transformation to *EF***: This block transforms body velocities and positions to EF which can be used for earth velocity trim and navigation purposes for future works.

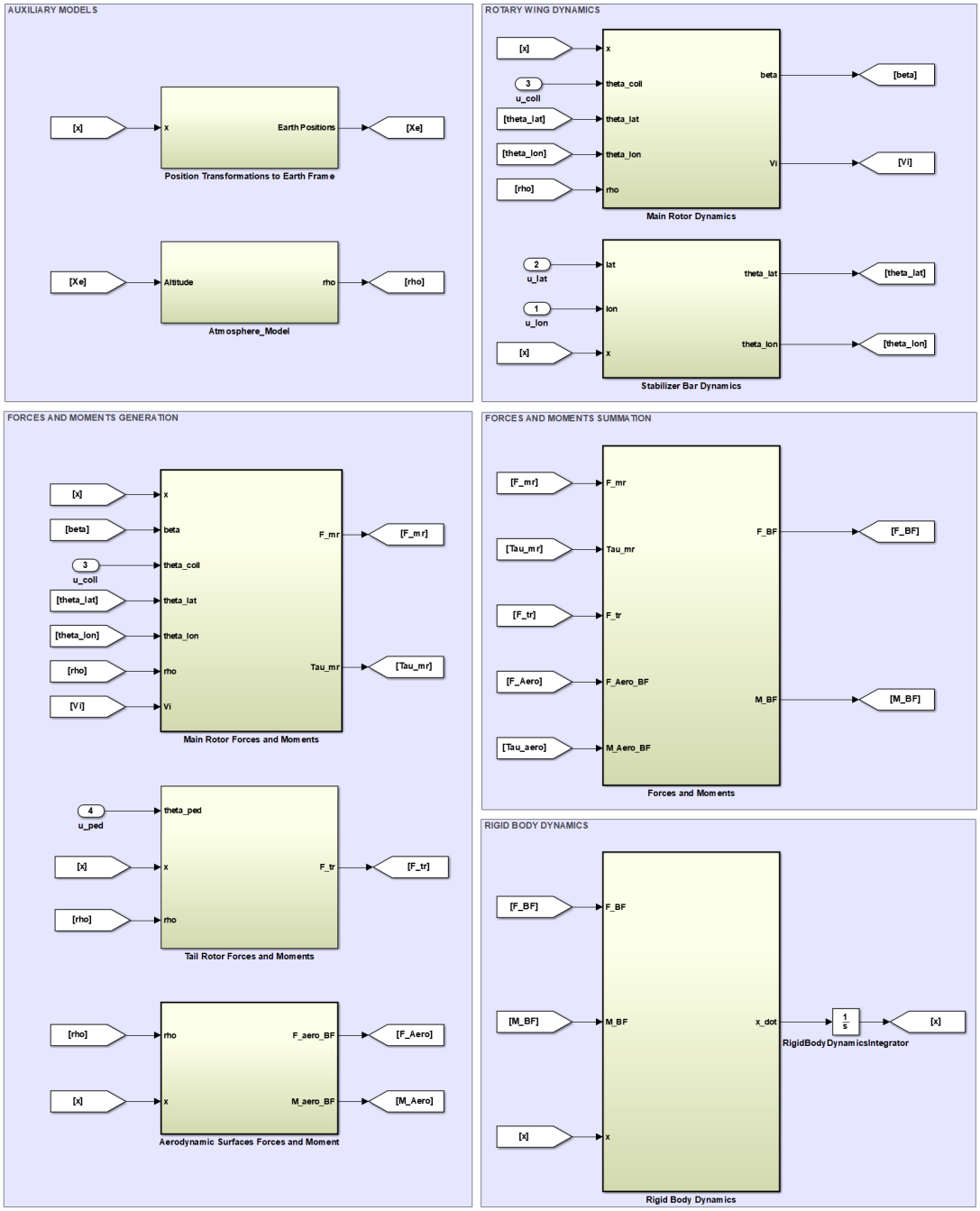

Figure 2.1: MATLAB-Simulink Blocks of the Mathematical Model

2.1.1 Model Assumptions

There are some assumptions which are considered during modeling of the helicopter dynamics. These assumptions are mostly because of complexity and nonlinearity of the helicopter dynamics. In order to work in a simulation environment and solve

nonlinear differential equations, the following assumptions are made in modeling:

- Wind velocity are assumed as zero.
- Constant inflow speed on the blade is considered.
- Blades are not twisted.
- Earth is assumed flat and stationary.
- Helicopter mass is constant during simulations.
- Moment of inertias are constant.
- Non-diagonal terms in inertia matrix are zero due to plane of symmetry assumption around x_B-z_B axis.
- The helicopter is considered as a rigid body.
- There is an enough engine power to keep main rotor rotating at a constant angular velocity.
- CG location is constant during simulations.
- Main rotor blades are rotating in clockwise direction.
- Only flapping dynamics are considered in main rotor dynamics. Lead-lag and feathering dynamics are ignored.
- Ground effect is not considered for low level flights.

2.1.2 Reference Frames

There will be two main and five auxiliary reference frames and notations to describe the helicopter flight dynamics. The main reference frames are Body Fixed Reference Frame and Earth Fixed Reference Frame. In order to facilitate helicopter dynamic modeling, five auxiliary reference frames, Hub Fixed, Tail Rotor Fixed, Flapping Hinge Fixed, Blade Fixed and Spatial, are defined. The orientation and center points of each frame are shown in Figure 2.2.

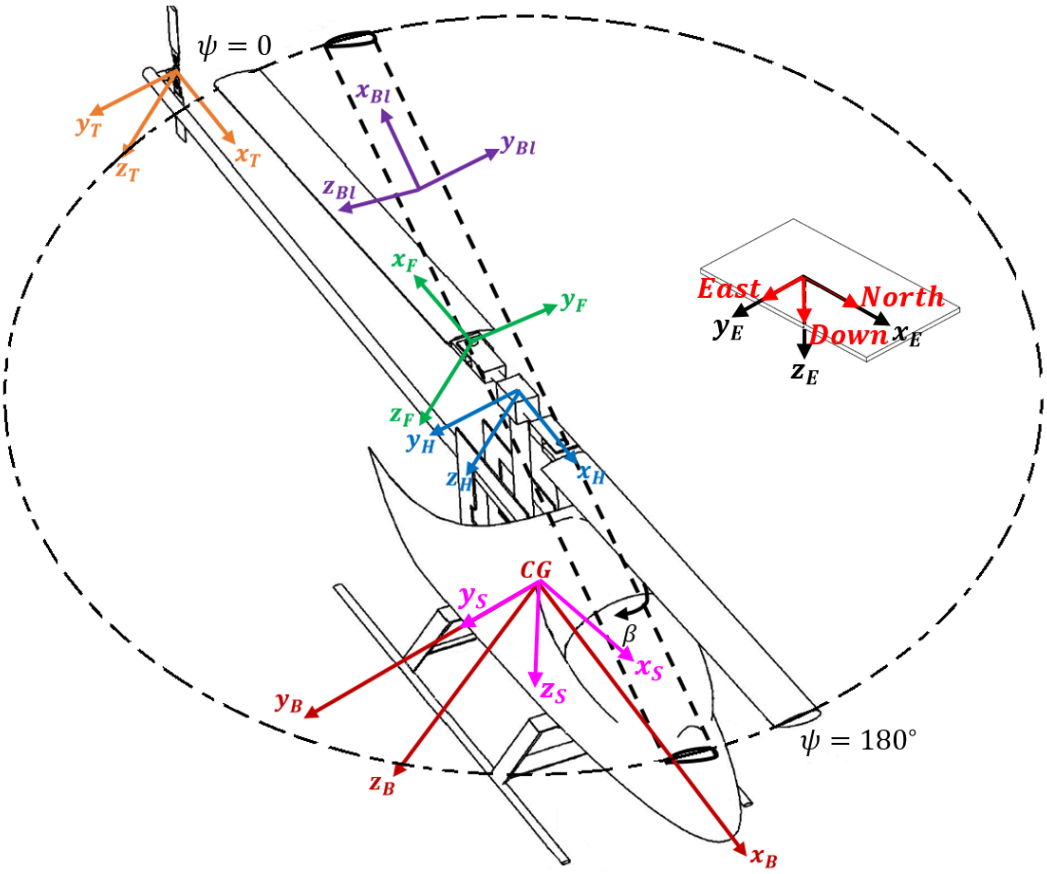

Figure 2.2: Orientation of Reference Frames [39]

2.1.2.1 Body Fixed Reference Frame

Considering equations of motion, it is necessary that a frame where inertia of the helicopter is constant. This frame is called by Body Fixed Reference Frame, abbreviated by BF and its orientation is defined as a right handed coordinate system. Origin of BF is fixed at the center of mass of the helicopter and it moves and rotates with the helicopter. The basis vector of BF is expressed by (x_B, y_B, z_B). The x_B axis points out the nose of the helicopter from CG position. The y_B axis points through the right side seen from the back of the helicopter. The z_B axis is perpendicular to both x_B and y_B and it points through downward from the bottom of the helicopter.

2.1.2.2 Earth Fixed Reference Frame

In order to use Newtonian mechanics and develop equations of motions, a non-rotating and non-accelerating frame is needed. This frame is called as Inertial Coordinate Frame. With the assumptions of that Earth is flat and stationary and the speed of the helicopter is not high, Earth Fixed Coordinate Frame, abbreviated by EF, is taken as Inertial Coordinate Frame [43]. Origin of EF is located arbitrarily on the Earth surface with fixed orientation. The basis vector of EF is expressed by (x_E,y_E,z_E). The x_E axis points out North direction. The y_E axis points out East direction. The z_E axis is perpendicular to both x_E and y_E and it points through downward to the center of the Earth.

2.1.2.3 Hub Fixed Reference Frame

In order to express main rotor forces and moments, Hub Fixed Reference Frame, abbreviated by HF, is defined as an auxiliary reference frame. Origin of HF is located at the top of the main rotor hub. The basis vector of HF is expressed by (x_H,y_H,z_H). The orientation of HF is same with BF.

2.1.2.4 Tail Rotor Fixed Reference Frame

In order to express tail rotor forces and moments, Tail Rotor Fixed Reference Frame, abbreviated by TF, is defined as the second auxiliary reference frame. Origin of TF is located at the top of the tail rotor hub and its orientation is same with BF. The basis vector of TF is expressed by (x_T,y_T,z_T).

2.1.2.5 Spatial Reference Frame

The third auxiliary reference frame is Spatial Reference Frame, abbreviated by SF, used in transformation of forces and moments from BF to a non-rotating reference frame. Origin of SF is same with BF, which is center of the mass of the helicopter, and same orientation with EF. The basis vector of SF is expressed by (x_S, y_S, z_S).

2.1.2.6 Flapping Hinge Fixed Reference Frame

The forth auxiliary reference frame is Flapping Fixed Reference Frame, abbreviated by FF, origin of the FF is fixed at the flapping hinge and it rotates with the main rotor rotation. The basis vector of FF is expressed by (x_F, y_F, z_F).

2.1.2.7 Blade Fixed Reference Frame

The last auxiliary reference frame is Blade Fixed Reference Frame, abbreviated by BFF, origin of the BFF is fixed at the main rotor blade and it rotates with main rotor flapping. The basis vector of BFF is expressed by (x_{Bl}, y_{Bl}, z_{Bl}).

2.2 Rigid Body Dynamics

According to Newtonian mechanics, time derivatives of linear and angular momentum are equal to the external forces and moments of the body, respectively [36].

$$\begin{aligned} \sum \vec{F}_B &= \frac{d}{dt}(\vec{L}_B) = \frac{d}{dt}(m_h \vec{V}_B) \\ \sum \vec{\tau}_B &= \frac{d}{dt}(\vec{H}_B) = \frac{d}{dt}(I\vec{\omega}_B) \end{aligned} \tag{2.1}$$

2.2.1 Euler Angles and Rotation Matrix

In order to define vectors between BF and SF, a transformation matrix should be defined in terms of attitude of the helicopter. Euler angles $\Theta = \begin{bmatrix} \phi \\ \theta \\ \psi \end{bmatrix}^T$ are used to represent helicopter attitude. Therefore, SF should be rotated around its z axis by ψ, y axis by θ, and x axis by ϕ respectively to reach the identical coordinate system with BF.

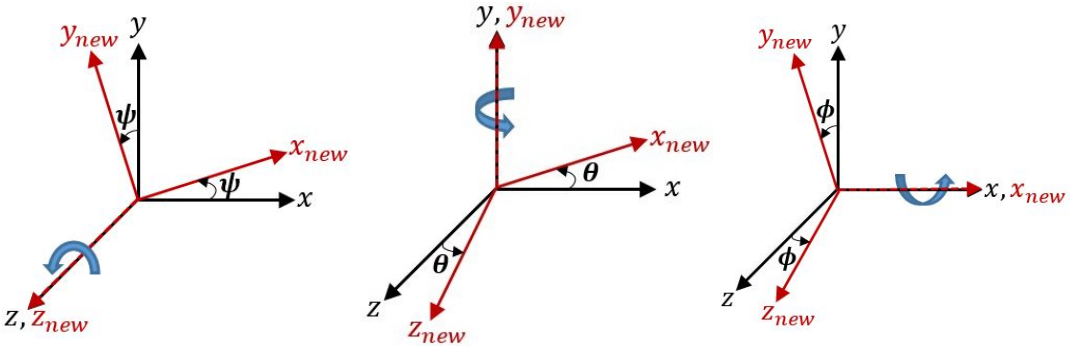

(a) z-rotation (b) y-rotation (c) x-rotation

Figure 2.3: Rotations around three axis

Figure 2.3 shows that rotations around z-y-x axis, respectively. As a mathematical fact, any new reference frame can be obtained by rotating any coordinate frame one-by-one around each axis.

First rotating SF around its z axis by ψ,

$$\begin{aligned} x_1 &= x_S \cos\psi + y_S \sin\psi \\ y_1 &= -x_S \sin\psi + y_S \cos\psi \\ z_1 &= z_S \end{aligned} \tag{2.2}$$

In matrix form,

$$\begin{bmatrix} x_1 \\ y_1 \\ z_1 \end{bmatrix} = \begin{bmatrix} \cos\psi & \sin\psi & 0 \\ -\sin\psi & \cos\psi & 0 \\ 0 & 0 & 1 \end{bmatrix} \begin{bmatrix} x_S \\ y_S \\ z_S \end{bmatrix} = R_z(\psi) \begin{bmatrix} x_S \\ y_S \\ z_S \end{bmatrix} \tag{2.3}$$

Then, rotating the new coordinates system around y axis by θ,

$$\begin{aligned} x_2 &= x_1 \cos\theta - z_1 \sin\theta \\ y_2 &= y_1 \\ z_2 &= x_1 \cos\theta + z_1 \cos\theta \end{aligned} \tag{2.4}$$

In matrix form,

$$\begin{bmatrix} x_2 \\ y_2 \\ z_2 \end{bmatrix} = \begin{bmatrix} \cos\theta & 0 & -\sin\theta \\ 0 & 1 & 0 \\ \sin\theta & 0 & \cos\theta \end{bmatrix} \begin{bmatrix} x_1 \\ y_1 \\ z_1 \end{bmatrix} = R_y(\theta) \begin{bmatrix} x_1 \\ y_1 \\ z_1 \end{bmatrix} \tag{2.5}$$

Finally, rotating the last coordinate system around x axis by ϕ,

$$\begin{aligned} x_3 &= x_2 \\ y_3 &= y_2\cos\theta + z_2\sin\theta \\ z_3 &= -y_2\sin\theta + z_2\cos\theta \end{aligned} \tag{2.6}$$

In matrix form,

$$\begin{bmatrix} x_3 \\ y_3 \\ z_3 \end{bmatrix} = \begin{bmatrix} 1 & 0 & 0 \\ 0 & \cos\phi & \sin\phi \\ 0 & -\sin\phi & \cos\phi \end{bmatrix} \begin{bmatrix} x_2 \\ y_2 \\ z_2 \end{bmatrix} = R_x(\varphi) \begin{bmatrix} x_2 \\ y_2 \\ z_2 \end{bmatrix} \tag{2.7}$$

After the last rotation,

$$\begin{bmatrix} x_B \\ y_B \\ z_B \end{bmatrix} = \begin{bmatrix} x_3 \\ y_3 \\ z_3 \end{bmatrix} = R_x(\phi)R_y(\theta)R_z(\psi) \begin{bmatrix} x_S \\ y_S \\ z_S \end{bmatrix} = R_{SB}(\Theta) \begin{bmatrix} x_S \\ y_S \\ z_S \end{bmatrix} \tag{2.8}$$

where

$$R_{SB}(\theta) = \begin{bmatrix} \cos\theta\cos\psi & \cos\theta\sin\psi & -\sin\theta \\ \sin\phi\sin\theta\cos\psi - \cos\phi\sin\psi & \sin\phi\sin\theta\sin\psi + \cos\phi\cos\psi & \sin\phi\cos\theta \\ \cos\phi\sin\theta\cos\phi + \sin\phi\sin\psi & \cos\phi\sin\theta\sin\psi - \sin\phi\cos\psi & \cos\phi\cos\theta \end{bmatrix} \tag{2.9}$$

Since the transformation matrix is orthogonal, the inverse of it is equals to its transpose, that is:

$$R_{BS}(\theta) = \begin{bmatrix} \cos\theta\cos\psi & \sin\phi\sin\theta\cos\psi - \cos\phi\sin\psi & \cos\phi\sin\theta\cos\psi + \sin\phi\sin\psi \\ \cos\theta\sin\psi & \sin\phi\sin\theta\sin\psi & \cos\phi\sin\theta\sin\psi - \sin\phi\cos\psi \\ -\sin\theta & \sin\phi\cos\theta & \cos\phi\cos\theta \end{bmatrix} \tag{2.10}$$

2.2.2 Transformation of Reference Frames

In this part, transformation of the reference frames described in Section 2.1.2 between each other is presented. These transformation matrices will be helpful in mathematical model derivation.

2.2.2.1 Transformation of Earth Frame to Body Frame

In Equation 2.9, the relation between SF and BF is shown. Since the orientation of SF and EF are same as stated in Section 2.1.2.5, transformation matrix in Equation 2.9 can be used for transformation of EF to BF,

$$R_{EB}(\Theta) = \begin{bmatrix} \cos\theta\cos\psi & \cos\theta\sin\psi & -\sin\theta \\ \sin\phi\sin\theta\cos\psi - \cos\phi\sin\psi & \sin\phi\sin\theta\sin\psi + \cos\phi\cos\psi & \sin\phi\cos\theta \\ \cos\phi\sin\theta\cos\phi + \sin\phi\sin\psi & \cos\phi\sin\theta\sin\psi - \sin\phi\cos\psi & \cos\phi\cos\theta \end{bmatrix} \tag{2.11}$$

2.2.2.2 Transformation from Body Frame to Hub Frame

As described in Section 2.1.2.3, hub axis is fixed and has exactly the same orientation with BF. In matrix form,

$$\begin{bmatrix} x_H \\ y_H \\ z_H \end{bmatrix} = R_{BH}(\Theta) \begin{bmatrix} x_B \\ y_B \\ z_B \end{bmatrix} = \begin{bmatrix} 1 & 0 & 0 \\ 0 & 1 & 0 \\ 0 & 0 & 1 \end{bmatrix} \begin{bmatrix} x_B \\ y_B \\ z_B \end{bmatrix} \tag{2.12}$$

2.2.2.3 Transformation from Hub Frame to Flapping Hinge Frame

FF is obtained by rotating HF about its z axis amount of ψ degrees.

$$\begin{aligned} \begin{bmatrix} x_F \\ y_F \\ z_F \end{bmatrix} &= R_z(\psi) \begin{bmatrix} x_H \\ y_H \\ z_H \end{bmatrix} \\ &= \begin{bmatrix} cos\psi & sin\psi & 0 \\ -sin\psi & cos\psi & 0 \\ 0 & 0 & 1 \end{bmatrix} \begin{bmatrix} x_H \\ y_H \\ z_H \end{bmatrix} \\ &= R_{HF}(\Theta) \begin{bmatrix} x_H \\ y_H \\ z_H \end{bmatrix} \end{aligned} \tag{2.13}$$

2.2.2.4 Transformation from Flapping Hinge Frame to Blade Fixed Frame

BFF is obtained by rotating FF about its y axis amount of β degrees.

$$\begin{aligned}\begin{bmatrix} x_{Bl} \\ y_{Bl} \\ z_{Bl} \end{bmatrix} &= R_y(\beta) \begin{bmatrix} x_F \\ y_F \\ z_F \end{bmatrix} \\ &= \begin{bmatrix} \cos\beta & 0 & -\sin\beta \\ 0 & 1 & 0 \\ \sin\beta & 0 & \cos\beta \end{bmatrix} \begin{bmatrix} x_F \\ y_F \\ z_F \end{bmatrix} \\ &= R_{FBl}(\beta) \begin{bmatrix} x_F \\ y_F \\ z_F \end{bmatrix}\end{aligned} \tag{2.14}$$

2.2.3 Euler Rates

There is another transformation matrix which will be required in defining the relation of angular velocities with Euler angle rates. It is important to notice that while Euler angle rates $\left(\dot{\Theta} = \begin{bmatrix} \dot{\phi} \\ \dot{\theta} \\ \dot{\psi} \end{bmatrix}^T\right)$ are the rates of change of the Euler angles with respect to SF, angular velocity $\left(\vec{\omega}_B = \begin{bmatrix} p \\ q \\ r \end{bmatrix}^T\right)$ is the helicopter body angular velocity vector. The equation expressing the relation between $\dot{\theta}$ and ω is written by kinematics [43],

$$\vec{\omega}_B = \begin{bmatrix} p \\ q \\ r \end{bmatrix} = \begin{bmatrix} \dot{\phi} \\ 0 \\ 0 \end{bmatrix} + R_x(\phi) \begin{bmatrix} 0 \\ \dot{\theta} \\ 0 \end{bmatrix} + R_x(\phi)R_y(\theta) \begin{bmatrix} 0 \\ 0 \\ \dot{\psi} \end{bmatrix} = C_{BS}(\Theta)\dot{\Theta} \tag{2.15}$$

where,

$$C_{BS}(\Theta) = \begin{bmatrix} 1 & 0 & -\sin\theta \\ 0 & \cos\phi & \sin\phi.\cos\theta \\ 0 & -\sin\phi & \cos\phi.\cos\theta \end{bmatrix} \tag{2.16}$$

By inverting the transformation matrix, Euler rates are defined in terms of body angular velocities:

$$\dot{\Theta} = C_{BS}^{-1}(\Theta)\vec{\omega}_B$$
$$\begin{bmatrix} \dot{\phi} \\ \dot{\theta} \\ \dot{\psi} \end{bmatrix} = C_{SB}(\Theta) \begin{bmatrix} p \\ q \\ r \end{bmatrix} \tag{2.17}$$

where,

$$C_{SB}(\Theta) = C_{BS}^{-1}(\Theta) = \frac{1}{\cos\theta} \begin{bmatrix} \cos\theta & \sin\phi.\sin\theta & \cos\phi.\sin\theta \\ 0 & \cos\phi.\cos\theta & -\sin\phi.\cos\theta \\ 0 & \sin\phi & \cos\phi \end{bmatrix} \tag{2.18}$$

Finally, rotation matrix $R_{EB}(\Theta)$ in Equation 2.11 will be used for mapping Earth position vector and rotation matrix $C_{SB}(\Theta)$ in Equation 2.18 will be used for mapping angular velocities from BF to SF.

2.2.4 Translational Accelerations

Using Equation 2.1 and assuming helicopter mass is constant with time [36],

$$\sum \vec{F}_B = \frac{d}{dt}(m_h \vec{V}_B^I) = m_h \frac{d}{dt}\vec{V}_B^I \tag{2.19}$$

where $\sum \vec{F}_B = [\vec{F}_x \quad \vec{F}_y \quad \vec{F}_z]^T$ are total external forces of three axis generated by the helicopter components. m_h is the mass of the helicopter. $\vec{V}_B = [\vec{u}_B \quad \vec{v}_B \quad \vec{w}_B]^T$ are translational body velocities of the three axis with respect to inertial frame. This velocity is written as,

$$\vec{V}_B^I = \vec{V}_B + \vec{\omega}_B^I \times \vec{r}_B^I \tag{2.20}$$

where $\vec{\omega}_B^I = [p \quad q \quad r]^T$ are angular velocities of three axis and $\vec{r}_B^I$ is the helicopter body position vector. Taking derivative of Equation 2.20,

$$\frac{d}{dt}\vec{V}_B^I = \dot{\vec{V}}_B + \vec{\omega}_B^I \times \vec{V}_B^I \tag{2.21}$$

Then,

$$\begin{aligned} \sum \vec{F}_B = \frac{d}{dt}(m_h \vec{V}_B^I) &= m_h \left(\dot{\vec{V}}_B + \vec{\omega}_B^I \times \vec{V}_B^I \right) \\ \Rightarrow \dot{\vec{V}}_B &= \frac{\sum \vec{F}_B}{m_h} - \omega_B^I \times V_B^I \end{aligned} \tag{2.22}$$

After writing cross product in matrix notation,

$$\dot{\vec{V}}_B = \begin{bmatrix} \dot{\vec{u}}_B \\ \dot{\vec{v}}_B \\ \dot{\vec{w}}_B \end{bmatrix} = \frac{\sum \vec{F}_B}{m_h} - \begin{bmatrix} 0 & -r & q \\ r & 0 & -p \\ -q & p & 0 \end{bmatrix} \begin{bmatrix} \vec{u}_B \\ \vec{v}_B \\ \vec{w}_B \end{bmatrix} \tag{2.23}$$

Finally, translational accelerations are derived as,

$$\begin{aligned} \dot{\vec{u}}_B &= \frac{\sum \vec{F}_x}{m_h} + \vec{v}_B r - \vec{w}_B q \\ \dot{\vec{v}}_B &= \frac{\sum \vec{F}_y}{m_h} - \vec{u}_B r + \vec{w}_B p \\ \dot{\vec{w}}_B &= \frac{\sum \vec{F}_z}{m_h} + \vec{u}_B q - \vec{v}_B p \end{aligned} \tag{2.24}$$

2.2.5 Rotational Accelerations

Using Equation 2.1 [36],

$$\sum \vec{M}_B = \frac{d}{dt}\vec{H}_B^I = \frac{d}{dt}\vec{H}_B^B + \omega_B^I \times \vec{H}_B^I \tag{2.25}$$

Where $\sum \vec{M}_B = [\vec{M}_x \quad \vec{M}_y \quad \vec{M}_z]^T$ are total external moments of three axis generated by the helicopter components and $\vec{H}_B$ is the angular momentum vector about center of gravity position of the helicopter and it is defined as,

$$\vec{H}_B = I\vec{\omega}_B \tag{2.26}$$

Where I is the inertia matrix of the helicopter,

$$I = \begin{bmatrix} I_{xx} & -I_{xy} & -I_{xz} \\ -I_{yx} & I_{yy} & -I_{yz} \\ -I_{zx} & -I_{zy} & I_{zz} \end{bmatrix} \tag{2.27}$$

For a symmetric aircraft, xz plane is assumed as plane of symmetry and inertia matrix can be taken as,

$$I = \begin{bmatrix} I_{xx} & 0 & -I_{xz} \\ 0 & I_{yy} & 0 \\ -I_{zx} & 0 & I_{zz} \end{bmatrix} \tag{2.28}$$

Taking derivative of angular momentum equation in Equation 2.25 with respect to BF,

$$\frac{d}{dt}\vec{H}_B^B = \frac{d}{dt}I.\vec{\omega}_B^B + I.\frac{d}{dt}\vec{\omega}_B^B \tag{2.29}$$

Since change in inertia vector with time is assumed as zero,

$$\begin{aligned} \frac{d}{dt}I &= 0 \\ \frac{d}{dt}\vec{H}_B^B &= I.\vec{\omega}_B \end{aligned} \tag{2.30}$$

$$\begin{aligned} \Rightarrow \sum \vec{M}_B &= \begin{bmatrix} I_{xx} & 0 & -I_{xz} \\ 0 & I_{yy} & 0 \\ -I_{zx} & 0 & I_{zz} \end{bmatrix} \begin{bmatrix} \dot{p} \\ \dot{q} \\ \dot{r} \end{bmatrix} + \begin{bmatrix} p \\ q \\ r \end{bmatrix} \times \begin{bmatrix} I_{xx} & 0 & -I_{xz} \\ 0 & I_{yy} & 0 \\ -I_{zx} & 0 & I_{zz} \end{bmatrix} \begin{bmatrix} p \\ q \\ r \end{bmatrix} \\ &= \begin{bmatrix} \vec{M}_x \\ \vec{M}_y \\ \vec{M}_z \end{bmatrix} = \begin{bmatrix} I_{xx}\dot{p} - I_{xz}\dot{r} - q(I_{zx}p - I_{zz}r) - I_{yy}qr \\ I_{yy}\dot{q} + p(l_{zx}p - I_{zz}r) + r(I_{xx}p - I_{xz}r) \\ I_{zz}\dot{r} - I_{zx}\dot{p} - q(I_{xx}p - I_{xz}r) + I_{yy}pq \end{bmatrix} \end{aligned} \tag{2.31}$$

Then, the rotational accelerations are derived as,

$$\begin{aligned} \dot{p} &= \frac{\vec{M}_x + I_{xz}\dot{r} + q(I_{zx}p - I_{zz}r) + I_{yy}qr}{I_{xx}} \\ \dot{q} &= \frac{\vec{M}_y - p(I_{zx}p - I_{zz}r) - r(I_{xx}p - I_{xx}r)}{I_{yy}} \\ \dot{r} &= \frac{\vec{M}_z + I_{zx}\dot{p} + q(I_{xx}p - I_{xz}r) - I_{yy}pq}{I_{zz}} \end{aligned} \tag{2.32}$$

Finally, all rigid body dynamics equations are obtained. There are nine unknowns and six differential equations described in Equation 2.24 and Equation 2.32. In order to solve these nonlinear equations, three more equations are essential and they come from kinematic relation in Equation 2.17. After deriving all equations, $\sum \vec{F}_B = [\vec{F}_x \quad \vec{F}_y \quad \vec{F}_z]^T$ and $\sum \vec{M}_B = [\vec{M}_x \quad \vec{M}_y \quad \vec{M}_z]^T$ are needed to be calculated to solve rigid body dynamics equations.

2.3 Rotary Wing Dynamics

In this section, main rotor and stabilizer bar dynamics are described. As mentioned in model assumptions in Section 2.1.1, only flapping motion is considered in deriving equations. Flapping of the rotary wing is the most important dynamics for a helicopter [6]. It is primary source of lift force and it does not only keep the helicopter in air, but also it decides direction of the helicopter. Since it is a very complex physical structure, most of the model assumptions are made in defining and deriving this dynamics.

2.3.1 Main Rotor Flapping Dynamics

In order to describe main rotor flapping dynamics, it is necessary to determine the source of this dynamics. Therefore, pitch angle of each blade is defined. Pitch angle of blades are controlled by swash plate with harmonically varying angles. Only first order harmonics are considered [41]. That is,

$$\theta_{bl} = \theta_{coll} + \theta_{lat}\cos\psi - \theta_{lon}\sin\psi + \theta_{tw}\frac{e+r}{R} - K_s\beta_{bl} \tag{2.33}$$

where,
θ_{bl} is the pitch angle of the blade,
θ_{col} is the collective pitch angle,
θ_{lon} is the longitudinal pitch angle,
θ_{lat} is the lateral pitch angle,
ψ is the angular position of the blade,
θ_{tw} is the blade twist angle,
e is the distance from flapping hinge to the main rotor hub,
r is the distance from flapping hinge to a blade element,
R is the main rotor radius,
K_s is the cross-coupling between the flapping angle and the pitch angle,
β_{bl} is the flapping angle of the main rotor blade.

In Equation 2.33, it is seen that θ_{coll} are not multiplied with any term related with the blade position. This means that collective pitch angle of blades are equal at any azimuth angle ψ. Moreover, according to model assumptions in Section 2.1.1, blade twist angle and flapping-pitch angle cross coupling are zero. Then,

$$\theta_{bl} = \theta_{coll} + \theta_{lat}\cos\psi - \theta_{lon}\sin\psi \tag{2.34}$$

After defining the source of the flapping dynamics, the resulting motion is need to be defined. Since pitch angle of the blades are defined as a harmonic function, resulting flapping motion are also be defined harmonically. Considering ideal phase shift (90°), flapping motion is defined as [36],

$$\beta_{bl} = \beta_0 - \beta_{1c}\cos\psi + \beta_{1s}\sin\psi \tag{2.35}$$

In order to determine signs in Equation 2.35, corresponding flapping motion is considered after 90° phase shift from the swash plate input is given. The main principle is that maximum flapping occurs 90° after maximum pitch is given.

After determining inputs and results of flapping motion, aerodynamic forces and moments on a blade are considered in order to derive flapping dynamics equations. For this purpose, Blade Element Method is widely used in literature [40]. This method basically presents examining forces and moments on a small element of a blade, then calculating total forces and moments by integration along blade length.

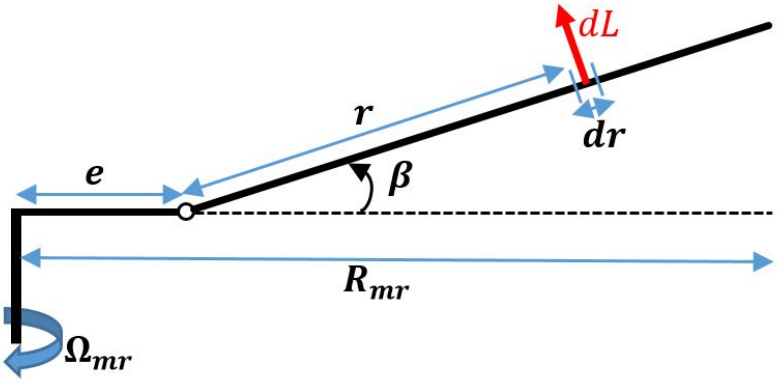

Figure 2.4: Cross section of the helicopter main rotor blades

In Figure 2.4, a small blade element dr is shown. By using basic aerodynamics [36], corresponding lift force dL is calculated. e is the hinge offset in the same unit with R_{mr} and calculated by multiplying hinge offset percent with main rotor radius length.

First step of blade element method is to calculate lift and drag force on a small element. Figure 2.5 illustrates the blade cross section and corresponding dL and dD forces acting on the blade. Resulting air velocity U_b is perpendicular to dL and is parallel to dD.

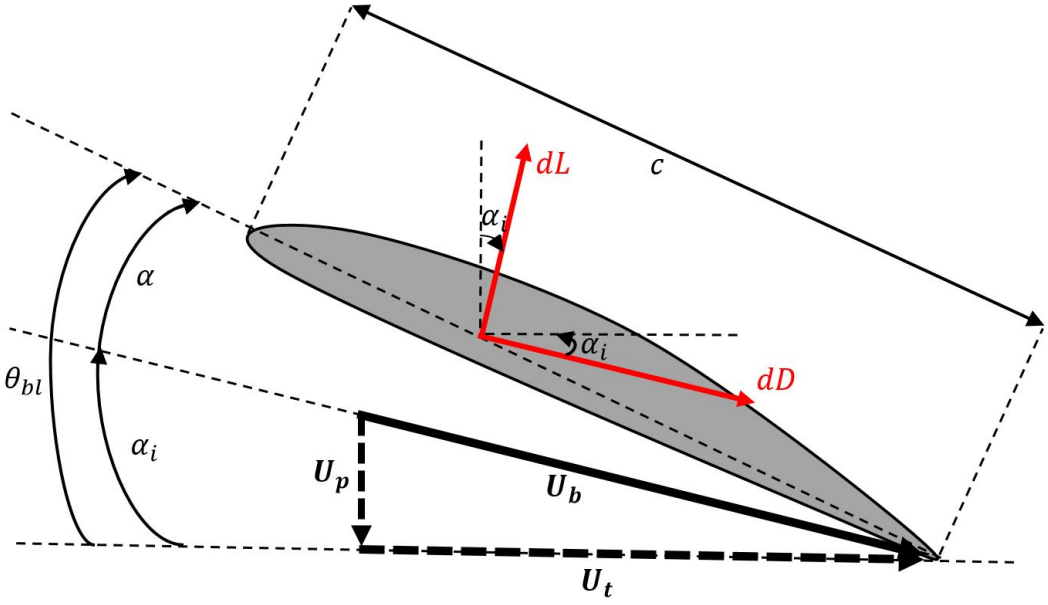

Figure 2.5: Cross section of the helicopter main rotor blades

The increment of lift force dL on a small element dr is described by basic aerodynamics [36],

$$dL = \frac{\rho}{2} U_b^2 C_L c dr \tag{2.36}$$

where,

ρ is the density of the air

U_b is the air velocity

C_L is the blade lift coefficient

c is the cord length of the blade

Blade lift coefficient C_L can be assumed as it has a constant lift curve slope C_{L_α}, then Equation 2.36 becomes,

$$dL = \frac{\rho}{2} U_b^2 C_{L_\alpha} \alpha c dr \tag{2.37}$$

Considering local inflow angle α_i very small, it is assumed that $|U_t| >> |U_p|$.

$$\begin{aligned} \alpha &= \theta_{bl} - \alpha_i \\ &= \theta_{bl} - \tan^{-1}(\frac{U_p}{U_t}) \\ &\approx \theta_{bl} - \frac{U_p}{U_t} \end{aligned} \tag{2.38}$$

$$\begin{aligned} U_b &= \sqrt{U_t^2 + U_p^2} \\ &\approx U_t \end{aligned} \tag{2.39}$$

Then, lift force acting on a small blade element dL is described,

$$dL = \frac{\rho}{2} U_t^2 C_{L_\alpha} (\theta_{bl} - \frac{U_p}{U_t}) c dr \tag{2.40}$$

Drag force acting on a small element dD is derived by same procedure,

$$dD = \frac{\rho}{2} U_t^2 C_d c dr \tag{2.41}$$

where C_d is the blade drag coefficient.

In Equations 2.40 and 2.41, there are two unknowns which need to be defined. These are horizontal and vertical blade velocities. Primary source of horizontal blade velocity is the main rotor rotation speed. Other source that contributes to U_t is translational velocities of the helicopter. On the other hand, primary source of vertical blade velocity is main rotor inflow. Other contributors are helicopter translational velocities, helicopter rotational velocities and main rotor flapping rates. Considering all contributions to horizontal and vertical velocity of the blade, these velocities can be defined [5].

$$\begin{aligned} U_t &= \Omega_{mr}(e + r\cos\beta) + u_B \sin\psi - v_B \cos\psi \\ U_p &= -w_B \cos\beta + u \sin\beta \cos\psi + v \sin\beta \sin\psi + v_i \cos\beta + \dot{\beta} r \\ &\quad + (e + r\cos\beta)(p \sin\psi - q \cos\psi) \end{aligned} \tag{2.42}$$

Assuming small angle assumption to flapping angle β ($\sin\beta \approx \beta$ and $\cos\beta \approx 1$), Equation 2.42 becomes,

$$\begin{aligned} U_t &= \Omega_{mr}(e + r) + u_B \sin\psi - v_B \cos\psi \\ U_p &= -w_B + u\beta \cos\psi + v\beta \sin\psi + v_i + \dot{\beta} r \\ &\quad + (e + r)(p \sin\psi - q \cos\psi) \end{aligned} \tag{2.43}$$

Now, each unknown term in Equations 2.40 and 2.41 is defined . This means that forces acting on a blade can be calculated by simple integration over the blade. Moving on to torques acting on the blades, it can be said that resulting torque needs to be equal to aerodynamic torque generated dominantly by lift force on the blade for equilibrium. Resulting torque is defined by Euler equations of rotation which is based on

total moment of all external forces about a fixed point is equal to time rate of change in total angular momentum [14].

$$\sum M_{aero} = (\vec{r}_{cg} m_{bl} \times \vec{a}_{hinge}) + \dot{\vec{H}}_{0_{bl}} + \vec{\omega}_{bl} \times \vec{H}_{0_{bl}} + \vec{M}_{sp} \tag{2.44}$$

In Equation 2.44, there are some new terms need to be defined,

- $\vec{\omega}_{bl}$: Rotational velocity at blade
- $\vec{a}_{hinge}$: Translational acceleration at flapping hinge point
- $\vec{M}_{sp}$ is the restraint torque due to spring at flapping hinge.
- $\vec{H}_{0_{bl}}$: Angular momentum around hinge center

In order to define these unknown terms, transformation matrices are frequently used. Starting to define angular velocities at BF, HF and FF,

$$\vec{\omega}_B = \begin{bmatrix} p \\ q \\ r \end{bmatrix} \tag{2.45}$$

$$\vec{\omega}_H = R_{BH}(\Theta)\vec{\omega}_B \tag{2.46}$$

$$\vec{\omega}_F = R_{HF}(\Theta)\vec{\omega}_H \tag{2.47}$$

$$\vec{\omega}_{bl} = R_{FBl}(\beta)\vec{\omega}_F + \begin{bmatrix} 0 \\ \dot{\beta} \\ 0 \end{bmatrix} + R_{FBl}(\beta) \begin{bmatrix} 0 \\ 0 \\ \Omega_{mr} \end{bmatrix} \tag{2.48}$$

Note that main rotor rotation $\left(\begin{bmatrix} 0 \\ 0 \\ \Omega_{mr} \end{bmatrix} \right)$ is defined in FF and flapping rate $\left(\begin{bmatrix} 0 \\ \dot{\beta} \\ 0 \end{bmatrix} \right)$ is defined in BFF.

Next, translational acceleration of the hinge point is defined with general planar motion [14],

$$\vec{a}_{Bl_{hinge}} = R_{FBl}\left[\vec{a}_{F_{hinge}} + \dot{\vec{\omega}}_F \times \vec{e} + \vec{\omega}_F \times (\vec{\omega}_F \times \vec{e})\right] \tag{2.49}$$

where $\vec{a}_{F_{hinge}} = 0$ because it is the translational acceleration of flapping hinge fixed reference frame relative to itself. $\vec{e} = \begin{bmatrix} e_{mr} \\ 0 \\ 0 \end{bmatrix}$ is the hinge offset vector fixed at flapping hinge in FF.

Next, $\vec{M}_{Bl_{sp}} = \begin{bmatrix} 0 \\ K_s\beta \\ 0 \end{bmatrix}$ is the restraint torque and its source is the virtual spring at the flapping hinge. It always generates torque against flapping motion.

The last term needs to be defined $\vec{H}_{0_{bl}} = I\vec{\omega}_{bl}$ is the angular momentum of the blade with respect to flapping hinge point. Therefore, $\dot{\vec{H}}_{0_{bl}} = I\dot{\vec{\omega}}_{bl}$.

After determining all unknown terms in total moment equation in Equation 2.44, total lift force and aerodynamics moment can be calculated by using lift force acting on a small blade element [36],

$$\sum M_{aero} = \int rdL = \int_0^{R_{mr}-e} \frac{\rho}{2} U_t^2 C_{L_\alpha} (\theta_{bl} - \frac{U_p}{U_t}) crdr \tag{2.50}$$

In Equation 2.50, all terms are previously defined. Inserting 2.50 into total moment equation in Equation 2.44, total flapping dynamics equation is obtained. That is,

$$\int_0^{R_{mr}-e} \frac{\rho}{2} U_t^2 C_{L_\alpha} (\theta_{bl} - \frac{U_p}{U_t}) crdr - \left[(\vec{r}_{cg} m_{bl} \times \vec{a}_{hinge}) + \dot{\vec{H}}_{0_{bl}} + \vec{\omega}_{bl} \times \vec{H}_{0_{bl}} + \vec{M}_{sp} \right] = 0 \tag{2.51}$$

It should be noticed that pitch angle and flapping angle of the blades are defined as a first order harmonic function. This results in using harmonic balancing [41] to solve Equation 2.51. In order to do this, all sine, cosine and constant terms are separated from each other and equated to zero.

Finally second order flapping equations are derived as $\ddot{\beta}_0$, $\ddot{\beta}_{1s}$ and $\ddot{\beta}_{1c}$. $\ddot{\beta}_0$ is the solution of constant terms in Equation 2.51. $\ddot{\beta}_{1s}$ is the solution of sine terms in Equation 2.51. Lastly, $\ddot{\beta}_{1c}$ is the solution of cosine terms in Equation 2.51. Implicit solutions of second order flapping angles equations can be seen in Appendix A.

2.3.2 Main Rotor Inflow

Main rotor inflow is the most important parameter affecting thrust generation by the main rotor. For the induced velocity calculation, momentum theory with a recursive solution is used and main rotor inflow is assumed constant over blade. Thrust

generated by the main rotor is described as [16],

$$T_{mr} = (w_b - v_i)\frac{\rho\Omega_{mr}R_{mr}C_{L_\alpha}NcR_{mr}}{4} \tag{2.52}$$

$$v_i^2 = \sqrt{(-\frac{\hat{v}^2}{2})^2 + (\frac{T_{mr}}{2\rho A_{mr}})^2} - \frac{\hat{v}^2}{2} \tag{2.53}$$

where,

$$w_b = w_r + \frac{2}{3}\Omega_{mr}R_{mr}(\theta_{coll} + \frac{3}{4}\theta_{tw}) \tag{2.54}$$

$$w_r = w + (\beta_{1c} + i_s)u_B - \beta_{1s}v_B \tag{2.55}$$

$$\hat{v}^2 = u_B^2 + v_B^2 + w_r(w_r - 2v_i) \tag{2.56}$$

$$A_{mr} = \pi R_{mr}^2 \tag{2.57}$$

where ρ is the air density, Ω_{mr} is the main rotor angular velocity, C_{L_α} is the lift curve slope, R_{mr} is the main rotor radius, N is the number of blades, c is the chord length, w_b is the main rotor blade velocity, w_r is main rotor disc velocity and and v_i is the induced velocity.

2.3.3 Stabilizer Bar Flapping Dynamics

In order to describe stabilizer bar flapping dynamics, its function and use of purpose are necessary to be defined. Basically, stabilizer bar acts like a rate feedback controller in pitch and roll axes to decrease bandwidth and weights of cyclic control inputs. Stabilizer bar does not have a coning angle, it only flaps in lateral and longitudinal directions. Similar procedure with main rotor flapping derivation is applied for stabilizer bar flapping dynamics. It uses longitudinal and lateral swash plate input [39],

$$\theta_{sb} = \theta_{sw_{lat}}cos\psi - \theta_{sw_{lon}}sin\psi \tag{2.58}$$

And stabilizer bar flapping is defines as[39],

$$\beta_{sb} = -\beta_{1c_{sb}}cos\psi + \beta_{1s_{sb}}sin\psi \tag{2.59}$$

Horizontal and vertical velocities on the stabilizer bar paddle and angle between them is written as[39],

$$U_{t_{sb}} = \Omega_{mr} r + u_B \sin\psi - v_B \cos\psi \tag{2.60}$$

$$U_{p_{sb}} = -w_B + u_B \beta_{sb} \cos\psi + v_B \beta_{sb} \sin\psi + v_i + \dot{\beta}_{sb} r + r(p \sin\psi - q \cos\psi) \tag{2.61}$$

$$\begin{aligned} \alpha &= \theta_{sb} - \tan^{-1}(\frac{U_p}{U_t}) \\ &\approx \theta_{sb} - \frac{U_{p_{sb}}}{U_{t_{sb}}} \end{aligned} \tag{2.62}$$

After using the whole procedure and applying harmonic balancing [41], first order stabilizer bar flapping equations are derived implicitly. $\dot{\beta}_{1c_{sb}}$ and $\dot{\beta}_{1s_{sb}}$ equations can be found in Appendix A.

Stabilizer bar flapping and swash plate inputs are mixed and fed to the main rotor. This mixing relation is the mechanical links connecting swash plate, stabilizer bar and main rotor. Bell-Hiller gains are used to define this relation [39].

$$\begin{aligned} \theta_{lat} &= K_{sw} \theta_{sw_{lat}} + K_{sb} \beta_{1s_{sb}} \\ \theta_{lon} &= K_{sw} \theta_{sw_{lon}} - K_{sb} \beta_{1c_{sb}} \\ \theta_{coll} &= \theta_{sw_{coll}} \end{aligned} \tag{2.63}$$

2.4 Forces and Moments

In this section, forces and moments acting on the helicopter body are described. Primary sources of the forces are main rotor and tail rotor. The most important torque contribution of main rotor is drag torque around z_H due to main rotor rotation. The main role of tail rotor is to create anti-torque to main rotor drag torque. Fuselage, horizontal tail and vertical fin also generate a force on the helicopter body; however, these forces are small relative to main rotor and tail rotor. Stabilizer bar is assumed as it does not create a significant force on the helicopter.

2.4.1 Forces and Moments Generation

In order to understand helicopter motion, forces and moments generated by the components of helicopter model should be derived particularly. These forces can be derived at different reference frames. It will be transformed into BF in Forces and Moment Summation in Section 2.4.2.

2.4.1.1 Main Rotor Forces and Moments

Main rotor generates forces and moments in three axis in HF. These forces and moments are $F_{x_{mr}}$, $F_{y_{mr}}$, $F_{z_{mr}}$ and $M_{x_{mr}}$, $M_{y_{mr}}$ and $M_{z_{mr}}$. In order to define these forces, blade element theory is again used. Lift and drag force on the blade are the main sources of main rotor forces and moments. They can be seen in Figure 2.5. According to Figure 2.5 and small angle assumption to α_i, forces at zero azimuth are defined as [41],

$$\begin{aligned} dF_{y_{Bl}} &= -dL\sin\alpha_i - dD\cos\alpha_i \\ &\approx -(dL\alpha_i + dD) \end{aligned} \tag{2.64}$$

$$\begin{aligned} dF_{z_{Bl}} &= -dL\cos\alpha_i + dD\sin\alpha_i \\ &\approx -dL \end{aligned} \tag{2.65}$$

$$\begin{aligned} dF_{x_{Bl}} &= dF_{z_{Bl}}\sin\beta \\ &\approx -dL\beta \end{aligned} \tag{2.66}$$

$$\Rightarrow dF_{Bl} = \begin{bmatrix} dF_{x_{Bl}} \\ dF_{y_{Bl}} \\ dF_{z_{Bl}} \end{bmatrix} = \begin{bmatrix} -dL\beta \\ -(dL\alpha_i + dD) \\ -dL \end{bmatrix} \tag{2.67}$$

In order to write main rotor forces in HF, transformation matrices are used. The angle between BFF and HF is $(180+\psi)$ degrees.

$$dF_H = R_z(180^\circ+\psi)dF_{Bl} = \begin{bmatrix} \cos(180^\circ+\psi) & \sin(180^\circ+\psi) & 0 \\ -\sin(180^\circ+\psi) & \cos(180^\circ+\psi) & 0 \\ 0 & 0 & 1 \end{bmatrix} dF_{Bl} \tag{2.68}$$

$$\Rightarrow dF_{x_H} = -dF_{x_{Bl}} \cos\psi + dF_{y_{Bl}} \sin\psi = dL\beta \cos\psi - (dL\alpha_i + dD)\sin\psi$$
$$\Rightarrow dF_{y_H} = -dF_{x_{Bl}} \sin\psi - dF_{y_{Bl}} \cos\psi = dL\beta \sin\psi + (dL\alpha_i + dD)\cos\psi \quad (2.69)$$
$$\Rightarrow dF_{z_H} = dF_{z_{Bl}} = -dL$$

Then, infinitesimal main rotor forces in HF are integrated over blade length, that is from 0 to $(R_{mr} - e)$. Since forces are changing with azimuth angle ψ, average main rotor forces are found by integrating along azimuth angle from 0 to 2π, multiplying with number of main rotor blades and by dividing 2π [36].

$$H_{mr} = \frac{N_{mr}}{2\pi} \int_0^{2\pi} \int_0^{R_{mr}-e} dF_{x_H} dr d\psi \quad (2.70)$$

$$Y_{mr} = \frac{N_{mr}}{2\pi} \int_0^{2\pi} \int_0^{R_{mr}-e} dF_{y_H} dr d\psi \quad (2.71)$$

$$T_{mr} = \frac{N_{mr}}{2\pi} \int_0^{2\pi} \int_0^{R_{mr}-e} dF_{z_H} dr d\psi \quad (2.72)$$

Finally, main rotor forces in HF is derived.

$$F_{mr_H} = \begin{bmatrix} H_{mr} \\ Y_{mr} \\ T_{mr} \end{bmatrix} \quad (2.73)$$

Same procedure is applied for deriving main rotor moments. It should be noted that moments are taken around flapping hinge point [36].

$$M_{z_H} = Q_{mr} = \frac{N_{mr}}{2\pi} \int_0^{2\pi} \int_0^{R_{mr}-e} (e + r) dF_{y_{Bl}} d\psi \quad (2.74)$$

$$M_{x_H} = M_{x_{mr}} = \frac{N_{mr}}{2\pi} \int_0^{2\pi} \int_0^{R_{mr}-e} -(e \sin\psi) dF_{z_{Bl}} d\psi + K_s \beta \sin\psi d\psi \quad (2.75)$$

$$M_{y_H} = M_{y_{mr}} = \frac{N_{mr}}{2\pi} \int_0^{2\pi} \int_0^{R_{mr}-e} (e \cos\psi) dF_{z_{Bl}} d\psi + K_s \beta \cos\psi d\psi \quad (2.76)$$

It is seen that while $F_{z_{Bl}}$ force generates $M_{x_{mr}}$ and $M_{y_{mr}}$, $F_{y_{Bl}}$ force is the source of main rotor drag torque Q_{mr}. Note that K_s is the flapping hinge spring constant and $K_s\beta$ is the its contribution, known as restraint torque.

After inserting Equation 2.38, final main rotor force and moments equations in HF in Equations 2.71–2.76 are derived.

$$F_{mr_H} = \begin{bmatrix} H_{mr} \\ Y_{mr} \\ T_{mr} \end{bmatrix} = \begin{bmatrix} \frac{N_{mr}}{2\pi}\int_0^{2\pi}\int_0^{R_{mr}-e} dL\beta\cos\psi - (dL(\theta_{bl}-\frac{U_p}{U_t})+dD)\sin\psi dr d\psi \\ \frac{N_{mr}}{2\pi}\int_0^{2\pi}\int_0^{R_{mr}-e} dL\beta\sin\psi + (dL(\theta_{bl}-\frac{U_p}{U_t})+dD)\cos\psi dr d\psi \\ \frac{N_{mr}}{2\pi}\int_0^{2\pi}\int_0^{R_{mr}-e} -dL dr d\psi \end{bmatrix} \tag{2.77}$$

$$M_{mr_H} = \begin{bmatrix} M_{x_{mr}} \\ M_{y_{mr}} \\ Q_{mr} \end{bmatrix} = \begin{bmatrix} \frac{N_{mr}}{2\pi}\int_0^{2\pi}\int_0^{R_{mr}-e}\Big[dL(e\sin\psi)+K_s\beta\sin\psi\Big]d\psi \\ \frac{N_{mr}}{2\pi}\int_0^{2\pi}\int_0^{R_{mr}-e}\Big[-dLe\cos\psi+K_s\beta\cos\psi\Big]d\psi \\ \frac{N_{mr}}{2\pi}\int_0^{2\pi}\int_0^{R_{mr}-e} -(e+r)\Big[dL(\theta_{bl}-\frac{U_p}{U_t})+dD\Big]d\psi \end{bmatrix} \tag{2.78}$$

2.4.1.2 Tail Rotor Forces and Moments

In derivation of tail rotor forces and moments, it is assumed that tail rotor only generates thrust force in y_T axis and tail rotor drag force is neglected. Unlike main rotor, tail rotor does not have longitudinal and lateral inputs. Collective pedal input θ_{tr} generates tail thrust force T_{tr}. In order to derive tail rotor thrust, momentum theory with a recursive solution is used like main rotor inflow. Tail rotor does not generate any torque on center of TF. Thrust generated by the tail rotor is described as [16],

$$T_{tr} = (w_{b_{tr}} - v_{i_{tr}})\frac{\rho\Omega_{tr}R_{tr}C_{L_{\alpha_{tr}}}N_{tr}c_{tr}R_{tr}}{4} \tag{2.79}$$

$$v_{i_{tr}}^2 = \sqrt{(-\frac{\hat{v}_{tr}^2}{2})^2 + (\frac{T_{tr}}{2\rho A_{tr}})^2} - \frac{\hat{v}_{tr}^2}{2} \tag{2.80}$$

where,

$$w_{b_{tr}} = w_{r_{tr}} + \frac{2}{3}\Omega_{tr}R_{tr}(\theta_{tr} + \frac{3}{4}\theta_{tw_{tr}}) \tag{2.81}$$

$$w_{r_{tr}} = -v + rR_{x_{TR}} - pR_{z_{TR}} \tag{2.82}$$

$$\hat{v}_{tr}^2 = u_B^2 + (w_B + qR_{x_{TR}})^2 + w_{r_{tr}}(w_{r_{tr}} - 2v_{i_{tr}}) \tag{2.83}$$

$$A_{tr} = \pi R_{tr}^2 \tag{2.84}$$

where ρ is the air density, Ω_{tr} is the tail rotor angular velocity, $C_{L_{\alpha_{tr}}}$ is the tail rotor lift curve slope, R_{tr} is the tail rotor radius, N_{tr} is the number of blades of tail rotor, c_{tr} is the chord length of the tail rotor, $w_{b_{tr}}$ is the tail rotor blade velocity, $w_{r_{tr}}$ is tail rotor disc velocity and and $v_{i_{tr}}$ is the induced velocity of the tail rotor.

Final tail rotor force equations are described.

$$F_{tr_B} = F_{tr_T} = \begin{bmatrix} 0 \\ -T_{tr} \\ 0 \end{bmatrix} \tag{2.85}$$

2.4.1.3 Fuselage Forces and Moments

Fuselage creates drag forces defined in all axes in BF. These forces are assumed at CM; therefore, they do not create any significant moment on CG position. Fuselage forces are described using quadratic drag function [36],

$$F_{fus_B} = \begin{bmatrix} -\frac{1}{2}\rho u_B |u_B| C_{d_x} A_{fus_x} \\ -\frac{1}{2}\rho v_B |v_B| C_{d_y} A_{fus_y} \\ -\frac{1}{2}\rho w_B |w_B| C_{d_z} A_{fus_z} \end{bmatrix} \tag{2.86}$$

Where C_{d_x}, C_{d_y} and C_{d_z} are drag coefficients and A_{fus_x}, A_{fus_y} and A_{fus_z} are the equivalent flat plate areas in the related axis.

2.4.1.4 Empennage Forces and Moments

The last components which generate forces and moments on the helicopter body are horizontal stabilizer and vertical fin. The main intended purpose of vertical fin is to create extra anti-torque when the helicopter is in forward flight and air is flowing across the lifting surface. On the other hand, horizontal tail is used for holding fuselage flat in forward flight. Drag force on both vertical fin and horizontal stabilizer can be neglected, since they are relatively small and thin components. Lift force generated by vertical fin and horizontal stabilizer are defined as [36],

$$F_{hs_B} = \begin{bmatrix} F_{x_{hs}} \\ F_{y_{hs}} \\ F_{z_{hs}} \end{bmatrix} = \begin{bmatrix} 0 \\ 0 \\ -\frac{1}{2}\rho u_B |u_B| C_{L_{\alpha_{hs}}} \alpha_{hs} A_{hs} \end{bmatrix} \tag{2.87}$$

$$F_{vf_B} = \begin{bmatrix} F_{x_{vf}} \\ F_{y_{vf}} \\ F_{z_{vf}} \end{bmatrix} = \begin{bmatrix} 0 \\ -\frac{1}{2}\rho u_B |u_B| C_{L_{\alpha_{vf}}} \alpha_{vf} A_{vf} \\ 0 \end{bmatrix} \tag{2.88}$$

Where $C_{L_{\alpha_{hs}}}$ and $C_{L_{\alpha_{vf}}}$ are lift curve slopes of horizontal tail and vertical fin, respectively. A_{hs} and A_{vf} are the horizontal stabilizer and vertical fin areas. Angle of attack of these components are defines as [36],

$$\begin{aligned} \alpha_{hs} &= \arctan(w_{hs}/u_B) \\ \alpha_{vf} &= \arctan(v_{vf}/u_B) \end{aligned} \tag{2.89}$$

Velocities passing over the lifting surfaces are defined as,

$$\begin{aligned} w_{hs} &= w_B + qR_{x_{hs}} \\ v_{vf} &= v_B - rR_{x_{vf}} \end{aligned} \tag{2.90}$$

Moving on torques generated by empennage forces,

$$M_{hs_B} = \begin{bmatrix} M_{x_{hs}} \\ M_{y_{hs}} \\ M_{z_{hs}} \end{bmatrix} = \begin{bmatrix} F_{z_{hs}} R_{y_{hs}} - F_{y_{hs}} R_{z_{hs}} \\ F_{x_{hs}} R_{z_{hs}} - F_{z_{hs}} R_{x_{hs}} \\ F_{y_{hs}} R_{x_{hs}} - F_{x_{hs}} R_{y_{hs}} \end{bmatrix} \tag{2.91}$$

$$M_{vf_B} = \begin{bmatrix} M_{x_{vf}} \\ M_{y_{vf}} \\ M_{z_{vf}} \end{bmatrix} = \begin{bmatrix} F_{z_{vf}} R_{y_{vf}} - F_{y_{vf}} R_{z_{vf}} \\ F_{x_{vf}} R_{z_{vf}} - F_{z_{vf}} R_{x_{vf}} \\ F_{y_{vf}} R_{x_{vf}} - F_{x_{vf}} R_{y_{vf}} \end{bmatrix} \tag{2.92}$$

Where $R_{x_{hs}}$, $R_{y_{hs}}$, $R_{z_{hs}}$, $R_{x_{vf}}$, $R_{y_{vf}}$ and $R_{z_{vf}}$ are the distances of horizontal stabilizer and vertical fin to CG in x_B, y_B and z_B axis.

2.4.2 Forces and Moments Summation

After deriving forces and moments generated by the components, the last step is to transform them to BF in order to use in Rigid Body Dynamics in Section 2.2. First, total moment around CG due to main rotor and tail rotor are defined.

$$\begin{aligned} M_{mr_B} &= M_{mr_H} + R_{MR} \times F_{mr_H} \\ M_{tr_B} &= R_{TR} \times F_{tr_H} \end{aligned} \tag{2.93}$$

Beside these forces generated in Section 2.4.1, gravitational force is defined in SF and always act in z_S direction. Transforming all forces and moments to BF,

$$\begin{aligned} F_B &= R_{SB}\begin{bmatrix} 0 \\ 0 \\ m_h g \end{bmatrix} + R_{HB}F_{mr_H} + F_{tr_B} + F_{fus_B} + F_{hs_B} + F_{vf_B} \\ \tau_B &= M_{mr_B} + M_{tr_B} + M_{hs_B} + M_{vf_B} \end{aligned} \tag{2.94}$$

Then, using Equation 2.93 in Equation 2.94, final moment equation in BF are derived.

Where $R_{MR} = \begin{bmatrix} R_{x_{mr}} \\ R_{y_{mr}} \\ R_{z_{mr}} \end{bmatrix}$ and $R_{TR} = \begin{bmatrix} R_{x_{tr}} \\ R_{y_{tr}} \\ R_{z_{tr}} \end{bmatrix}$ are the distances of main rotor and tail rotor to CG position, respectively.

2.5 Analysis of Mathematical Model

In this part, mathematical model of the helicopter is implemented and analysed. After deriving necessary dynamics, these equations need to be related with each other. Looking at the structure by considering inputs and outputs of each subparts,

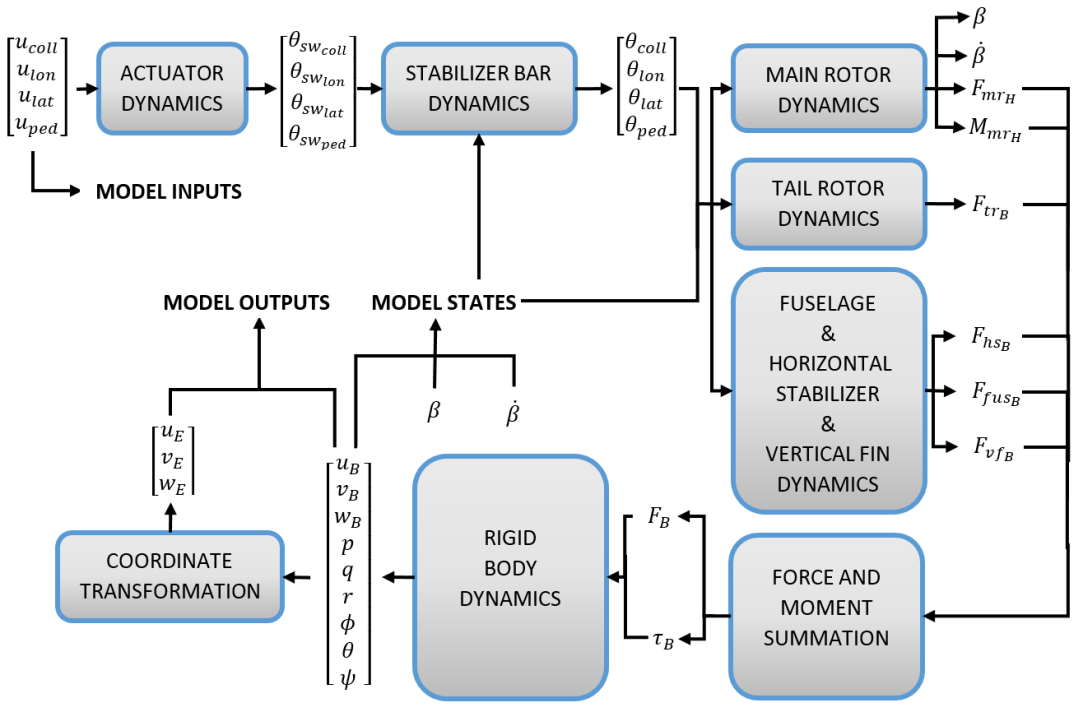

Figure 2.6: Model Inputs, States and Outputs

Considering full mathematical model, there are four inputs, fifteen states and twelve outputs. States are translational body velocities, rotational velocities, Euler Angles,

main rotor flapping angles and flapping rates. Outputs are translational body velocities, rotational velocities, Euler angles and translational Earth velocities.

$$
\begin{aligned}
u &= \begin{bmatrix} u_{coll} & u_{lon} & u_{lat} & u_{ped} \end{bmatrix}^T \\
x &= \begin{bmatrix} u_B & y_B & w_B & p & q & r & \phi & \theta & \psi & \beta_0 & \beta_{1s} & \beta_{1c} & \dot{\beta}_0 & \dot{\beta}_{1s} & \dot{\beta}_{1c} \end{bmatrix}^T \\
y &= \begin{bmatrix} u_B & y_B & w_B & p & q & r & \phi & \theta & \psi & u_E & v_E & w_E \end{bmatrix}^T
\end{aligned}
\tag{2.95}
$$

After constructing the helicopter mathematical model, a sample helicopter model need to be selected. This helicopter should be a small-sized model helicopter because of the assumptions in Section 2.1.1. Having a hinge offset and a stabilizer bar are other important properties for the sample helicopter selection. After searching literature, R-50 helicopter is found appropriate to be tested with the mathematical model derived. R-50 helicopter parameters can be found in Appendix B [28].

Using sample helicopter parameters and defining trim condition, trimming process of the nonlinear mathematical model is done. Then, in order to obtain linear system and design a linear controller, nonlinear model is linearized around specified equilibrium point. Finally, linear model order is reduced considering the least effective states for the helicopter behavior.

2.5.1 Trimming and Linearization of the Mathematical Model

2.5.1.1 Trimming Process

Trim point is defined as a condition where all resultant forces and moments around center of gravity position of the helicopter are zero. Any force acting a position different than c.g. produces moments on the aircraft and it is desired that rotation should be zero at trim condition. Trimming is an important job because there will be residual forces and moments which ruin the exact nonlinear character if working with random point rather than trim point.

$$\sum \vec{F} = \sum \vec{M} = 0 \tag{2.96}$$

In addition, mathematically, trim point is the point where all state derivatives equal to zero [35]. For trimming of nonlinear helicopter model, MATLAB Linear Analysis

Tool is used for its reliability, simplicity and accuracy. The sample helicopter parameters is substituted into mathematical model equations and trim input and state values is obtained at specified trim conditions. Trim condition is decided to be hover at 100 ft altitude.

$$\dot{x}_{trim} = f(x_{trim}, u_{trim}, t) = 0 \tag{2.97}$$

Constraints for the trim condition are decided as follows,

$$\begin{gathered} u_B = v_B = w_B = p = q = r = U = 0 \\ h = 100ft \end{gathered} \tag{2.98}$$

where U is the airspeed and h is the altitude of the helicopter.

Result of the trimming process is,

$$u_{trim} = \begin{bmatrix} u_{coll_{trim}}[rad] \\ u_{lon_{trim}}[rad] \\ u_{lat_{trim}}[rad] \\ u_{ped_{trim}}[rad] \end{bmatrix} = \begin{bmatrix} 0.106516 \\ 0.00019 \\ 0.0035 \\ 0.02312 \end{bmatrix}, \qquad x_{trim} = \begin{bmatrix} u_{B_{trim}}[m/s] \\ v_{B_{trim}}[m/s] \\ w_{B_{trim}}[m/s] \\ p_{trim}[rad/s] \\ q_{trim}[rad/s] \\ r_{trim}[rad/s] \\ \phi_{trim}[rad] \\ \theta_{trim}[rad] \\ \psi_{trim}[rad] \\ \beta_{1c_{sbtrim}}[rad] \\ \beta_{1s_{sbtrim}}[rad] \\ \beta_0[rad] \\ \beta_{1s}[rad] \\ \beta_{1c}[rad] \\ \dot{\beta}_0[rad] \\ \dot{\beta}_{1s}[rad] \\ \dot{\beta}_{1c}[rad] \\ X[m] \\ Y[m] \\ Z[m] \end{bmatrix} = \begin{bmatrix} 0 \\ 0 \\ 0 \\ 0 \\ 0 \\ 0 \\ 0.003516 \\ -0.000112 \\ 0 \\ 0.00011 \\ 0.001204 \\ 0.037341 \\ 0.00013 \\ 0.001236 \\ 0 \\ 0 \\ 0 \\ 0 \\ 0 \\ 0 \\ 30.48 \end{bmatrix} \tag{2.99}$$

2.5.1.2 Linearization Process

Linearization process is made according to small perturbation theory. Writing states and input variables as a perturbation value addition to trim value [35],

$$\begin{aligned} x &= x_{trim} + \Delta x \\ u &= u_{trim} + \Delta u \end{aligned} \tag{2.100}$$

where Δx and Δu are perturbation values. Then,

$$\dot{x} = f((x_{trim} + \Delta x), (u_{trim} + \Delta u), t) \tag{2.101}$$

For more compact form of the linearized system after neglecting second and higher order terms,

$$\begin{aligned}\dot{x}(t) &= f(x,u,t)\\ \dot{x}_{trim}+\Delta\dot{x}(t) &= f((x_{trim}+\Delta x(t)),(u_{trim}+\Delta u(t)),t)\\ &= f(x_{trim},u_{trim},t)+\frac{\partial f}{\partial x}\Big|_{\substack{x(t)=x_{trim}(t)\\u(t)=u_{trim}(t)}}\times\Delta x(t)+\frac{\partial f}{\partial u}\Big|_{\substack{x(t)=x_{trim}(t)\\u(t)=u_{trim}(t)}}\times\Delta u(t)\end{aligned} \tag{2.102}$$

Combining Equation 2.97 and Equation 2.102,

$$\Delta\dot{x}(t)=\frac{\partial f}{\partial x}\Big|_{\substack{x(t)=x_{trim}(t)\\u(t)=u_{trim}(t)}}\times\Delta x(t)+\frac{\partial f}{\partial u}\Big|_{\substack{x(t)=x_{trim}(t)\\u(t)=u_{trim}(t)}}\times\Delta u(t) \tag{2.103}$$

Finally, nonlinear system is linearized and state-space representation of the linear system is defined as,

$$\Delta\dot{x}(t)=A(t)\Delta x(t)+B(t)\Delta u(t) \tag{2.104}$$

where $A(t)=\frac{\partial f}{\partial x}\Big|_{\substack{x(t)=x_{trim}(t)\\u(t)=u_{trim}(t)}}$ and $B(t)=\frac{\partial f}{\partial u}\Big|_{\substack{x(t)=x_{trim}(t)\\u(t)=u_{trim}(t)}}$

$A(t)$ and $B(t)$ are the Jacobian Linearized matrices of the nonlinear system around specified trim condition. In order to obtain $A(t)$ and $B(t)$, MATLAB Linear Analysis Tool is used.

2.5.2 Order Reduction of Linearized Mathematical Model

After linearization, the next step to do with the model is the order reduction. For controller design purpose, lower order linear model is appropriate unless discarded model states do not affect the system characteristics. Eigenvalue analysis of the full order linear system and reduced order linear systems are required to make sure that general behavior of the systems are the same. There are two main types of model reduction: Truncation and Matched DC gain methods. For truncation method, states considered as to be eliminated are directly removed on the system matrix of the linear system since they are ineffective in system dynamics manner. Matched DC gain method is a model reduction method considering the effects of the eliminated states on remaining states of the system. In this method, time derivatives of the eliminated

states are taken as zero. First, consider a state vector to be partitioned to x_1 and x_2.

$$\begin{bmatrix} \dot{x}_1 \\ \dot{x}_2 \end{bmatrix} = \begin{bmatrix} A_{11} & A_{12} \\ A_{21} & A_{22} \end{bmatrix} \begin{bmatrix} x_1 \\ x_2 \end{bmatrix} + \begin{bmatrix} B_1 \\ B_2 \end{bmatrix} u \tag{2.105}$$

After taking the time derivative of x_2 as zero, reduced system dynamics are described as follows.

$$\dot{x}_1 = \left[A_{11} - A_{12}A_{22}^{-1}A_{21}\right]x_1 + \left[B_1 - A_{12}A_{22}^{-1}B_2\right]u \tag{2.106}$$

By looking the states of the full linear model, flapping angles and flapping rates are the states which are needed to be eliminated with Matched DC Gain method since they are faster dynamics than helicopter rigid body dynamics but they affect the general behavior at the least. Earth positions states are the eliminated states by truncation method. They do not have a role on system dynamics.

Consequently, there are three different models; nonlinear model, full order linear model at hover condition and reduced order linear model at hover condition. Eigenvalue comparison of reduced order model and the linear model of R-50 type helicopter in literature [28] are compared and can be found in Appendix C. As the last step of modeling part, different models obtained by linearization and model order reduction are tested by commanding step inputs of 1° to all channels. Comparison of the models is given in Figure 2.7.

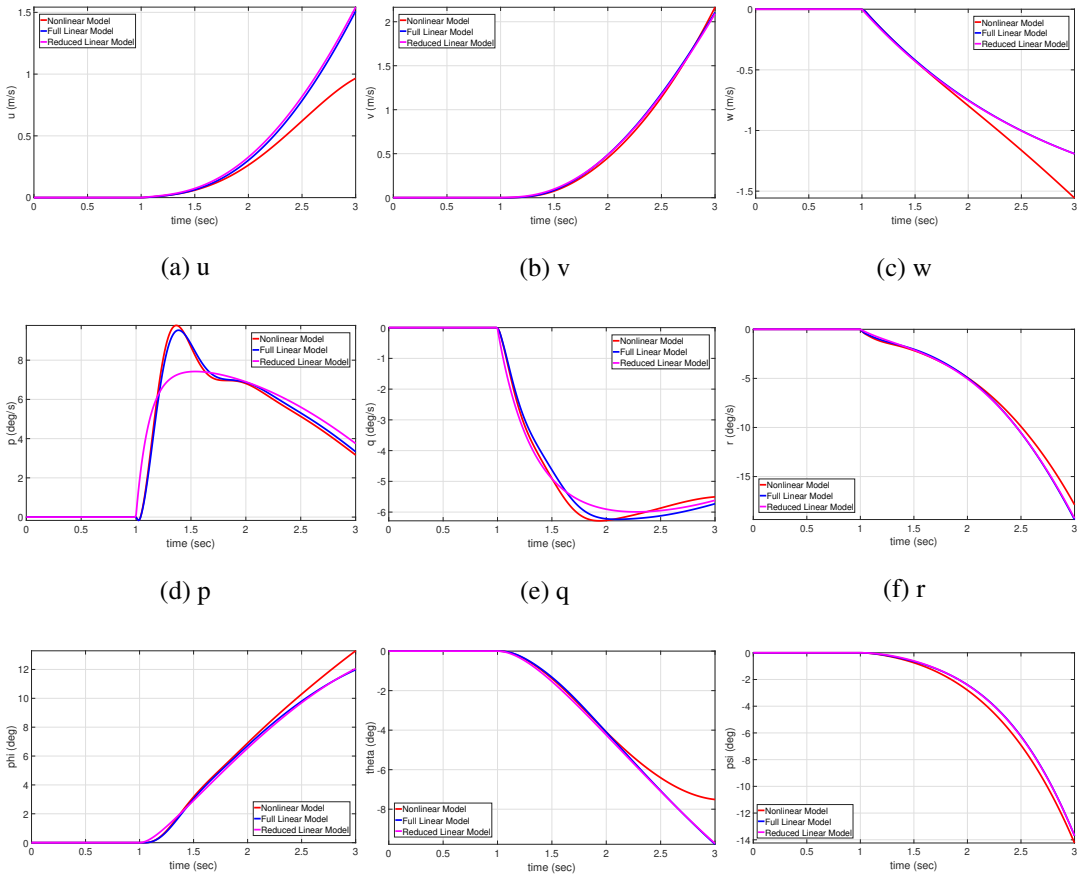

(a) u (b) v (c) w

(d) p (e) q (f) r

(g) phi (h) theta (i) psi

Figure 2.7: Comparison of Nonlinear Model, Full Order Linear Model and Reduced Order Linear Model Response

As seen in Figure 2.7, all models have similar response. Difference between linear model and nonlinear model is because of the getting far away the trim point of the linear model and this is expected result. Finally, it can be concluded that reduced order linear model can be used in controller design.

CHAPTER 3

MODEL REFERENCE ADAPTIVE CONTROL

In this chapter, MRAC design procedures are given for an uncertain MIMO system. The purpose of MRAC is to make the uncertain plant track the desired reference model [4]. Reference model design, deciding uncertainty parametrization method and weight update law are the main steps in controller design. Reference model is the desired system response and the plant should follow it in spite of uncertainties. Uncertainty parametrization is the component that is used to define and cancel out uncertainties. Lastly, weight update law is the estimation algorithm of controller gains required for adaptive control. For the nonadaptive baseline controller, any control method can be selected. Uncertain plant, reference model, baseline and MRAC controller are the total system to be considered and design scheme is given in Figure 3.1.

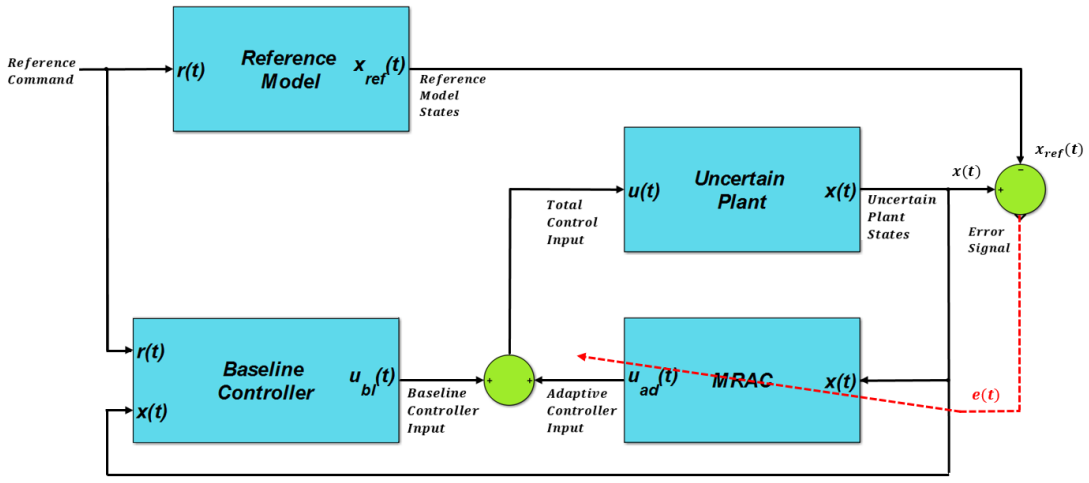

Figure 3.1: Augmentation of MRAC controller to baseline controller

3.1 Reference Model Design

The first part of designing MRAC controller is to decide the reference model to be tracked. This process can also be called as baseline controller design. The main property of this controller is that to make the actual system follow the reference model without any uncertainty and disturbance effects. This implies that there should not be any transient and steady state error between the reference model and closed loop dynamics with baseline controller. Another property of the baseline controller is having a feasible design and appropriate to be tested on the nonlinear mathematical model. Considering the baseline controller design specifications, Linear Quadratic Optimal Conroller with an Integrator is decided to be suitable for baseline controller design. First, consider a plant defined by [11],

$$\begin{aligned} \dot{x}_p(t) &= A_p x_p(t) + B_p u(t) \\ y_p(t) &= C_p x_p(t) \end{aligned} \tag{3.1}$$

Where $x_p(t) \in R^{n_p}$ is the plant state vector, $u(t) \in R^m$ is the control input signal, $y_p(t)$ is the plant output vector. $A_p \in R^{n_p x n_p}$, $B_p \in R^{n_p x m}$ and $C_p \in R^{n_p x n_p}$ are the system, input and output matrices of the plant, respectively.

The main aim of the controller is to find a control input signal such that the regulated plant output tracks the reference input command. The error between the plant regulated output and the reference input command is defined by,

$$e_y(t) = y(t) - r(t) = C_p x_p(t) - r(t) \tag{3.2}$$

In order to write it in a state space form, integral of output error is defined [11].

$$e_{yi}(t) = \int_0^t \Big(y(\tau) - r(\tau) \Big) d\tau = \frac{e_y(t)}{s} \tag{3.3}$$

Combining both equations, augmented system dynamics with output error can be represented with [11],

$$\begin{aligned} \dot{x}(t) &= \begin{bmatrix} e_y(t) \\ \dot{x}_p(t) \end{bmatrix} = \begin{bmatrix} 0_{m\times m} & C_p \\ 0_{n_p\times m} & A_p \end{bmatrix} \begin{bmatrix} e_{yi}(t) \\ x_p(t) \end{bmatrix} + \begin{bmatrix} 0_{m\times m} \\ B_p \end{bmatrix} u(t) + \begin{bmatrix} -I_{m\times m} \\ 0_{n_p\times m} \end{bmatrix} r(t) \\ y &= \begin{bmatrix} 0_{m\times m} & C_p \end{bmatrix} x(t) \end{aligned} \tag{3.4}$$

yields the extended open loop dynamics in the form of,

$$\begin{aligned} \dot{x}(t) &= Ax(t) + Bu(t) + B_{ref}r(t) \\ y(t) &= Cx(t) \end{aligned} \tag{3.5}$$

where $x(t) = \left[\begin{smallmatrix} e_{yi}(t) \\ x_p(t) \end{smallmatrix}\right] \in R^{n \times m}$ is the extended system state vector and corresponding state space matrices are defined by,

$$A = \begin{bmatrix} 0_{m\times m} & C_p \\ 0_{n_p\times m} & A_p \end{bmatrix}, \quad B = \begin{bmatrix} 0_{m\times m} \\ B_p \end{bmatrix}, \quad Bref = \begin{bmatrix} -I_{m\times m} \\ 0_{n_p\times m} \end{bmatrix}, \quad C = \begin{bmatrix} 0_{m\times m} & C_p \end{bmatrix} \tag{3.6}$$

Define the control input by LQR control law,

$$u(t) = -K_{lqr}x(t) \tag{3.7}$$

Where $K_{lqr} = R_{lqr}^{-1}B^T P_{lqr}$ and P_{lqr} is the solution of the associated Riccati Equation,

$$A^T P_{lqr} + P_{lqr}A - P_{lqr}BR_{lqr}^{-1}B^T P_{lqr} + Q_{lqr} = 0 \tag{3.8}$$

Where Q_{lqr} and R_{lqr} are the LQR controller state and input weight matrices, respectively.

Inserting Equation 3.7 to Equation 3.5,

$$\dot{x}(t) = \big(A - BK_{lqr}\big)x(t) + B_{ref}r(t) \tag{3.9}$$

This final form of the closed loop system is defined as a reference model to be followed by the actual system.

$$\dot{x}_{ref}(t) = A_{ref}x_{ref}(t) + B_{ref}r(t) \tag{3.10}$$

Then, matching condition is defined [11],

$$A_{ref} = A - BK_{lqr} \tag{3.11}$$

This completes the baseline controller design. Considering closed loop system performance and stability, reference model is designed by selecting appropriate weight matrices.

3.2 Model Reference Adaptive Control Design with Integral Action

The next part is to decide the controller structure and control law in order to keep the actual system tracks the reference model. Reference model is selected to be linear and without any uncertainty; therefore, the designed controller should need to cancel out uncertainties. Since these uncertainties on the system can be varying and mostly nonlinear, proposed controller is required to be also nonlinear. Model Reference Adaptive Control is considered as a suitable controller design technique for these purposes. The main idea of the controller is that while keeping baseline controller provides a reasonable tracking performance and stability, MRAC augmented controller structure gives the controller extra capability in uncertainty suppression manner.

First, consider an uncertain plant dynamics [11],

$$\begin{aligned} \dot{x}_p(t) &= A_p x_p(t) + B_p \Lambda\big(u(t) + f(x)\big) \\ y_p &= C_p x_p(t) \end{aligned} \tag{3.12}$$

Where $x_p \in R^{n_p}$ is the plant state vector, $u \in R^m$ is the control input signal, $r(t) \in R^m$ is the external bounded command signal, y_p is the regulated plant output vector. $A_p \in R^{n_p x n_p}$, $B_p \in R^{n_p x m}$ and $C_p \in R^{n_p x n_p}$ are the system, input and output matrices of the plant, respectively. $\Lambda \in R^{mxm}$ is the constant diagonal matrix which defines modeling errors or failures known as control effectiveness. Applying same approach with Section 3.1, augmented system dynamics is obtained.

$$\begin{aligned} \dot{x}(t) &= Ax(t) + B\Lambda\big(u(t) + f(x)\big) + B_{ref} r(t) \\ y &= Cx(t) \end{aligned} \tag{3.13}$$

Where $x(t) \in R^n$ is the augmented state vector, $u(t) \in R^m$ is the control input signal, $r(t) \in R^m$ is the external bounded command signal, $y(t)$ is the output vector. $A \in R^{nxn}$, $B \in R^{nxm}$ and $C \in R^{nxn}$ are the system, input and output matrices of the augmented system, respectively.

According to LQR control law described in Equation 3.7, baseline controller is selected [11].

$$u_{bl}(t) = -K_{lqr} x(t) = -K_{lqr} \begin{bmatrix} e_{yi}(t) \\ x_p(t) \end{bmatrix} = -K_i \frac{e_y(t)}{s} - K_p x_p(t) \tag{3.14}$$

where $K_{lqr} = \begin{bmatrix} K_i \\ K_p \end{bmatrix}$ is the baseline controller gain.

Assumption 1: $f(x) : R^n \rightarrow R^m$ is the matched uncertainty and each component of $f(x)$ can be represented in terms of locally Lipschitz continuous basis functions.

$$f(x) = W^T \beta(x) \tag{3.15}$$

Where $W \in R^{n_b xm}$ is the constant ideal weight matrix with unknown coefficients and $\beta(x) \in R^{n_b}$ is the vector of basis functions.

The controller objective is to design state feedback adaptive law to make the system tracks the predefined reference model in Equation 3.16 when there are parametric uncertainties Λ and $f(x)$.

$$\begin{aligned} \dot{x}_{ref} &= A_{ref} x_{ref}(t) + B_{ref} r(t) \\ y_{ref} &= C_{ref} x_{ref}(t) \end{aligned} \tag{3.16}$$

Where $x_{ref} \in R^n$ is the reference model state vector, y_{ref} is the reference model output vector. $A_{ref} \in R^{nxn}$, $B_{ref} \in R^{nxm}$ and $C_{ref} \in R^{nxn}$ are the system, input and output matrices of the reference model, respectively.

Assumption 2: Model matching condition is satisfied. There exists $K_1 \in R^{nxm}$ satisfying Equation 3.11 to given reference Hurwitz A_{ref} matrix .

Inserting model matching condition and Equation 3.16 into Equation 3.13,

$$\dot{x}(t) = A_{ref} x(t) + BK_{lqr} x + B\Lambda\big(u(t) + W^T \beta(x)\big) + B_{ref} r(t) \tag{3.17}$$

In order to satisfy controller tracking objective, define a control signal such that,

$$u(t) = u_{bl}(t) + u_{ad}(t) = -K_{lqr} x(t) + u_{ad}(t) \tag{3.18}$$

Then, closed loop system dynamics equation becomes,

$$\dot{x}(t) = A_{ref} x(t) + B\Lambda\big((I_{mxm} - \Lambda^{-1}) u_{bl}(t) + u_{ad}(t) + W^T \beta(x)\big) + B_{ref} r(t) \tag{3.19}$$

Alternatively, Equation 3.19 can be written in more compact form,

$$\dot{x}(t) = A_{ref} x(t) + B\Lambda\big(W^* \beta^*(x) + u_{ad}\big) + B_{ref} r(t) \tag{3.20}$$

where

$$\begin{aligned} W^* &= \begin{bmatrix} (I_{mxm} - \Lambda^{-1}) & W^T \end{bmatrix} \\ \beta^*(u_{bl}, x(t)) &= \begin{bmatrix} u_{bl} \\ \beta(x) \end{bmatrix} \end{aligned} \tag{3.21}$$

Since augmented system needs to be same dynamics with the reference model, adaptive component should be selected as [11],

$$u_{ad}(t) = -\hat{W}^{*^T}\beta^*(u_{bl}(t), x(t)) \tag{3.22}$$

Where $\hat{W}^* \in R^{n_b x m}$ is the unknown adaptive weight with unknown coefficients and $\beta^* \in R^{n_b}$ is the augmented vector of basis functions.

Inserting 3.22 into 3.20,

$$\begin{aligned} \dot{x}(t) &= A_{ref}x(t) + B\Lambda\left(W^*\beta^*(x) - \hat{W}^{*^T}\beta^*(u_{bl}(t), x(t))\right) + B_{ref}r(t) \\ &= A_{ref}x(t) + B\Lambda\tilde{W}\beta^*(u_{bl}(t), x(t)) + B_{ref}r(t) \end{aligned} \tag{3.23}$$

where $\tilde{W} = W^* - \hat{W}^*$ is the weight estimation error.

Defining a state tracking error and its time derivative,

$$\begin{aligned} e(t) &= x(t) - x_{ref}(t) \\ \dot{e}(t) &= \dot{x}(t) - \dot{x}_{ref}(t) \end{aligned} \tag{3.24}$$

Substituting closed loop system dynamics and reference model dynamics in Equation 3.23 and Equation 3.16 into 3.24

$$\begin{aligned} \dot{e}(t) &= \left(A_{ref}x(t) + B\Lambda\tilde{W}\beta^*(u_{bl}(t), x(t)) + B_{ref}r(t)\right) - \left(A_{ref}x_{ref}(t) + B_{ref}r(t)\right) \\ &= A_{ref}e(t) + B\Lambda\tilde{W}\beta^*(u_{bl}(t), x(t)) \end{aligned} \tag{3.25}$$

Then, in order to derive adaptive law and ensure that the closed loop stability, choose a Lyapunov function candidate such that,

$$V(e(t), \tilde{W}) = e^T Pe + tr(\tilde{W}^T\Gamma^{-1}\tilde{W}\Lambda) \tag{3.26}$$

The Lyapunov function candidate is selected as a radially unbounded one in quadratic form. $\Gamma = \Gamma^T > 0$ is the adaptive learning rate and $P \in R^{nxn}$ is the symmetric positive definite solution of the Lyapunov equation,

$$A_{ref}P + PA_{ref} = -Q \tag{3.27}$$

Also note that there exists unique $P \in R^{nxn}$ for every $Q \in R^{nxn}$ since A_{ref} is Hurwitz. Taking time derivative of Equation 3.26 along trajectories of Equation 3.25 [11],

$$\dot{V}(e(t), \tilde{W}) = -e^T Qe - 2e^T PB\Lambda\tilde{W}^T\beta^* + 2tr(\tilde{W}^T\Gamma^{-1}\dot{\hat{W}}^*\Lambda) \tag{3.28}$$

Using vector trace identity $\left(A^T B = tr(BA^T)\right)$, Equation 3.28 becomes,

$$\dot{V}(e(t),\tilde{W}) = -e^T Qe + 2tr\left(\tilde{W}^T\left(\Gamma^{-1}\dot{\hat{W}}^* - \beta^* e^T PB\right)\Lambda\right) \tag{3.29}$$

In order to satisfy that Lyapunov stability condition $\dot{V}(e(t),\tilde{W}) = -e^T Qe <= 0$, adaptive weight update law is selected in the form [4],

$$\dot{\hat{W}}^* = \Gamma\beta^* e^T PB \tag{3.30}$$

which completes the proof of uniform ultimate boundedness of $\left(e(t),\tilde{W}\right)$.

Consequently, Equation 3.30 is the well known classical adaptive control law and it guarantees that state tracking error $e(t) \to 0$ as $t \to \infty$. In addition, since Lyapunov candidate function is radially unbounded, the closed loop state tracking error dynamics are globally asymptotically stable. Similarly, output tracking error is defined,

$$\begin{aligned} e_y(t) &= y(t) - y_{ref}(t) = C(x(t) - x_{ref}(t)) = Ce(t) \\ \Rightarrow \lim_{t\to\infty} e_y(t) &= \lim_{t\to\infty} Ce(t) = 0 \end{aligned} \tag{3.31}$$

This concludes that for any bounded reference command, output of the closed loop system tracks the output of reference model, that is $e_y(t) \to 0$ as $t \to \infty$.

Substituting Equation 3.21 into Equation 3.30 and defining $\Gamma = \begin{bmatrix} \Gamma_{bl} & 0_{nxm} \\ 0_{n_b xm} & \Gamma_x \end{bmatrix}$,

$$\begin{bmatrix} \dot{\hat{K}}_{u_{bl}} \\ \dot{\hat{W}} \end{bmatrix} = \begin{bmatrix} \Gamma_{bl} & 0_{nxm} \\ 0_{n_b xm} & \Gamma_x \end{bmatrix} \begin{bmatrix} u_{bl} \\ \beta(x) \end{bmatrix} e^T PB \tag{3.32}$$

where $K_{u_{bl}} = (I_{mxm} - \Lambda^{-1})$ and $\hat{K}_{u_{bl}}$ is the estimation of $K_{u_{bl}}$.

Arranging Equation 3.32, final form of the adaptive law is obtained [11].

$$\begin{aligned} \dot{\hat{K}}_{u_{bl}} &= \Gamma_{bl} u_{bl} e^T PB \\ \dot{\hat{W}} &= \Gamma_x \beta(x) e^T PB \end{aligned} \tag{3.33}$$

Rewriting control law of the MRAC with integral connection,

$$\begin{aligned} u(t) &= u_{bl}(t) + u_{ad}(t) \\ &= -K_{bl} x(t) + \hat{K}_{u_{bl}} u_{bl}(t) + \hat{W}\beta(x) \end{aligned} \tag{3.34}$$

Equation 3.34 is the total control law of the closed loop system including baseline control input of LQR with integrator and augmented control input of MRAC controller. K_{bl} is the optimal controller gain calculated by LQR method and $\hat{K}_{bl}$ and $\hat{W}$ are the adaptive weights required to be estimated by adaptive laws in Equation 3.33. Initial values of the adaptive weights can be chosen arbitrarily.

3.3 MRAC Modifications

In Section 3.2, classical adaptive control law is derived for the augmented system. It is assumed that there is not any external disturbance and uncertainty on the system can be linearly parametrized. When there exists bounded external disturbances on the system, augmented system dynamics is written as [11],

$$\begin{aligned} \dot{x}(t) &= Ax(t) + B\Lambda\big(u(t) + f(x)\big) + B_{ref}r(t) + \zeta(t) \\ y &= Cx(t) \end{aligned} \tag{3.35}$$

where $\zeta(t)$ is the bounded external disturbances such that,

$$\|\zeta(t)\| \leq \zeta_{max}, \qquad where \quad \zeta_{max} \geq 0 \tag{3.36}$$

State error dynamics is updated as,

$$\dot{e}(t) = A_{ref}e(t) + B\Lambda\tilde{W}\beta^*(u_{bl}(t), x(t)) + \zeta_(t) \tag{3.37}$$

Choosing the same Lyapunov function candidate in Equation 3.26 and taking time derivative of it,

$$V(e(t), \tilde{W}) = e^T Pe + tr(\tilde{W}^T\Gamma^{-1}\tilde{W}\Lambda) \tag{3.38}$$

$$\dot{V}(e(t), \tilde{W}) = -e^T Qe + 2tr\big(\tilde{W}^T\big(\Gamma^{-1}\dot{\hat{W}}^* - \beta^* e^T PB\big)\Lambda\big) + 2e^T P\zeta_(t) \tag{3.39}$$

Assuming classical adaptive law in Equation 3.30 holds,

$$\dot{V}(e(t), \tilde{W}) = -e^T Qe + 2e^T P\zeta_(t) \leq -\lambda_{Q_{min}}\|e\|^2 + 2\|e\|\lambda_{P_{max}}\zeta_{max} \tag{3.40}$$

yields,

$\dot{V}(e(t), \tilde{W}) < 0$ in the outside of the set [11],

$$R_0 = \left\{(e(t), \tilde{W}) : \|e\| \leq 2\frac{\lambda_{P_{max}}}{\lambda_{Q_{min}}}\zeta_{max} = e_0\right\} \tag{3.41}$$

State error dynamics $e(t)$ trajectories are in the compact set Ω_0 in R_0, however, Ω_0 is unbounded since there is no limitation in estimating adaptive parameters. In other words, $\tilde{W}$ is not restricted in any region. Thus, $\dot{V}(e(t), \tilde{W})$ can be positive inside the compact set Ω_0. This makes adaptive parameter diverges and unbounded even if state error norm remains bounded. Consequently, classical adaptive law losses its

robustness with $\zeta(t)$. This problem is known as *parameter drift* in the literature. In order to keep robustness, some modifications can be done in the controller and adaptive law design.

3.3.1 Adaptive Weight Update Law Modifications

Weight update law is one of the most significant part in model reference adaptive controller design. In order to improve performance and robustness of the system with classical adaptive control law in Equation 3.30, some modifications are presented as solution. In adaptive control literature, while sigma-modification, e-modification and dead-zone modification are the modifications by adding extra damping term to the classical adaptive law, projection operator is the modification with a special mathematical operator.

3.3.1.1 Projection Operator

Projection operator aims restricting adaptive weight in a predefined bounded and convex set. This idea is required for sustaining robustness to parametric and nonparametric uncertainties.

Defining two convex sets

$$\begin{aligned} \Omega_0 &= \left\{ W \in R^n : f(W) \leq 0 \right\} = \left\{ W \in R^n : \|W\|_2 \leq \frac{W_{max}}{\sqrt{1+\varepsilon_0}} \right\} \\ \Omega_1 &= \left\{ W \in R^n : f(W) \leq 1 \right\} = \left\{ W \in R^n : \|W\|_2 \leq W_{max} \right\} \end{aligned} \tag{3.42}$$

Note that $\Omega_0 \subset \Omega_1$. Then, projection operator is defined by [20],

$$Proj(W,y) = \begin{cases} y - \frac{\Gamma \nabla f(W)(\nabla f(W))^T}{(\nabla f(W))^T \Gamma \nabla f(W)}, & \text{if} \quad f(W) > 0 \quad \text{and} \quad y^T \nabla f(W) > 0 \\ y, & \text{otherwise} \end{cases} \tag{3.43}$$

where $y \in R^n$ and $\Gamma \in R^{nxn}$ is a constant symmetric positive definite matrix and $\nabla f(W) = \frac{2(1+\varepsilon_0)}{\varepsilon_0 W_{max}^2} W$.

Projection operator ensures that all adaptive weights remain in a compact set for all $t \geq 0$. Adaptive law with projection operator is defined by,

$$\dot{\hat{W}}^* = Proj(\hat{W}^*, \Gamma \beta^* e^T PB) \tag{3.44}$$

3.3.1.2 Dead-Zone Modification

The main idea of dead-zone modification, first proposed by Peterson and Narendra [38], is to disable adaptation process when state tracking error norm becomes smaller relative to predefined error norm in order to maintain robustness. Adaptive law with dead-zone modification is described by,

$$\dot{\hat{W}}^* = \begin{cases} \Gamma\beta^* e^T PB, & \text{if } \|e\| > e_0 \\ 0, & \text{if } \|e\| \leq 0 \end{cases} \tag{3.45}$$

Although dead-zone modification provides uniform ultimate boundedness of $\tilde{W}$, it has some drawbacks in design and performance. One of them is the requirement of having information of the upper error norm bound so that e_0 is properly selected considering upper bounds of $e(t)$. The second drawback is chattering problem around $\|e\| = 0$. Although uniform ultimate boundedness is achieved, asymptotic stability is not proved at $\|e\| = 0$. Chattering problem can be solved by using smooth dead-zone modification first presented by Slotine and Coetsee [10]. Adaptive law with smooth dead-zone modification is described by,

$$\dot{\hat{W}}^* = \Gamma\beta^* \mu(\|e\|) e^T PB \tag{3.46}$$

where $\|e\| = max\big(0, min(1, \frac{\|e\|-\delta e_0}{(1-\delta)e_0})\big)$

3.3.1.3 Sigma Modification

The main objective of sigma modification first proposed by Ioannou and Kokotovic [15], is to add extra damping to adaptive law. This damping term tries to decrease adaptive weights when they become large. Adaptive law with sigma modification is described by,

$$\dot{\hat{W}}^* = \Gamma\beta^* e^T PB - \Gamma\sigma\hat{W}^* \tag{3.47}$$

Where $\sigma \geq 0$ is the modification term which increases damping of the adaptive law. Although sigma modification does not require the knowledge of upper bounds of error norm, extra damping term can be overconservative and costly in controller design especially when error norm is around zero. This is the most known disadvantage of sigma modification.

3.3.1.4 e-Modification

Another method to overcome with drawbacks of sigma modification is using e-modification in adaptive law. The main idea behind e-modification, firstly presented by Narendra and Annaswamy [29], is replacing constant damping term with a linear combination of the error. This solves the problem of undesired effects around $\|e\| = 0$. Adaptive law with e-modification is described by,

$$\dot{\hat{W}}^* = \Gamma \beta^* e^T PB - \Gamma \mu \|e^T PB\| \hat{W}^* \tag{3.48}$$

Where $\mu \geq 0$ is the modification term which increases damping of the adaptive law in terms of state tracking error norm.

3.4 Uncertainty Parametrization Methods

Another important part of the model reference adaptive controller design is uncertainty parametrization. In order to parametrize unstructured uncertainties, universal approximators can be used. The main idea behind using them in MRAC design is that every uncertain function can be represented with a universal approximator. Sigmoid Functions are one of the most used functions in adaptive control problems [32]. Although they are not common as Sigmoid Functions, Fourier Series Expansion and Chebyshev Orthogonal Polynomials are used in literature [13, 34].

$$f(x) = W^T \beta(x,t) + \varepsilon \tag{3.49}$$

Where $\beta(x,t)$ is the regression vector of the uncertainty parametrization method, W is the corresponding adaptive weights and ε is the approximation error.

Regression vectors depend on the uncertainty parametrization methods described in the following part of this section. Three different basis functions are considered as a regression vector. There are some advantages and disadvantages of each basis function and each one is described and evaluated.

3.4.1 Sigmoid Functions

Sigmoid functions are specific kind of mathematical functions in the form of S-shaped. Equilibrium point is $\beta_i(0) = 0$ and sigmoid functions are defined in the range of $-1 \leq \beta_i(x,t) \leq 1$ for $x \in (-\infty, \infty)$. Main advantage of sigmoid functions are that they are bounded, monotonic and differentiable at every $x(t)$. Detailed information about sigmoid functions can be found in [9]. Regression vector of Sigmoid Functions are formed as,

$$\beta(x,t) = \begin{bmatrix} 1 \\ \beta_1(x,t) \\ \beta_2(x,t) \\ \vdots \\ \beta_{n-1}(x,t) \\ \beta_n(x,t) \end{bmatrix} \tag{3.50}$$

Where $i = 1,2,\ldots,n$ and $\beta_i(x,t) = \frac{1-e^{-x_i(t)}}{1+e^{-x_i(t)}}$. Note that function length n is the only one design parameters for Sigmoid Functions.

3.4.2 Fourier Series Transform

Fourier Series is a combination of trigonometric and periodic functions. Thus, when the uncertainty on the system is periodic and unknown, these special form of series can be advantageous to use. There are two parameters of Fourier series; series length and period. Fourier Series length is the parameter to be selected by designer and period should be at least three times higher than simulation time. Proof of using Fourier Series in MRAC can be found in [13]. Regression vector of Fourier Series

Transform are formed as,

$$\beta(x,t) = \begin{bmatrix} 1 \\ \beta_{c1}(x,t) \\ \beta_{c2}(x,t) \\ \vdots \\ \beta_{cN}(x,t) \\ \beta_{s1}(x,t) \\ \beta_{s2}(x,t) \\ \vdots \\ \beta_{sN}(x,t) \end{bmatrix} \tag{3.51}$$

where $i = 1,2,\ldots,N$, $\beta_{ci}(x,t) = \cos(i\frac{2\pi}{T}t)$ and $\beta_{si}(x,t) = \sin(i\frac{2\pi}{T}t)$. Series length N and series period T are the design parameters for Fourier Series Transform.

3.4.3 Chebyshev Polynomials

Another universal approximators to parametrize uncertainty is Chebyshev Polynomials. The main properties of Chebyshev Polynomials are being orthogonal in the interval of $x(t) \in (-1,1)$ with respect to weight function $w(x) = 1/\sqrt{1-x^2}$. Restricting $x(t)$ to required interval is done by simple trigonometric transform, $x = \cos(t)$ where t stands for time. Then, it can be said that Chebyshev polynomials length is the only parameter to be decided in design. Proof of using Chebyshev Polynomials in MRAC can be found in [34]. Regression vector of Chebyshev Polynomials are formed as,

$$\beta(x,t) = \begin{bmatrix} T_0(x,t) \\ T_1(x,t) \\ \vdots \\ T_{N-1}(x,t) \\ T_N(x,t) \end{bmatrix} \tag{3.52}$$

where

$$T_0(x,t) = 1$$

$$T_1(x,t) = x$$

$$\vdots$$

$$T_{i+1}(x,t) = 2xT_i(x,t) - T_{i-1}(x,t)$$

where $i = 1,2,\ldots,n$. Only the series length N is the design parameters for using Chebyshev Polynomials.

This completes the describing methodology of the controller design. Deciding design parameters, tuning controller weights and other controller design and implementation parts will be given in Chapter 4.

CHAPTER 4

RESULTS AND DISCUSSIONS

4.1 Implementation of the Controllers

In Section 2.5, mathematical model inputs, states and outputs are described. Considering whole system, nonlinear helicopter model is implemented on Matlab/Simulink environment. There is also a need of a linear model for model reference adaptive control design since reference model is going to be a linear one. For ease of control design purpose, reference model outputs are selected as only translational velocities, angular velocities and Euler Angles. Therefore, open loop helicopter model needs to be reduced according to reference model states and outputs. Reduced order linear model described in Equation 2.106 is used for this purpose. Reduced order system has four inputs, nine states and four outputs. Firstly, Linear Quadratic Controller with an Integral action (LQI Controller) is designed for reduced order linear model. Then, open loop system is controlled with LQI controller and it is shown that matching condition in Equation 3.11 is hold and reduced order linear model and reference model have exactly same response. However, when there is an external disturbance of the system, this type of controller does not provide a reasonable tracking performance to reference model. Next, LQI controller is implemented to nonlinear helicopter model and it is seen that response with the external disturbance is same with the linear one. Because external disturbances may be mostly nonlinear and helicopter mathematical model is also nonlinear, there is a need of nonlinear controller which can overcome nonlinear disturbances. When there is not a disturbance on the system, designed controller should not play a big role on the system since LQI controller is already designed as a baseline/nominal controller. Considering these control design purposes, Model Reference Adaptive Controller seems suitable for both linear and nonlinear

systems. After deciding the control design method, the next step is implementation of the controller to linear and nonlinear helicopter models. The main difference of them is initial condition. While initial condition of the linear model is always zero for both inputs and states, nonlinear model inputs and states initial conditions are defined by trimming results described in Section 2.5.1. The other difference is the rate limiting functions at the inputs of the helicopter. These rate limiters have 8 deg/s cut-off frequency. The next step is analyzing LQI-MRAC controller on the nonlinear helicopter model. When there is not any external disturbance on the system, adaptive controller contribution to the helicopter inputs is inconsiderable and source of this input is the numerical errors during order reduction to obtain reduced order model, linearization error and numerical errors by the solver which is Runge-Kutta 4th Order Method. In addition to these uncertainties on the system, the helicopter model is disturbed externally. In the first MRAC design attempt, Sigmoid Functions are used in the uncertainty parametrization and classical MRAC adaptive law without any modification is used. Although tracking performance is not unacceptable as much as the system only with baseline controller, there are some performance related problems especially in transient part of the response of MRAC augmented LQI controller. Finally, it is decided that some modifications are implemented to the MRAC controller and their effects are analyzed on the nonlinear helicopter model.

4.2 Results

In this part, main design tasks and their results are presented. These are reference model design, LQI and MRAC controllers design, modifications on MRAC controller and further studies with modified MRAC, respectively.

4.2.1 Reference Model

Reference model is designed such that there will not be any transient and steady state error between the closed loop system with baseline controller and reference model to be followed. Baseline controller method is selected to be LQR Controller with an integrator (LQI). Outputs to be followed is chosen as to be pitch angle, roll angle,

vertical velocity and yaw angle of the helicopter. LQI weight matrices are tuned as:

$$Q_{lqr} = \begin{bmatrix} 500 & 0 & 0 & 0 & 0 & 0 & 0 & 0 & 0 & 0 & 0 & 0 \\ 0 & 500 & 0 & 0 & 0 & 0 & 0 & 0 & 0 & 0 & 0 & 0 \\ 0 & 0 & 5 & 0 & 0 & 0 & 0 & 0 & 0 & 0 & 0 & 0 \\ 0 & 0 & 0 & 5000 & 0 & 0 & 0 & 0 & 0 & 0 & 0 & 0 \\ 0 & 0 & 0 & 0 & 0 & 0 & 0 & 0 & 0 & 0 & 0 & 0 \\ 0 & 0 & 0 & 0 & 0 & 0 & 0 & 0 & 0 & 0 & 0 & 0 \\ 0 & 0 & 0 & 0 & 0 & 0 & 30 & 0 & 0 & 0 & 0 & 0 \\ 0 & 0 & 0 & 0 & 0 & 0 & 0 & 10 & 0 & 0 & 0 & 0 \\ 0 & 0 & 0 & 0 & 0 & 0 & 0 & 0 & 10 & 0 & 0 & 0 \\ 0 & 0 & 0 & 0 & 0 & 0 & 0 & 0 & 0 & 500 & 0 & 0 \\ 0 & 0 & 0 & 0 & 0 & 0 & 0 & 0 & 0 & 0 & 500 & 0 \\ 0 & 0 & 0 & 0 & 0 & 0 & 0 & 0 & 0 & 0 & 0 & 1000 \end{bmatrix}, \quad R_{lqr} = 1000 \times \begin{bmatrix} 1 & 0 & 0 & 0 \\ 0 & 1 & 0 & 0 \\ 0 & 0 & 0.1 & 0 \\ 0 & 0 & 0 & 0.01 \end{bmatrix} \tag{4.1}$$

Reference model is designed such that,

$$\dot{x}_{ref}(t) = A_{ref}x_{ref}(t) + B_{ref}r(t) \tag{4.2}$$

Main criteria in tuning controller weight matrices are settling time, steady state error and controller effort. Using matching condition, reference model is designed with an appropriate tracking performance. Step response of the reference model is shown in Figure 4.1.

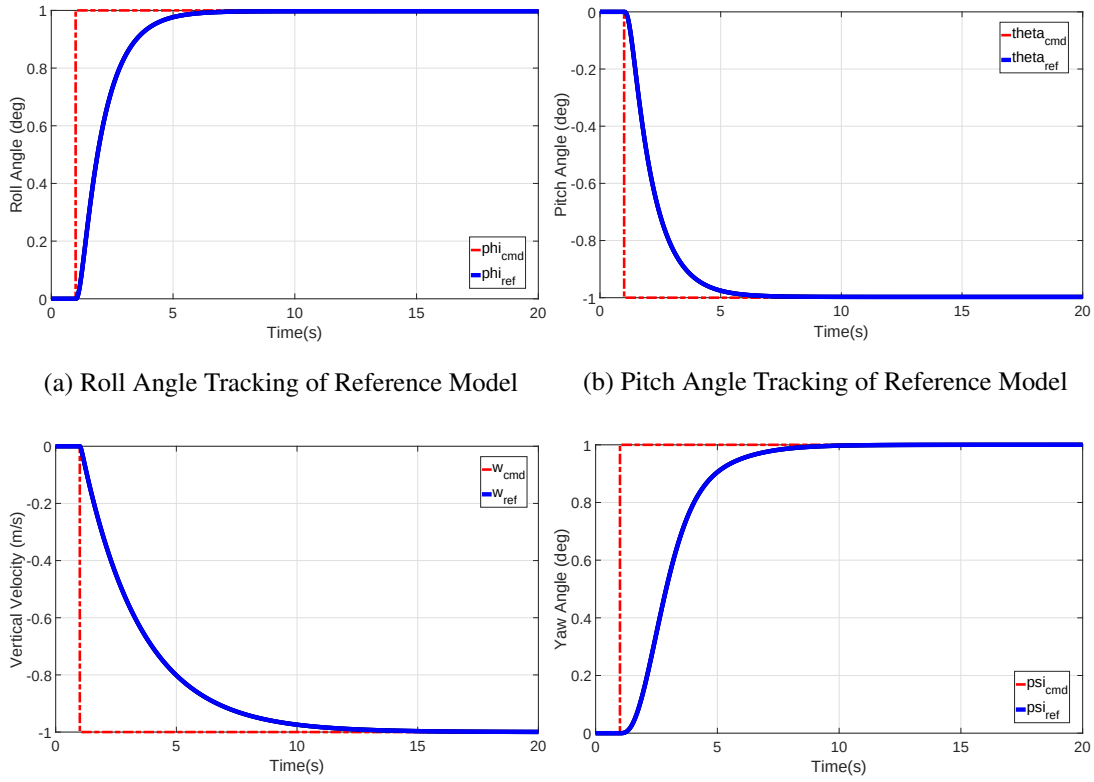

(a) Roll Angle Tracking of Reference Model

(b) Pitch Angle Tracking of Reference Model

(c) Vertical Vel. Tracking of Reference Model

(d) Yaw Angle Tracking of Reference Model

Figure 4.1: Reference Model Response to Step Command

4.2.2 LQI and MRAC Controllers

In this section, LQI and MRAC controllers are designed and compared. First, LQI controller is implemented to the open loop linear and nonlinear helicopter models. After ensuring that there are not any transient and steady state error between reference model and closed loop systems, MRAC controller is designed and implemented. For the basis function in uncertainty parametrization component, Sigmoid Functions are used since it is the most commonly used one in the literature. Then, step responses of systems with these controllers are plotted and compared. MRAC parameters are chosen and tuned as,

$$\begin{aligned} \Gamma &= diag(0.5, 0.5, 0.05, 1, 0, 0, 0.1, 100, 100, 100, 1000, 1000, 100) \\ Q &= diag(10, 10, 10, 10, 0.1, 0.1, 0.01, 0, 01, 0.01, 0.1, 0.05, 0.05, 0.1) \\ \beta(x,t) &= \begin{bmatrix} 1 & \beta_1(x,t) & \beta_2(x,t) & \dots & \beta_8(x,t) & \beta_9(x,t) \end{bmatrix}^T \end{aligned} \tag{4.3}$$

where $\beta_i(x,t) = \frac{1-e^{-x_i(t)}}{1+e^{-x_i(t)}}$ and $i = 1, 2, \dots, 9$.

4.2.2.1 Without External Disturbance

In the absence of external disturbance and noise on the system, it is expected that both controllers show almost same behavior on the linear system. The reason is that MRAC controller does not create a significant adaptive inputs to the system when there is not any uncertainty on the system. However, for nonlinear case, there can be internal uncertainties on the system caused by linearization, trimming and numerical calculations during simulation. For this case, MRAC create adaptive inputs to the system in order to keep tracking the reference model. Linear model step responses under different controllers are shown in Figure 4.2 without any external disturbance and noise to the system.

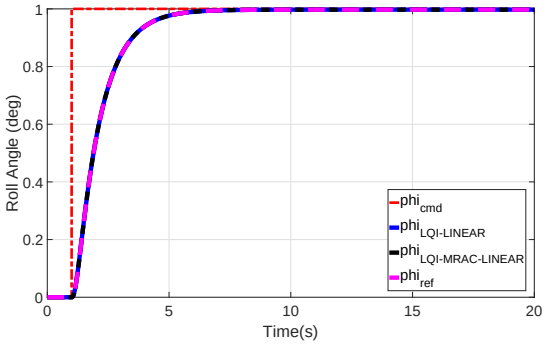

(a) Roll Angle Tracking of LQI and LQI-MRAC

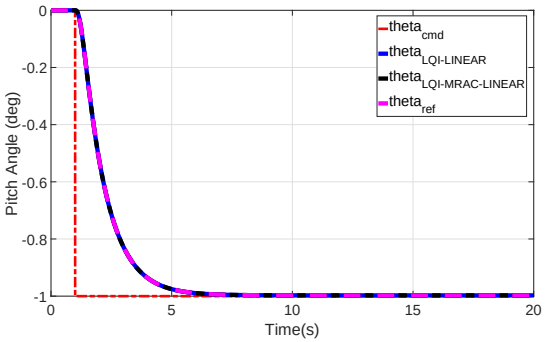

(b) Pitch Angle Tracking of LQI and LQI-MRAC

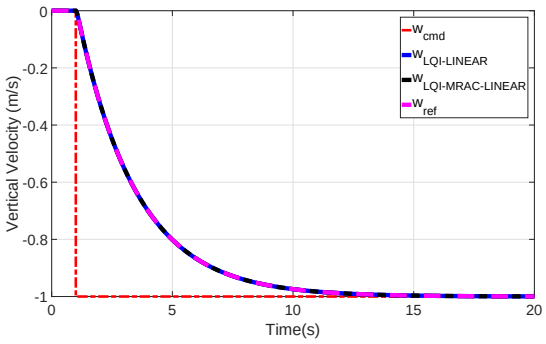

(c) Vertical Vel. Tracking LQI and LQI-MRAC

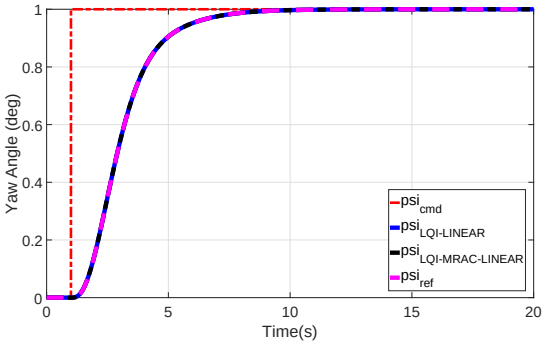

(d) Yaw Angle Tracking of LQI and LQI-MRAC

Figure 4.2: Linear Model Response with LQI and LQI-MRAC to Step Command

On the hand, executing same procedure for the nonlinear system,

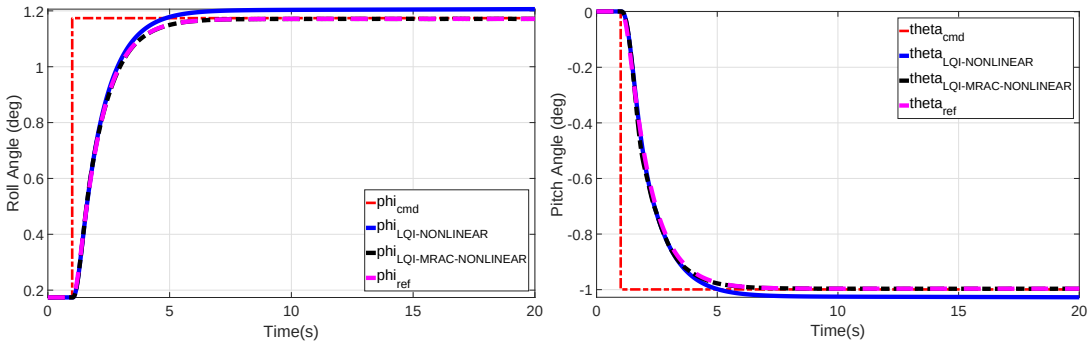

(a) Roll Angle Tracking of LQI and LQI-MRAC (b) Pitch Angle Tracking of LQI and LQI-MRAC

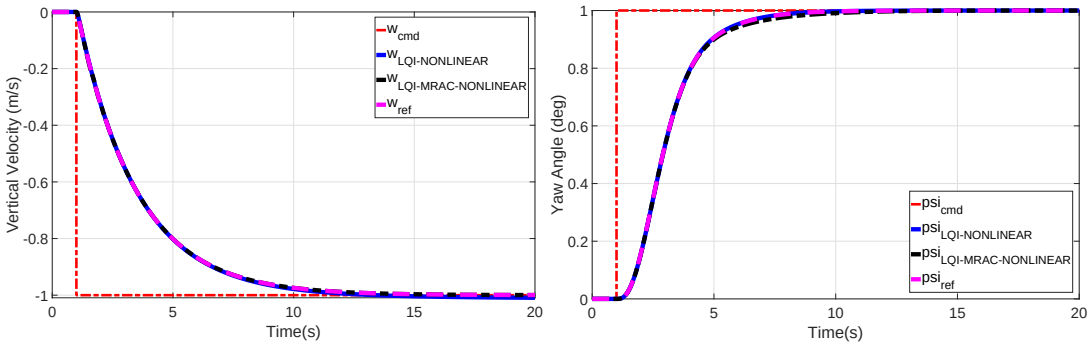

(c) Vertical Vel. Tracking LQI and LQI-MRAC (d) Yaw Angle Tracking of LQI and LQI-MRAC

Figure 4.3: Nonlinear Model Response with LQI and LQI-MRAC to Step Command

As seen in Figure 4.2 and Figure 4.3, MRAC augmented LQI controller counteracts the trimming, linearization and numerical errors and keeps tracking the reference model with zero steady state error. For the nonlinear system, LQI controller could not make steady state error zero in 20 seconds. Adaptive inputs that MRAC controller creates are effective in this manner and these adaptive inputs can be seen and compared with linear case in the following figure.

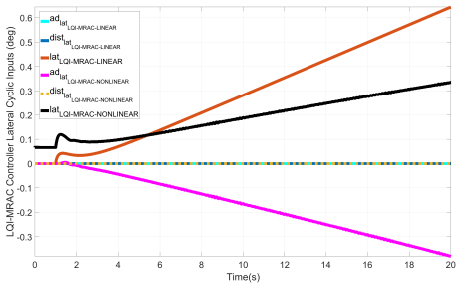

(a) Lateral Cyclic Inputs of Linear and Nonlinear LQI and LQI-MRAC Controller

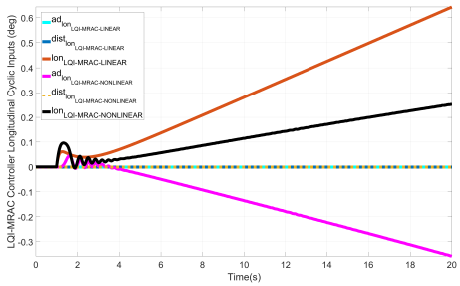

(b) Longitudinal Cyclic Inputs of Linear and Nonlinear LQI and LQI-MRAC Controller

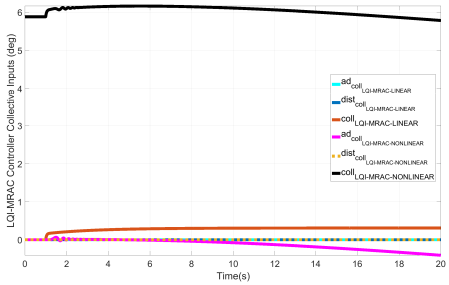

(c) Collective Inputs of Linear and Nonlinear LQI and LQI-MRAC Controller

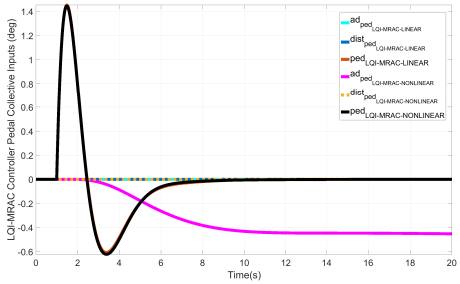

(d) Pedal Collective Inputs of Linear and Nonlinear LQI and LQI-MRAC Controller

Figure 4.4: Inputs of Linear and Nonlinear LQI and LQI-MRAC Controller

For the following simulation results, only nonlinear model responses will be shown since nonlinear model is more challenging than linear model in terms of uncertainties and responses to external disturbances.

4.2.2.2 With External Disturbance

In the presence of external disturbance on the system, adaptive controller is more effective. In addition to linearization and trimming errors, high amount of uncertainty is applied to the inputs and it is expected that controller retains the helicopter in reference model response. Three types of external disturbance are considered. The first one is constant disturbance. This type of uncertainty may be a crosswind. The second one is sinusoidal disturbance and turbulence can be an example for this. The last one is random external disturbance selected as a high order nonlinear function.

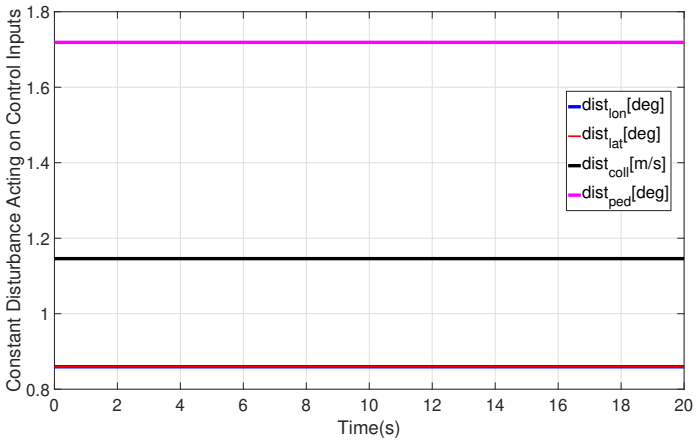

Figure 4.5: Constant Disturbance Acting on the System for Different Axis

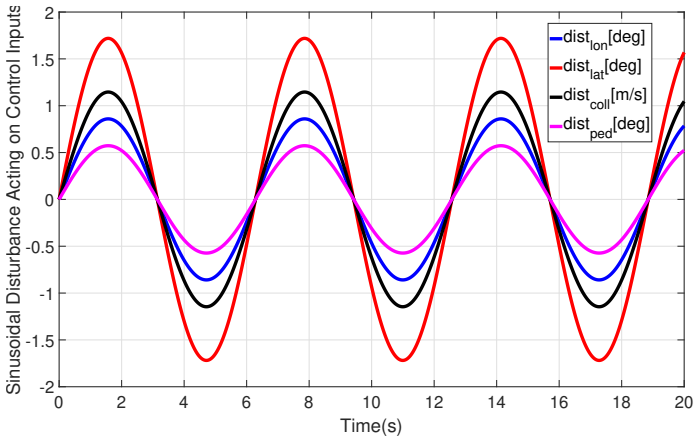

Figure 4.6: Sinusoidal Disturbance Acting on the System for Different Axis

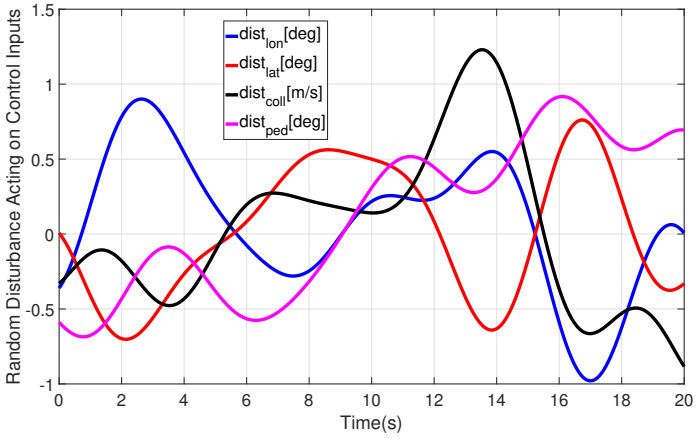

Figure 4.7: Random Disturbance Acting on the System for Different Axis

Constant External Disturbance: First, constant external disturbance is applied to the system. Projection operator and e-modification is used in MRAC controller and modification terms effects are shown in the same plot. Response of the helicopter is as follows:

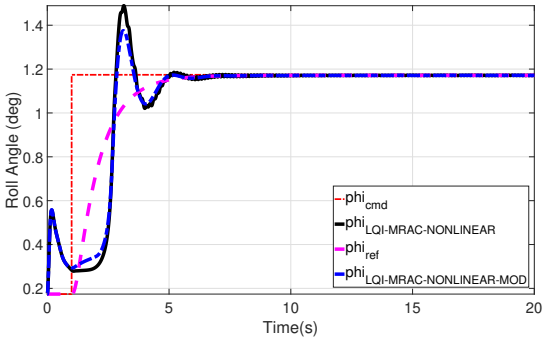

(a) Roll Angle Tracking of LQI and LQI-MRAC with Constant Dist.

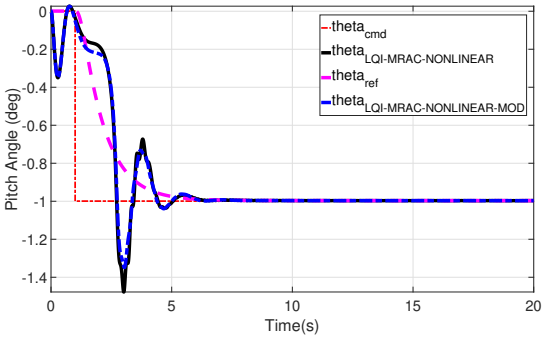

(b) Pitch Angle Tracking of LQI and LQI-MRAC with Constant Dist.

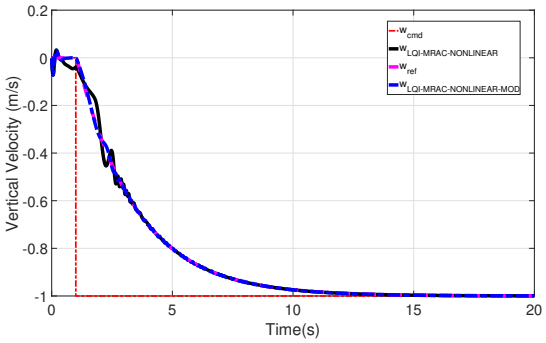

(c) Vertical Velocity Tracking LQI and LQI-MRAC with Constant Dist.

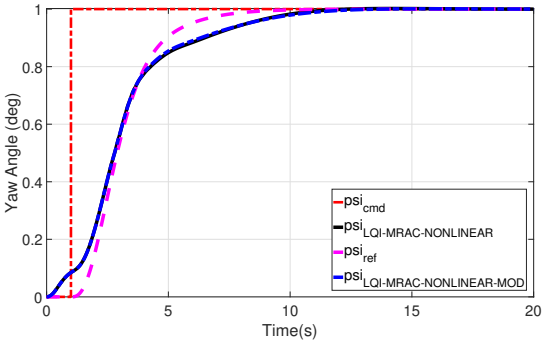

(d) Yaw Angle Tracking of LQI and LQI-MRAC with Constant Dist.

Figure 4.8: LQI-MRAC Controller Response with Constant Dist. to Step Command with and without Adaptive Law Modifications

Uncertainty exists on the system at the beginning of the simulation. As seen in Figure 4.8, LQI-MRAC controller removes the effect of uncertainty at the end of the simulation and keeps tracking the reference model. Although there are some oscillations in transient region, proposed controller successfully removes steady state error. In order to examine the effectiveness of the controller, uncertainty amount is kept high and this is the reason for the error in transient region. Modification term effects are seen in steady state region and they decrease control effort and overshoot.

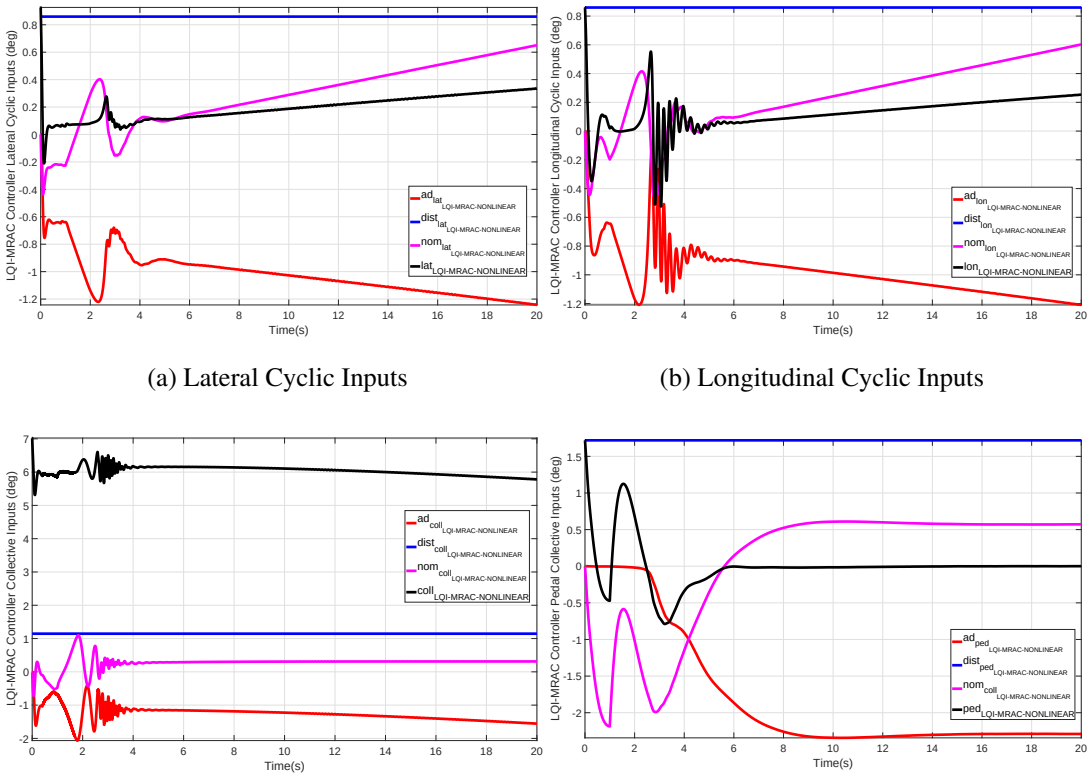

(a) Lateral Cyclic Inputs

(b) Longitudinal Cyclic Inputs

(c) Collective Inputs

(d) Pedal Collective Inputs

Figure 4.9: Inputs of LQI-MRAC Controller with Constant Dist. to Step Command

In Figure 4.9, different types of inputs acting on the helicopter are shown. It can be clearly seen that adaptive inputs are against to the disturbance on the relevant channel.

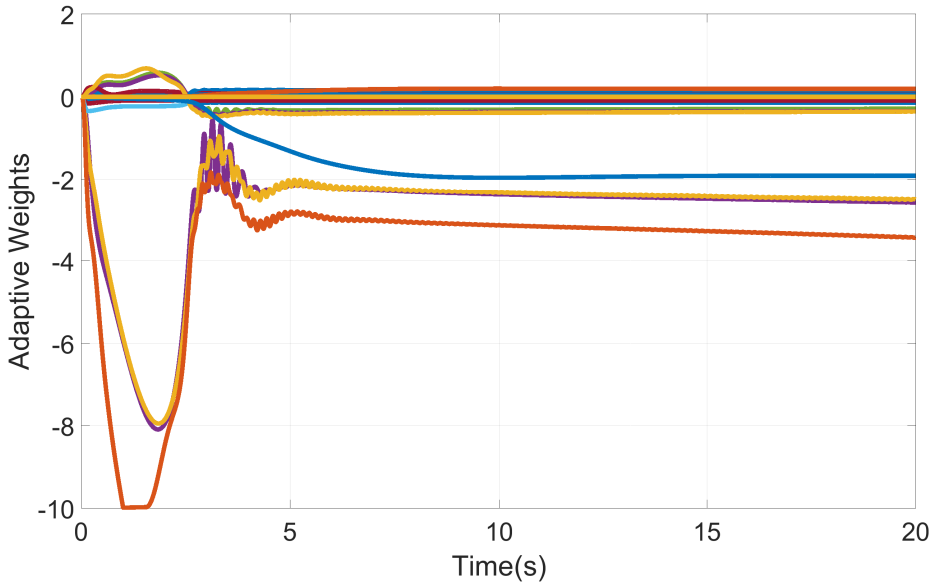

Figure 4.10: Adaptive Weights of LQI-MRAC with Constant Disturbance

In the figure 4.10, adaptive weights are shown. Adaptive controller finds appropriate weighs to cancel out the effect of the uncertainty. This is an extra profit because classical adaptive law does not guarantee that adaptive weight converges and equals to actual weights. Since actual weights are not known actually, converged weight values are assumed to be actual weights on the system.

Sinusoidal External Disturbance: Second disturbance example is sinusoidal type. Helicopter response is shown below when sinusoidal type of uncertainty is applied to system,

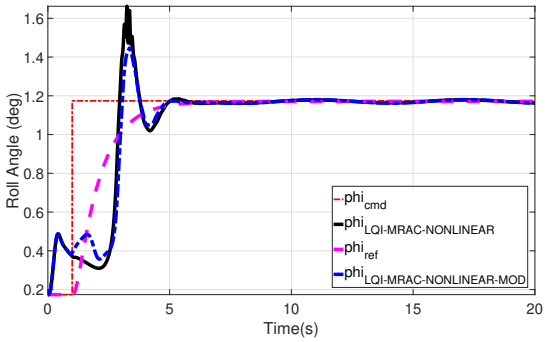

(a) Roll Angle Tracking of LQI and LQI-MRAC with Sinusoidal Dist.

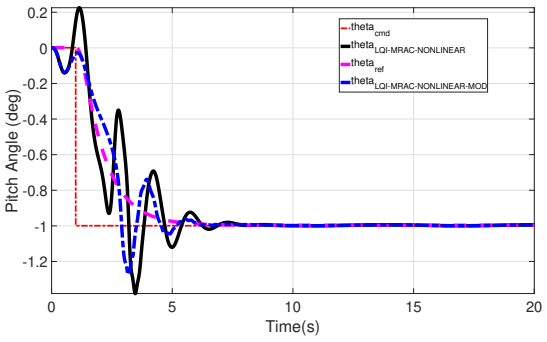

(b) Pitch Angle Tracking of LQI and LQI-MRAC with Sinusoidal Dist.

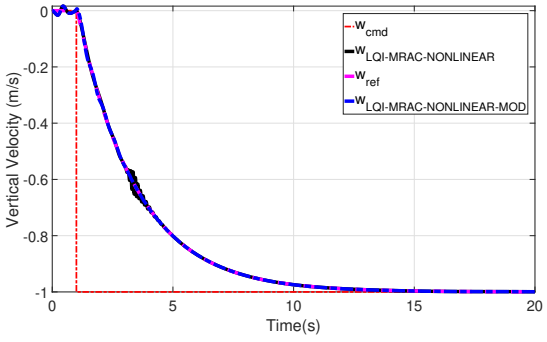

(c) Vertical Velocity Tracking LQI and LQI-MRAC with Sinusoidal Dist.

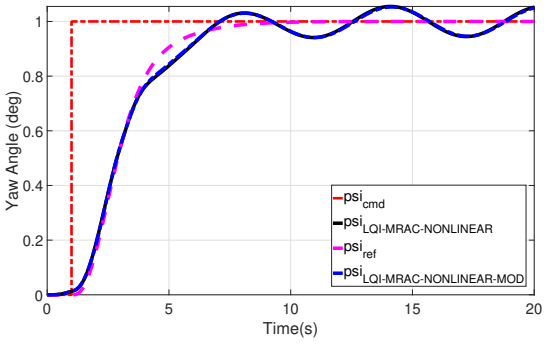

(d) Yaw Angle Tracking of LQI and LQI-MRAC with Sinusoidal Dist.

Figure 4.11: LQI-MRAC Controller Response with Sinusoidal Dist. to Step Command

Again, there exists external uncertainty from the beginning of the simulation. Although modification terms on adaptive law provides better tracking performance especially in transient region, it is seen that adaptive controller performance is not enough to track the reference model because of the oscillatory responses in the steady state region. Apart from yaw channel, tracking performance is reasonable. Next, inputs of the helicopter is shown in Figure 4.12,

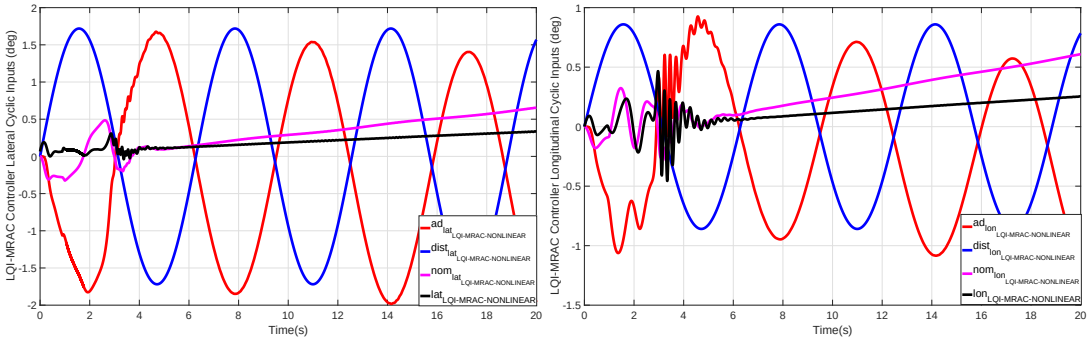

(a) Lateral Cyclic Inputs

(b) Longitudinal Cyclic Inputs

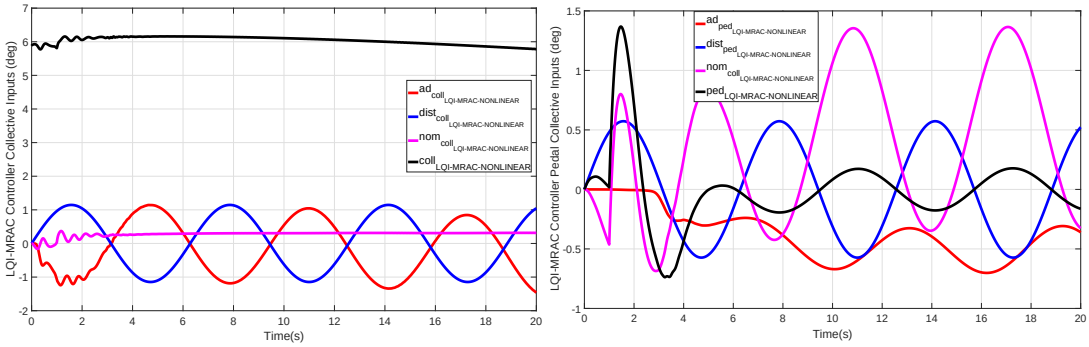

(c) Collective Inputs

(d) Pedal Collective Inputs

Figure 4.12: Inputs of LQI-MRAC Controller with Sinusoidal Dist. to Step Command

Adaptive control inputs are almost same magnitude with the disturbance in the negative direction. Adaptive controller could not remove all uncertainty effects on especially yaw channel and this result affects the reference model tracking.

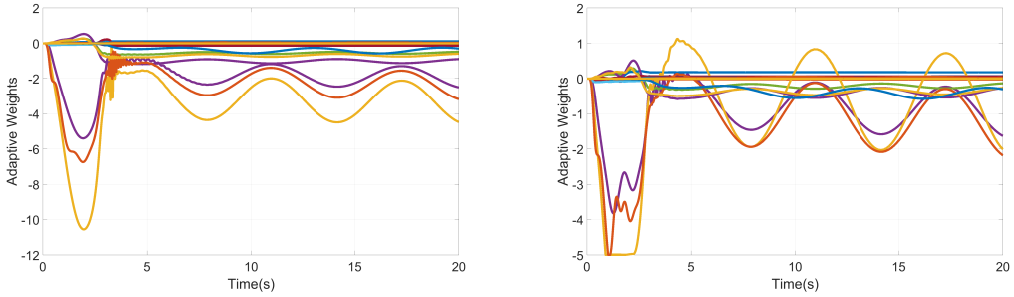

(a) Without Proj. Operator and e-mod

(b) With Projection Operator and e-modification

Figure 4.13: Adaptive Weights of LQI-MRAC with Sinusoidal Disturbance

In Figure 4.13, adaptive weights are shown when sinusoidal disturbance acts on the helicopter. Unlike constant disturbance, adaptive weights are not converged but they are bounded. It is clearly seen that while projection operator provides upper bounds to adaptive weights norm and keeps them smaller, e-modification provides better tracking performance relative to classical MRAC adaptive law.

Random External Disturbance: Lastly, random nonlinear function is added to the system as an external disturbance. Response of the model helicopter is shown in Figure 4.14,

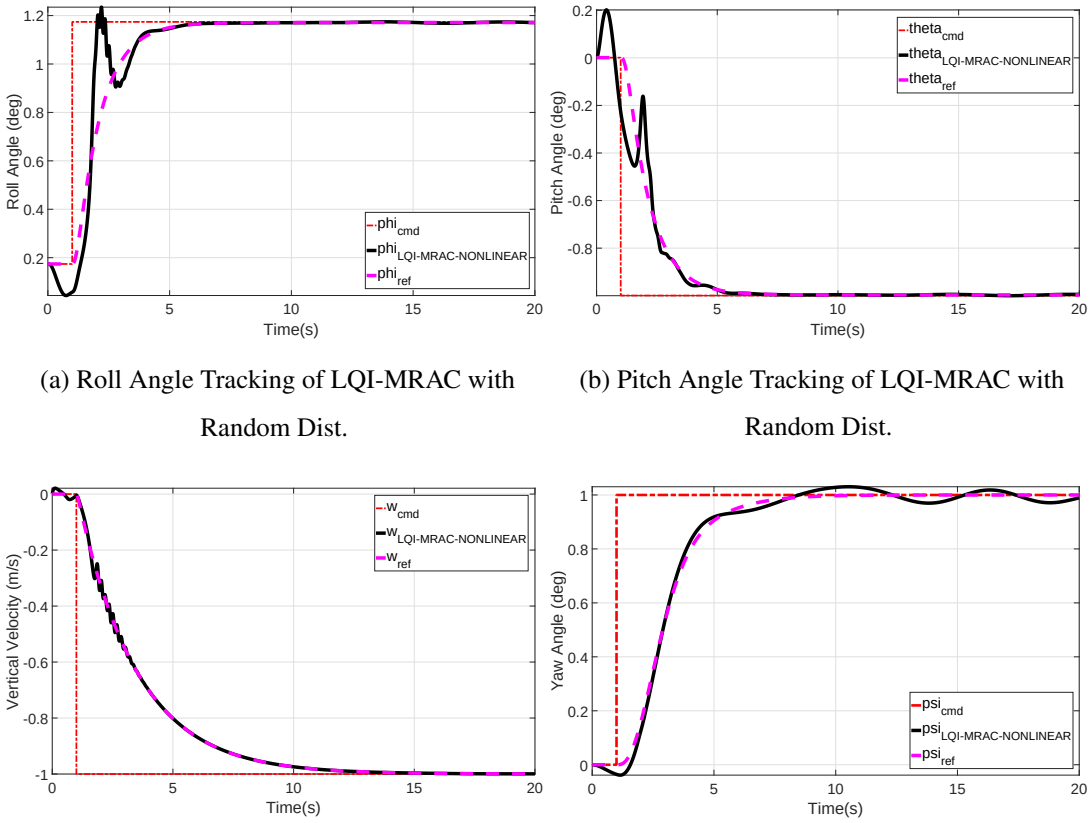

(a) Roll Angle Tracking of LQI-MRAC with Random Dist.

(b) Pitch Angle Tracking of LQI-MRAC with Random Dist.

(c) Vertical Velocity Tracking LQI-MRAC with Random Dist.

(d) Yaw Angle Tracking of LQI-MRAC with Random Dist.

Figure 4.14: LQI-MRAC Controller Response with Random Dist. Step Command

It is seen that steady state error is zero between the system with LQI-MRAC controller and reference model apart from yaw angle tracking. There is some oscillatory response again when random external disturbance is applied to the system input chan-

nels. Inputs and adaptive weights of the system are shown in the following figure.

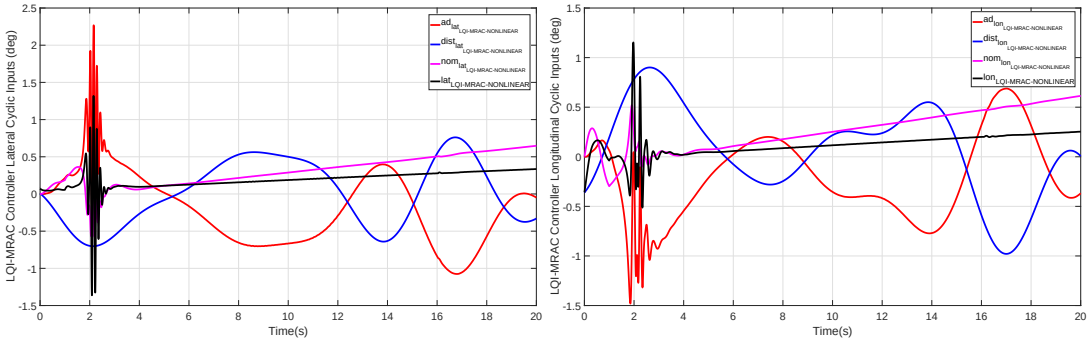

(a) Lateral Cyclic Inputs

(b) Longitudinal Cyclic Inputs

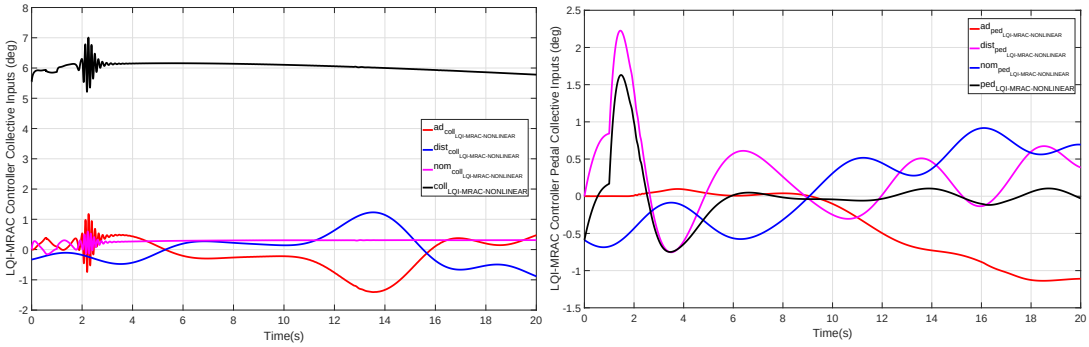

(c) Collective Inputs

(d) Pedal Collective Inputs

Figure 4.15: Inputs of LQI-MRAC Controller with Random Dist. to Step Command

Again, it seen that adaptive control inputs are opposed to the disturbance and adaptive weights are not converged. At the beginning of the simulation, adaptive controller shows an aggressive behavior to counteract the external disturbance. This creates undesired high frequency oscillations. Zero steady state error in pitch angle, roll angle and vertical velocity tracking performance can also be seen from that adaptive inputs and disturbances on the relative channel are at same magnitude with opposite sign.

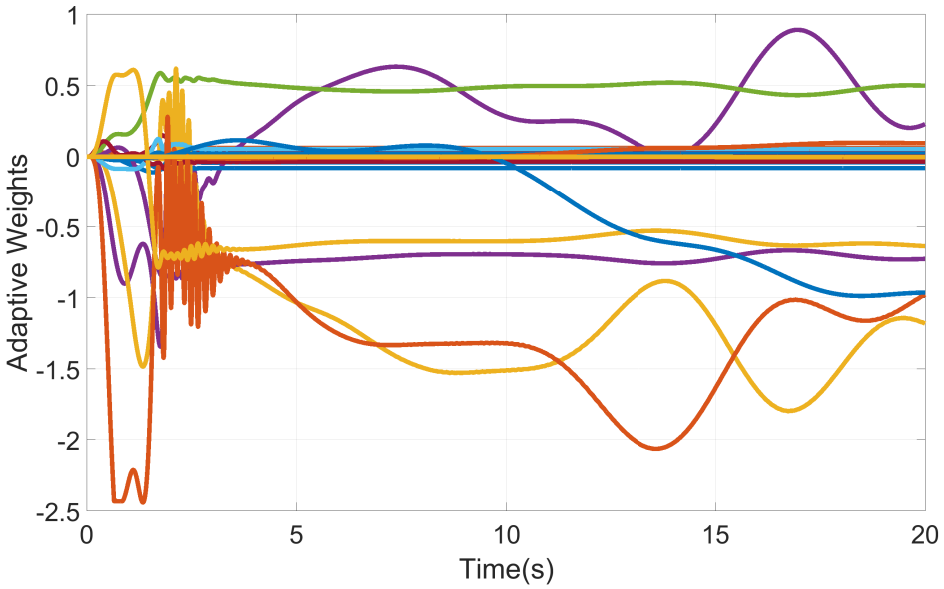

Figure 4.16: Adaptive Weights of LQI-MRAC with Random External Disturbance

In Figure 4.16, adaptive weights are shown when random external disturbance acts on the helicopter. Again, adaptive weights are not converged but they are bounded.

4.2.3 Modification of Uncertainty Parametrization in MRAC Controller

In this part, it will be focused on uncertainty parametrization methods of MRAC controller. First, Fourier Series is implemented and effects on the tracking performance is evaluated under three different external disturbance conditions. Then, Chebyshev Polynomials are replaced with Fourier Series and uncertainty parametrization performance is evaluated. Finally, Chebyshev Polynomials are defined in terms of time by using trigonometric relations and overall performance of time based uncertainty parametrization methods are shown.

4.2.3.1 Fourier Series Expansion

First, Fourier Series are written to be used in uncertainty parametrization,

$$\beta(x,t) = \begin{bmatrix} 1 \\ \beta_{c1}(x,t) \\ \beta_{c2}(x,t) \\ \vdots \\ \beta_{cN}(x,t) \\ \beta_{s1}(x,t) \\ \beta_{s2}(x,t) \\ \vdots \\ \beta_{sN}(x,t) \end{bmatrix}, \quad \beta_{ci}(x,t) = \cos(i\frac{2\pi}{T}t), \quad \beta_{ci}(x,t) = \sin(i\frac{2\pi}{T}t) \tag{4.4}$$

where $i = 1,2,\ldots,N$

Considering Fourier Series approximation accuracy and simulation speed, series length and period are selected and tuned as $N = 10$ and $T = 200s$. Then, adaptive control input is written as in Equation 4.5,

$$\begin{aligned} u_{ad}(t) &= \hat{W}^{*^T}\beta^*(x,t) \\ \beta^*(x,t) &= \begin{bmatrix} u_{bl}(t) \\ \beta(x,t) \end{bmatrix} \end{aligned} \tag{4.5}$$

Then, basis function and adaptive law parameters are decided as,

$$\beta(x,t) = \begin{bmatrix} 1 \\ \cos(\frac{2\pi}{200}t) \\ \cos(2\frac{2\pi}{200}t) \\ \vdots \\ \cos(10\frac{2\pi}{200}t) \\ \sin(\frac{2\pi}{200}t) \\ \sin(2\frac{2\pi}{200}t) \\ \vdots \\ \sin(10\frac{2\pi}{200}t) \end{bmatrix}, \quad \Gamma_{Fourier} = 0.1I_{21} \tag{4.6}$$

After deciding MRAC parameters, same external disturbance types are applied to

the system controlled with Fourier Series Based MRAC. Projection operator and e-modification is still hold in the weight update law.

Constant External Disturbance: First, constant external disturbance is applied to the system. Response of the helicopter is as follows:

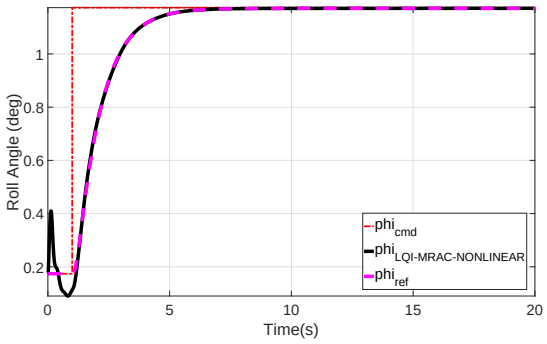

(a) Roll Angle Tracking of LQI-MRAC with Constant Dist.

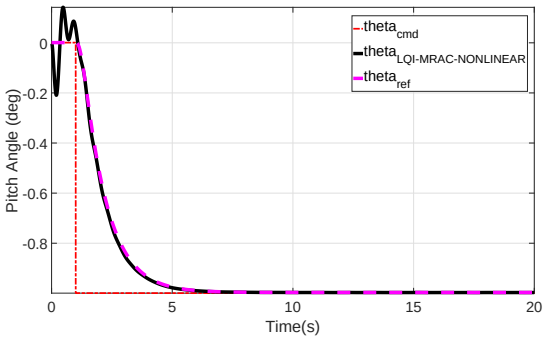

(b) Pitch Angle Tracking of LQI-MRAC with Constant Dist.

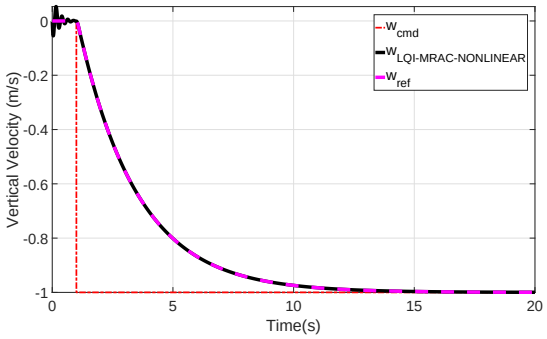

(c) Vertical Velocity Tracking LQI-MRAC with Constant Dist.

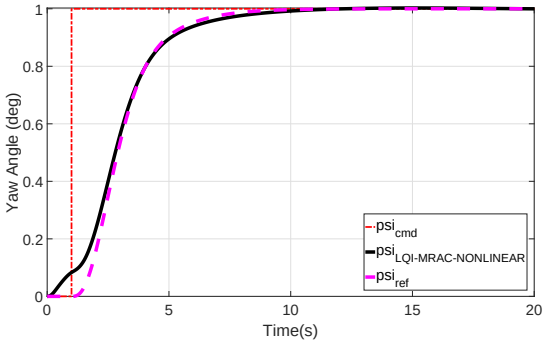

(d) Yaw Angle Tracking of LQI-MRAC with Constant Dist.

Figure 4.17: Fourier Series Based LQI-MRAC Controller Response with Constant Dist. Step Command

Again, uncertainty exists on the system at the beginning of the simulation. As seen in Figure 4.17, LQI-MRAC controller removes the effect of uncertainty at the end of the simulation and keeps tracking the reference model. It can be clearly said that Fourier Series performs better tracking performance in all axis when there is a constant uncertainty on the system.

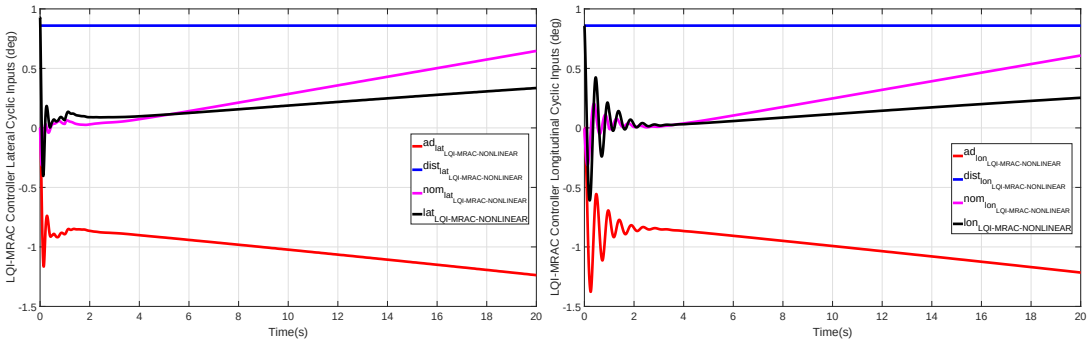

(a) Lateral Cyclic Inputs

(b) Longitudinal Cyclic Inputs

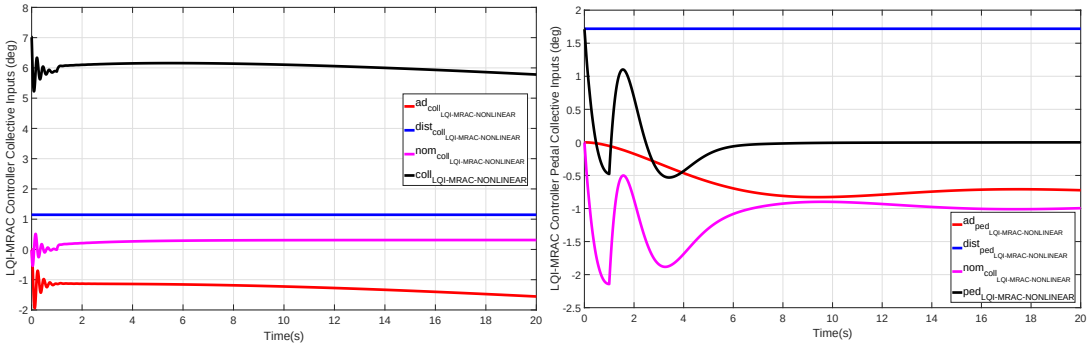

(c) Collective Inputs

(d) Pedal Collective Inputs

Figure 4.18: Inputs of Fourier Series Based LQI-MRAC Controller with Constant Dist. to Step Command

In Figure 4.18, nominal controller inputs, total inputs, adaptive inputs and disturbance acting on the helicopter are shown. It can be clearly seen that adaptive inputs are generated in order to cancel out constant disturbance. Moving on to adaptive weights,

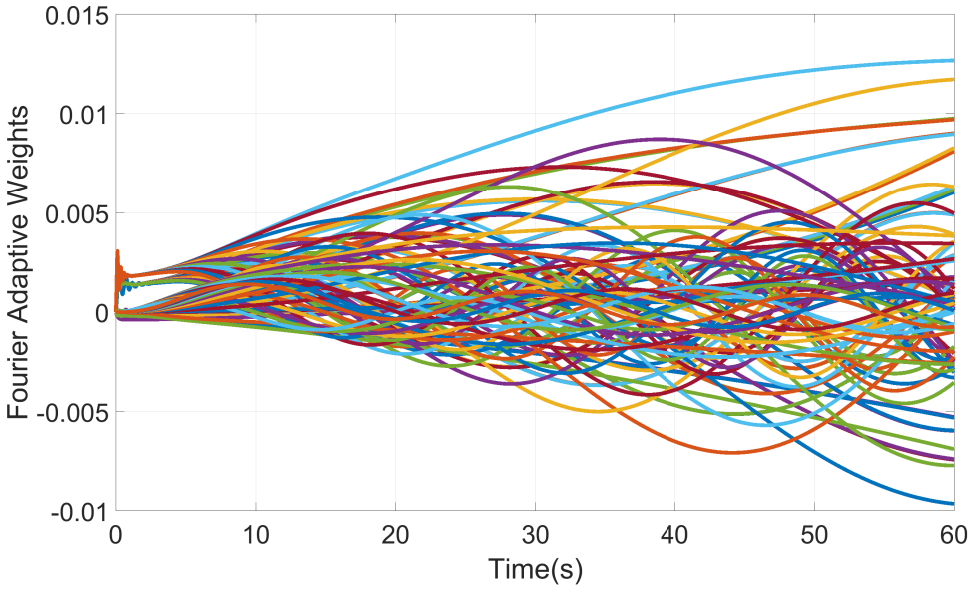

Figure 4.19: Adaptive Weights of Fourier Series Based LQI-MRAC with Constant External Disturbance

Unlike using Sigmoid functions in uncertainty parametrization, use of Fourier Series does not converge adaptive weights as in Figure 4.19. Since basis function elements β_i are periodic and sinusoidal functions, adaptive weights are also in similar structure to cancel out constant uncertainty on the system. Simulation length is kept longer to see the periodic behaviour of the adaptive weights.

Sinusoidal External Disturbance: Second, sinusoidal type uncertainty is applied to the system. Response of the helicopter is as follows:

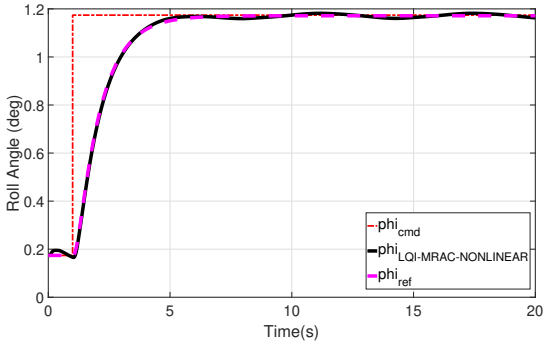

(a) Roll Angle Tracking of LQI-MRAC with Sinusoidal Dist.

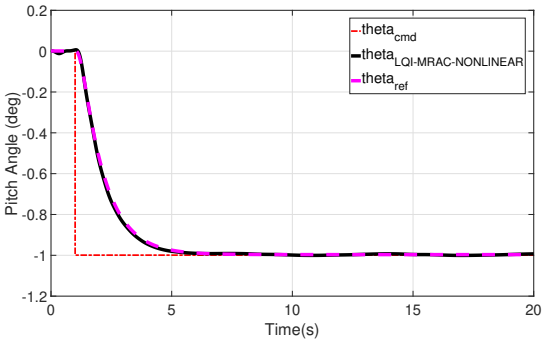

(b) Pitch Angle Tracking of LQI-MRAC with Sinusoidal Dist.

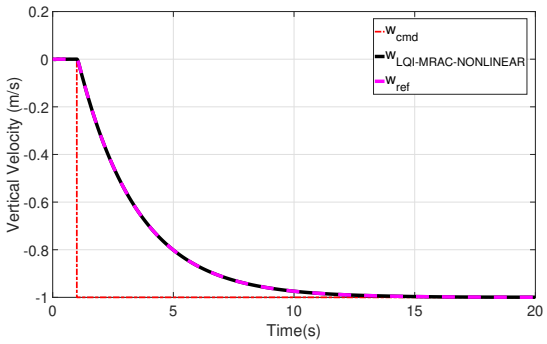

(c) Vertical Velocity Tracking LQI-MRAC with Sinusoidal Dist.

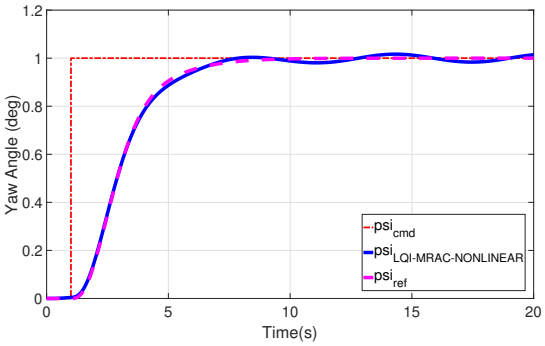

(d) Yaw Angle Tracking of LQI-MRAC with Sinusoidal Dist.

Figure 4.20: Fourier Series Based LQI-MRAC Controller Response with Constant Dist. Step Command

According to Figure 4.20, it is seen that system tracking performance to the reference model is improved especially in transient region when sinusoidal disturbance acts on the system. Oscillatory response is decreased significantly especially in yaw angle tracking relative to use of Sigmoid Functions in uncertainty parametrization. In addition, inputs of the helicopter is shown in Figure 4.21,

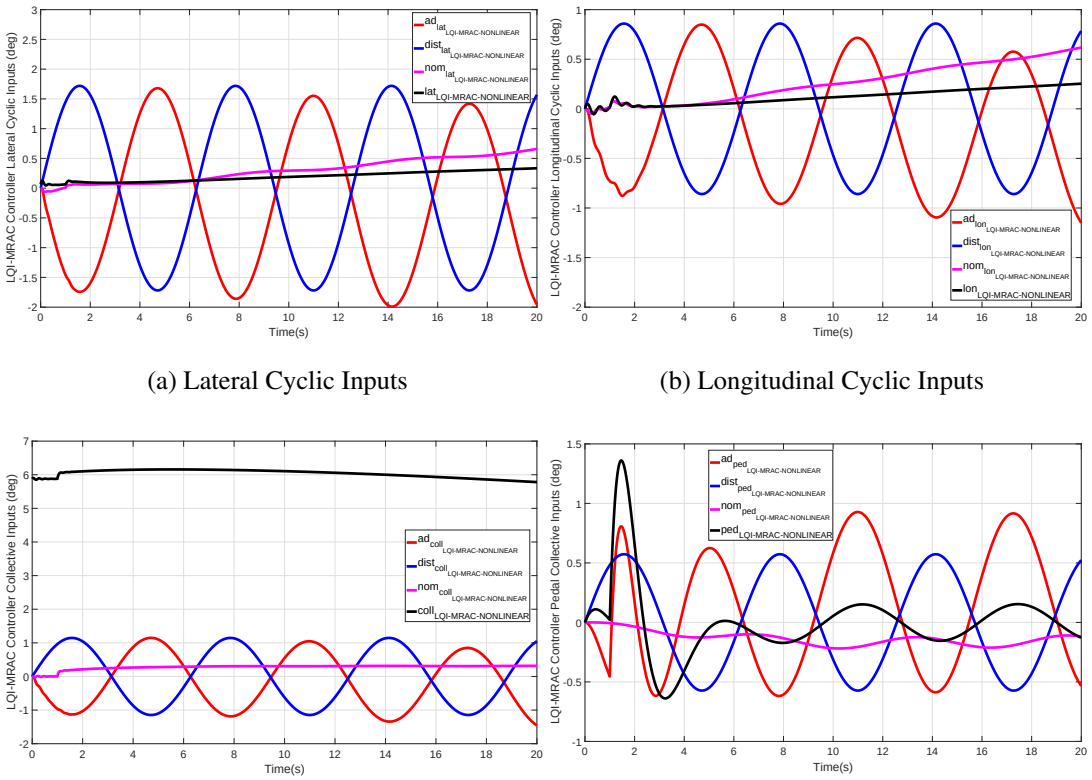

(a) Lateral Cyclic Inputs

(b) Longitudinal Cyclic Inputs

(c) Collective Inputs

(d) Pedal Collective Inputs

Figure 4.21: Inputs of Fourier Series Based LQI-MRAC Controller with Sinusoidal Dist. to Step Command

The improvement of MRAC controller and success of the uncertainty parametrization can be noticed by Figure 4.21. Unlike Sigmoid functions, use of Fourier series does not create high frequency oscillatory adaptive inputs and these inputs are almost same magnitude with opposite direction.

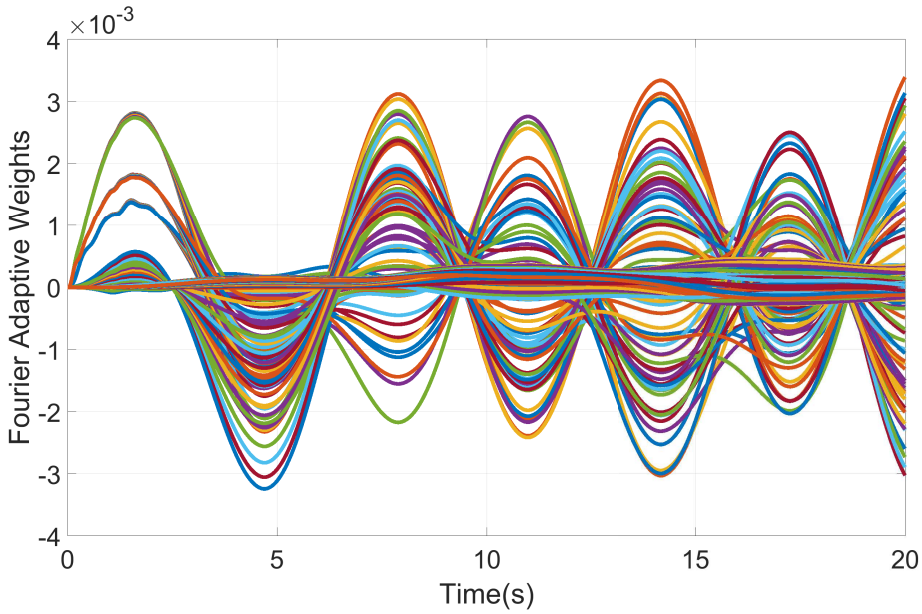

Figure 4.22: Adaptive Weights of Fourier Series Based LQI-MRAC with Sinusoidal External Disturbance

Figure 4.22 represents adaptive weights in MRAC where the uncertainty is parametrized with Fourier Series. By nature of Fourier Series, it is bounded and sinusoidal structure and this is also valid for adaptive weights of Fourier Series.

Random External Disturbance: Lastly, random nonlinear disturbance is implemented to the system as uncertainty. In addition to this, Gaussian type white noise is added to investigate that MRAC controller still works. Response of the helicopter is shown in Figure 4.23.

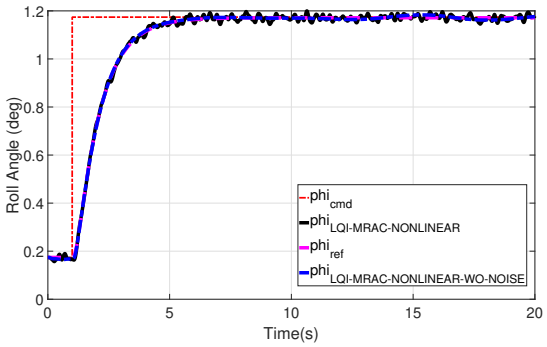

(a) Roll Angle Tracking of LQI-MRAC with Random Dist.

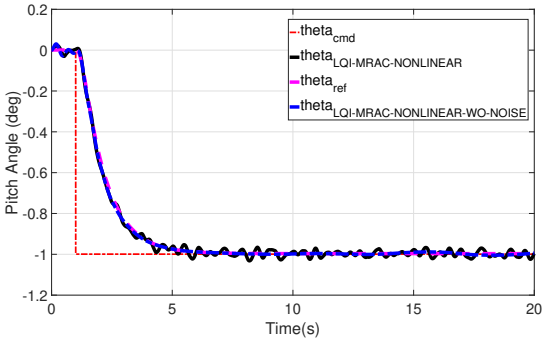

(b) Pitch Angle Tracking of LQI-MRAC with Random Dist.

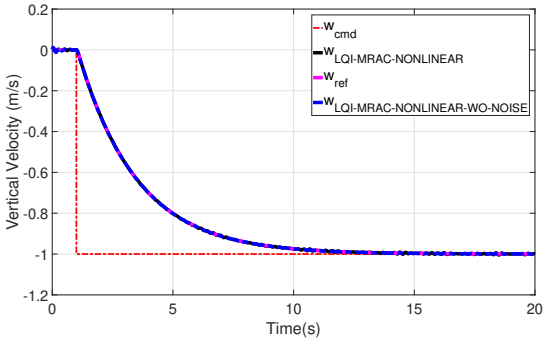

(c) Vertical Velocity Tracking LQI-MRAC with Random Dist.

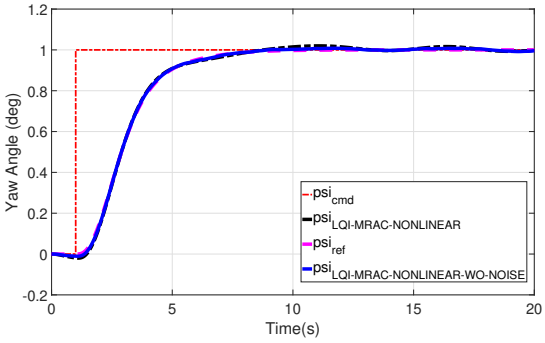

(d) Yaw Angle Tracking of LQI-MRAC with Random Dist.

Figure 4.23: Fourier Series Based LQI-MRAC Controller Response with Random Dist. Step Command

According to Figure 4.23, it is seen that system tracking performance is very similar with the sinusoidal disturbance case. Again, oscillatory response is decreased significantly. It can be said that use of Fourier Series in uncertainty parametrization handles with the predefined random type uncertainties. Moreover, inputs of the helicopter is shown in Figure 4.24.

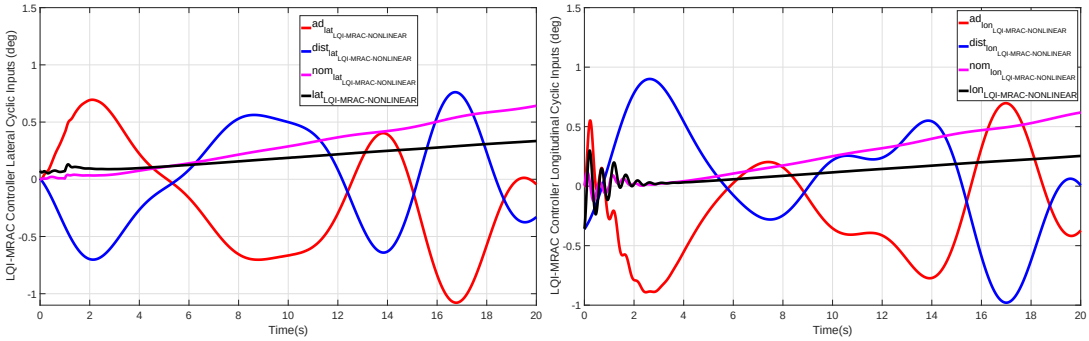

(a) Lateral Cyclic Inputs

(b) Longitudinal Cyclic Inputs

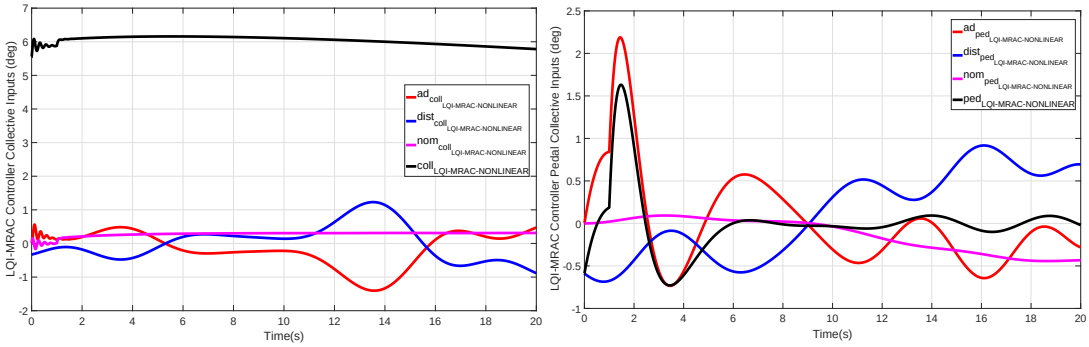

(c) Collective Inputs

(d) Pedal Collective Inputs

Figure 4.24: Inputs of Fourier Series Based LQI-MRAC Controller with Sinusoidal Dist. to Step Command

When inputs are examined in Figure 4.24, it is seen that adaptive inputs play an important role in suppressing the disturbance. They are in opposite directions and close in magnitude and the use of Fourier Series inhibits high frequency inputs as in the use of Sigmoid Functions.

Figure 4.25 represents the adaptive weight created by MRAC controller where uncertainty is parametrized with Fourier Series. Again, bounded and sinusoidal type adaptive weights are obtained due to the structure of Fourier Series.

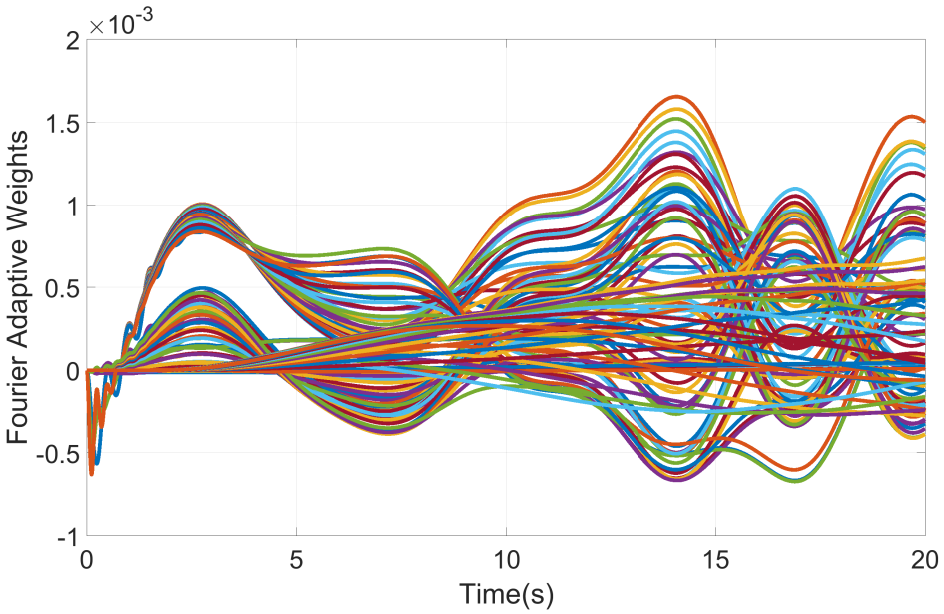

Figure 4.25: Adaptive Weights of Fourier Series Based LQI-MRAC with Random External Disturbance

4.2.3.2 Chebyshev Polynomials

Secondly, Chebyshev Polynomials are used in MRAC controller to parametrize uncertainties,

$$\beta(x,t) = \begin{bmatrix} T_0(x,t) \\ T_1(x,t) \\ \vdots \\ T_{N-1}(x,t) \\ T_N(x,t) \end{bmatrix}, \quad T_{i+1}(x,t) = 2xT_i(x,t) - T_{i-1}(x,t) \tag{4.7}$$

It is predefined that $T_0(x,t) = 1, \quad T_1(x,t) = x \quad \text{and} \quad i = 1,2,\ldots,N$. And, it is required that $|T_n(x,t)| \leq 1 \quad \text{and } x \in [-1,1] \quad \text{for } x \in N$ for orthogonality property.

The only one design parameter used Chebyshev Polynomials in uncertainty parametrization is polynomials length N. For simulation speed and performance, length is chosen

as $N = 5$. Rewriting adaptive control input as in Equation 4.8,

$$\begin{aligned} u_{ad}(t) &= -\hat{W}^{*^T}\beta^*(u_{bl}, x(t)) \\ \beta^*(u_{bl}, x(t)) &= \begin{bmatrix} u_{bl} \\ \beta(x,t) \end{bmatrix} \end{aligned} \tag{4.8}$$

Then, basis function and adaptive law parameters are decided as,

$$\beta(x,t) = \begin{bmatrix} T_0(x,t) \\ T_1(x,t) \\ \vdots \\ T_4(x,t) \\ T_5(x,t) \end{bmatrix}, \quad \Gamma_{Chebyshev} = 0.5I_6 \tag{4.9}$$

Implementation of Chebyshev Polynomials into adaptive law is same with the Fourier Series Expansion. After it is implemented in MRAC, controller is tested under same types of disturbances. Projection operator and e-modification is kept in controller design.

State Based Chebyshev Polynomials

In order to satisfy orthogonality property and use Chebyshev polynomials as a universal approximators, all state values need to be limited within the range of [-1,1]. System states used in controller design are output error integrals, translational velocities, rotational velocities and Euler angles. Since rotational velocities and Euler angles are in radians, their absolute values are always less than one in all flight condition for all simulations. Translational velocities may be greater than one; however, it may be limited between the required range by a simple unit conversion to mile/s.

Unfortunately, there is one more problem in using Chebyshev Polynomials in MRAC for MIMO systems. Because the polynomials are in term of system states and there are thirteen system states, basis function is going to be very large. This does not seem reasonable for simulation speed. If basis function is written in terms of system states

using Chebyshev Polynomials,

$$\beta(x,t) = \begin{bmatrix} T_0x_1(x,t) \\ T_0x_2(x,t) \\ \vdots \\ T_0x_n(x,t) \\ T_1x_1(x,t) \\ T_1x_2(x,t) \\ \vdots \\ T_1x_n(x,t) \\ \vdots \\ \vdots \\ T_Nx_1(x,t) \\ T_Nx_2(x,t) \\ \vdots \\ T_Nx_n(x,t) \end{bmatrix} \tag{4.10}$$

where $n = 13$ and $N = 5$.

Consequently, augmented basis function is a column matrix with 82 elements (4 for u_{bl} and 78 for $\beta(x,t)$) and there will be 4×82 elements in the adaptive weight matrix considering four input channel of the helicopter model. This implies that numerical calculations to estimate adaptive weights are not easy and simulation performance is not going to be as desired.

As done for all MRAC design and modifications up to this point, three types of disturbance are applied to the system. However, MRAC controller could not find appropriate weights to remove the uncertainty effect. Simulation result for the constant disturbance case is shown as an example.

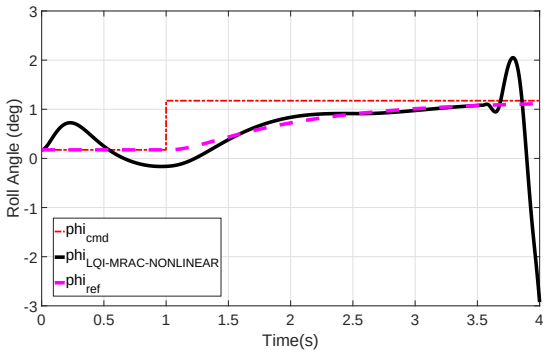

(a) Roll Angle Tracking of LQI-MRAC with Constant Dist.

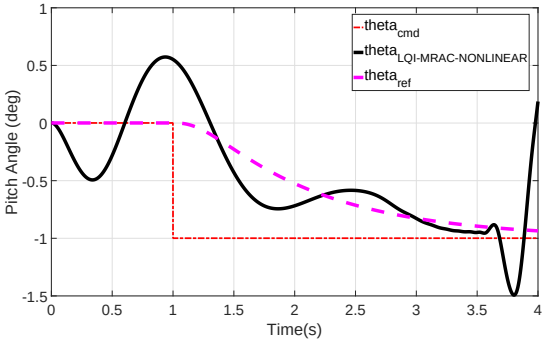

(b) Pitch Angle Tracking of LQI-MRAC with Constant Dist.

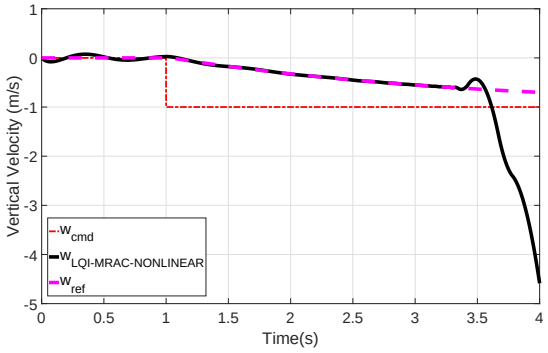

(c) Vertical Velocity Tracking LQI-MRAC with Constant Dist.

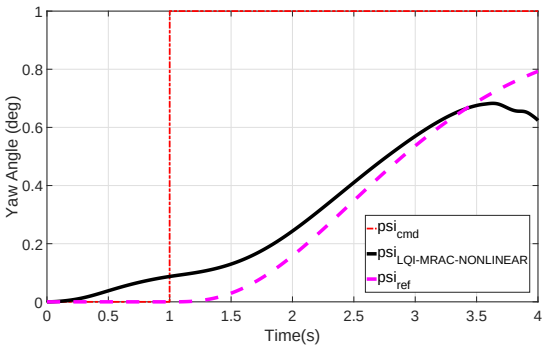

(d) Yaw Angle Tracking of LQI-MRAC with Constant Dist.

Figure 4.26: State Dependent Chebyshev Polynomials Based LQI-MRAC Controller Response with Constant Dist. to Step Command

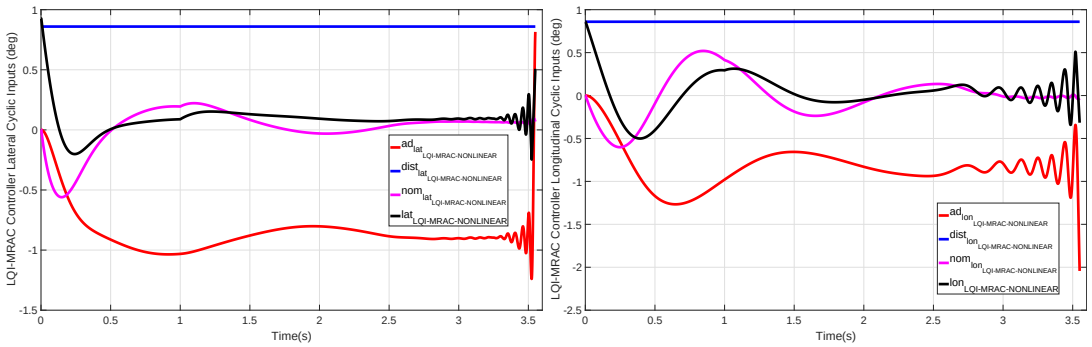

(a) Lateral Cyclic Inputs

(b) Longitudinal Cyclic Inputs

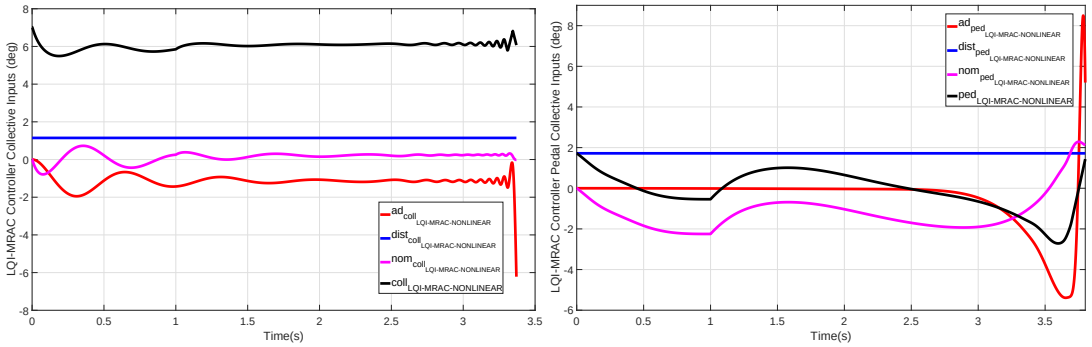

(c) Collective Inputs

(d) Pedal Collective Inputs

Figure 4.27: Inputs of State Dependent Chebyshev Polynomials Based LQI-MRAC Controller with Constant Dist. to Step Command

As seen in Figure 4.26 and Figure 4.27, adaptive element in MRAC could not found appropriate weights and could not create adaptive inputs to cancel out uncertainty on the system. After about four seconds, simulation is stopped.

When defining Chebyshev Polynomials in system state based, uncertainty is tried to be parametrized with system states one by one. That is, coupled terms are not considered. For example, generated adaptive input by State Based Chebyshev Polynomials MRAC is in the form of:

$$\begin{aligned}\left[u_{ad}(t)\right]_{4x1} &= \hat{K}_{u_{bl}} u_{bl}(t) + \hat{W}\beta(x,t) \\ &= \left[\hat{K}_{u_{bl}}\right]_{4x4} \times \left[u_{bl}(t)\right]_{4x1} + \left[\hat{W}\right]_{4x78} \times \left[\beta(x,t)\right]_{78x1}\end{aligned} \tag{4.11}$$

$$
\begin{aligned}
\Rightarrow [u_{ad}(t)]_{j,1} &= \hat{K}_{u_{bl}}(j,:) \times u_{bl}(:,j) \\
&+ \hat{W}^*_{j,1} T_0 x_1(x,t) + \hat{W}^*_{j,2} T_0 x_2(x,t) + \cdots + \hat{W}^*_{j,n} T_0 x_n(x,t) \\
&+ \hat{W}^*_{j,n+1} T_1 x_1(x,t) + \hat{W}^*_{j,n+2} T_1 x_2(x,t) + \cdots + \hat{W}^*_{j,2n} T_1 x_n(x,t) \\
&\vdots \\
&+ \hat{W}^*_{j,5n+1} T_N x_1(x,t) + \hat{W}^*_{j,5n+2} T_N x_2(x,t) + \cdots + \hat{W}^*_{j,6n} T_6 x_n(x,t)
\end{aligned}
$$

where $j = 1,2,3,4$, $n = 13$ and

$$
\begin{aligned}
T_{0x_i}(x,t) &= 1 \\
T_{1x_i}(x,t) &= x_i \\
T_{2x_i}(x,t) &= 2x_i^2 - 1 \\
T_{3x_i}(x,t) &= 4x_i^3 - 3x_i \\
T_{4x_i}(x,t) &= 8x_i^4 - 8x_i^2 + 1 \\
T_{5x_i}(x,t) &= 16x_i^5 - 20x_i^3 + 5x_i
\end{aligned}
\tag{4.12}
$$

for $i = 1,2,\ldots,13$.

With this form, multiplication of different states are not taken into account. Therefore, uncertainty is not parametrized successfully and MRAC controller does not create appropriate adaptive input.

Time Based Chebyshev Polynomials

Parametrizing uncertainty with Chebyshev Polynomials are not straightforward and successful with system states. Alternatively, defining Chebyshev Polynomials in time only could be a solution for this complexity of use. By trigonometric relation,

$$
\begin{aligned}
\cos(0) &= 1 \\
\cos(\phi) &= \cos\phi \\
\cos(2\phi) &= 2\cos^2\phi - 1 \\
\cos(3\phi) &= 4\cos^3\phi - 3\cos\phi \\
\cos(4\phi) &= 8\cos^4\phi - 8\cos^2\phi + 1 \\
\cos(5\phi) &= 16\cos^5\phi - 20\cos^3\phi + 5\cos\phi
\end{aligned}
\tag{4.13}
$$

Selecting $\phi = t$ and $T_n = \cos(nt)$,

$$\begin{aligned} T_0 &= 1 \\ T_1 &= \cos(t) \\ T_2 &= 2\cos^2(t) - 1 \\ T_3 &= 4\cos^3(t) - 3\cos(t) \\ T_4 &= 8\cos^4(t) - 8\cos^2(t) + 1 \\ T_5 &= 16\cos^5(t) - 20\cos^3(t) + 5\cos(t) \end{aligned} \tag{4.14}$$

Finally, equations in Equation 4.14 are in the form of Chebyshev Polynomials. Note that orthogonality property of Chebyshev Polynomials still hold. That is, $|T_n(x,t)| <= 1$ and $x \in [-1,1]$ for $x \in N$.

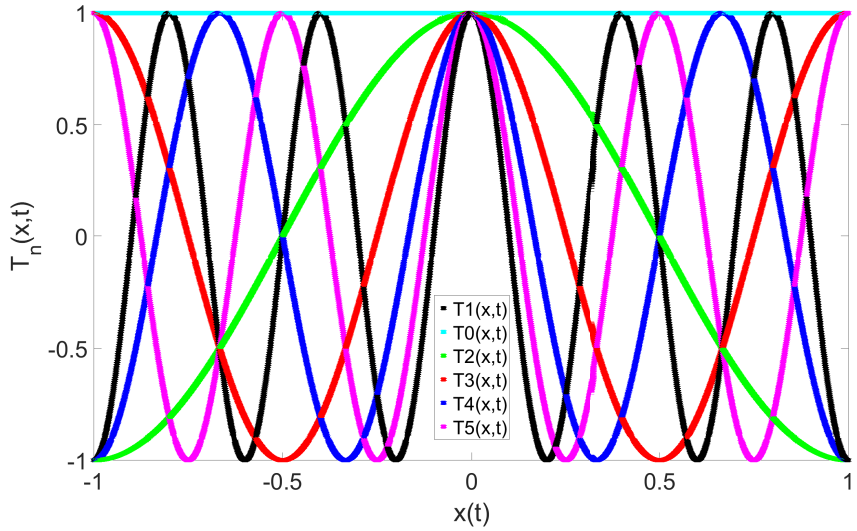

Figure 4.28: Chebyshev Polynomials (1^{st} Kind)

Figure 4.28 shows first six members of 1^{st} kind Chebyshev polynomials. It is clearly seen that orthogonal property is kept.

After defining time dependent Chebyshev Polynomials, same simulation procedures are done in order to analyze the effect of modification.

Constant and Sinusoidal External Disturbance: As done in other modifications, first, constant external disturbance is applied to the system. Since time based Cheby-

shev Polynomials are in trigonometric form, helicopter response is compared with the case that Fourier Series is used in uncertainty parametrization.

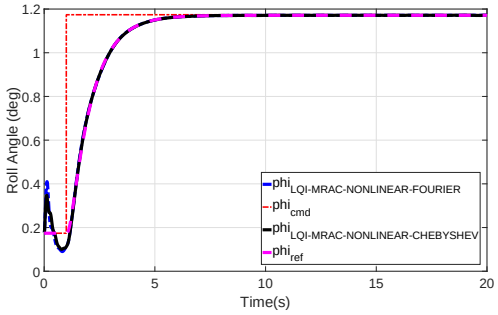

(a) Roll Angle Tracking of LQI-MRAC with Constant Dist.

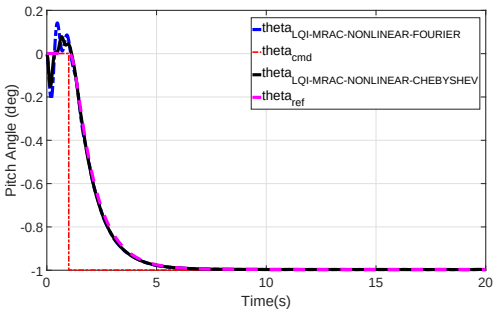

(b) Pitch Angle Tracking of LQI-MRAC with Constant Dist.

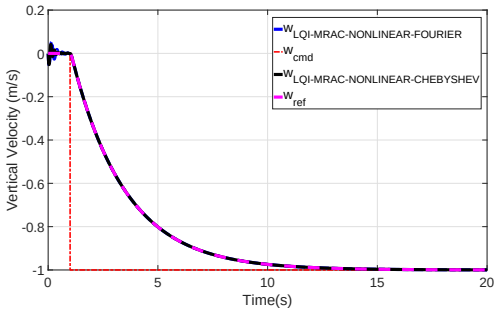

(c) Vertical Velocity Tracking LQI-MRAC with Constant Dist.

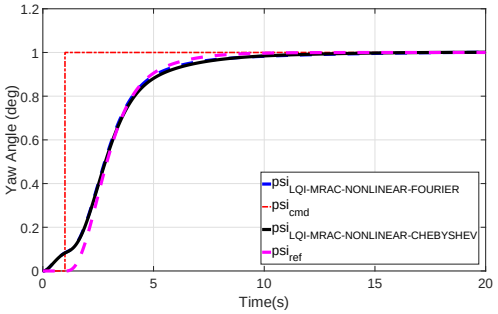

(d) Yaw Angle Tracking of LQI-MRAC with Constant Dist.

Figure 4.29: Time Dependent Chebyshev Polynomials and Fourier Based LQI-MRAC Controller Response with Constant Dist. to Step Command

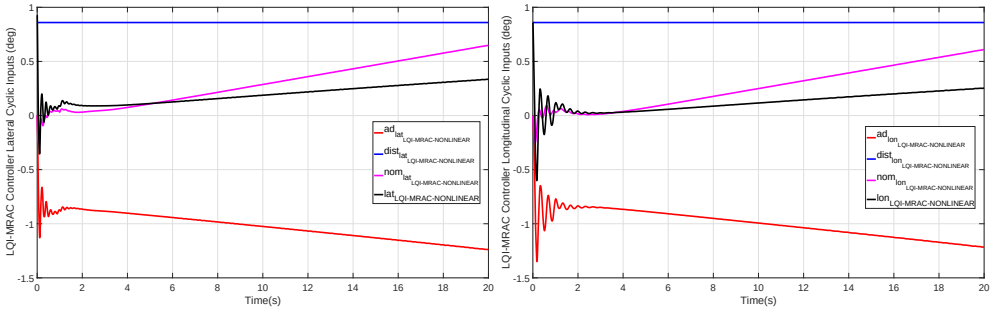

(a) Lateral Cyclic Inputs

(b) Longitudinal Cyclic Inputs

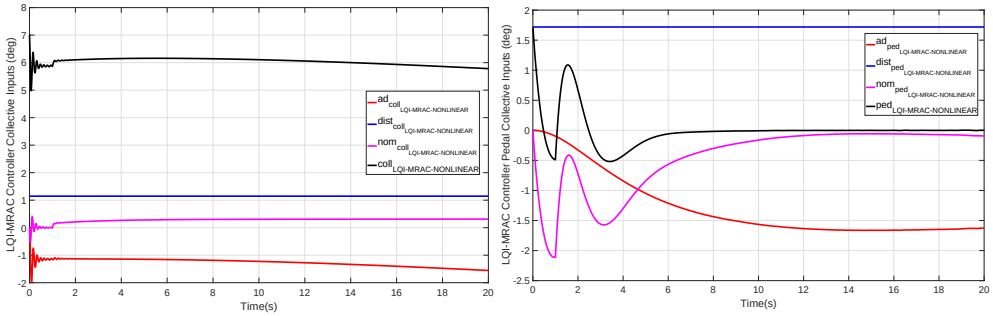

(c) Collective Inputs

(d) Pedal Collective Inputs

Figure 4.30: Inputs of Time Dependent Chebyshev Polynomials Based LQI-MRAC Controller with Constant Dist. to Step Command

Inputs of the Time Dependent Chebyshev Polynomials Based LQI-MRAC Controller and response to step command are given in Figure 4.29 and Figure 4.30. It is clearly seen that both systems show similar behavior and tracking performance. Although they converge to reference model successfully after $t = 1s$, system with Chebyshev Polynomials exhibit less amplitude oscillations before $t = 1s$. Adaptive input in the form of,

$$\begin{aligned}\left[u_{ad}(t)\right]_{4x1} &= \hat{K}_{u_{bl}} u_{bl}(t) + \hat{W}^T \beta(x,t) \\ &= \left[\hat{K}_{u_{bl}}\right]_{4x4} \times \left[u_{bl}\right]_{4x1} + \left[\hat{W}^T\right]_{4x6} \times \left[\beta(x,t)\right]_{6x1}\end{aligned} \tag{4.15}$$

$$\left[u_{ad}(t)\right]_{j,1} = \hat{K}_{u_{bl}}(j,:) \times u_{bl}(:,j) + \hat{W}_{j,1} T_0(t) + \hat{W}_{j,2} T_1(t) + \cdots + \hat{W}_{j,6} T_5(t) \tag{4.16}$$

where $j = 1,2,3,4$.

Adaptive weight matrix is formed with 4×10 elements for all input channels of the helicopter. Since there is not unique form for basis function elements, that is T_0, T_1,

$T_2, \ldots, T_5$ are in different form from each other, adaptive weights are not in a special form like Fourier Series.

Another difference between Fourier Series and Chebyshev Polynomials are MRAC design parameters. While Fourier Series need an appropriate period to parametrize uncertainty successfully, Chebyshev Polynomials do not need period as a parameter. In order to compare both approximators for different series period, sinusoidal type on disturbance is given to the system.

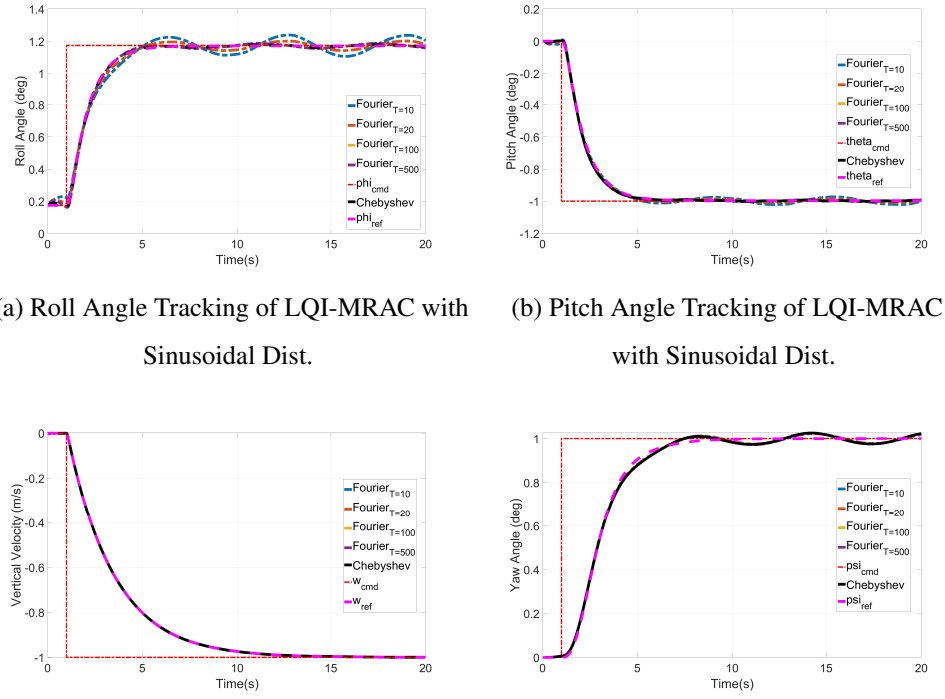

(a) Roll Angle Tracking of LQI-MRAC with Sinusoidal Dist.

(b) Pitch Angle Tracking of LQI-MRAC with Sinusoidal Dist.

(c) Vertical Velocity Tracking LQI-MRAC with Sinusoidal Dist.

(d) Yaw Angle Tracking of LQI-MRAC with Sinusoidal Dist.

Figure 4.31: Comparison of Time Dependent Chebyshev Polynomials and Fourier Based LQI-MRAC Controller Response with Sinusoidal Dist. and Different Periods

In Figure 4.31, use of Time Dependent Chebyshev Polynomials and Fourier Series in MRAC uncertainty parametrization is compared under sinusoidal external disturbance case. Although, system with Chebyshev Polynomials are not affected by period, simulations are repeated under different periods to show period effect in Fourier Series Approximation. As seen in especially Figure 4.31a and Figure 4.31b, Fourier Series are not effective with low periods like $T = 10s$ or $T = 20s$. Using Fourier Series

Approximation with high period length such as $T = 100s$ or $T = 500s$, both universal approximation methods show almost same tracking and uncertainty parametrization performance. For collective channel, uncertainty is canceled out successfully and system does almost perfect following of reference model with independent of period. Lastly, for yaw channel, oscillatory response still exists and both approximator could not remove all of the sinusoidal uncertainty.

Random External Disturbance: Finally, random disturbance is applied to the system with Time Based Chebyshev Polynomials LQI-MRAC controller. Since controller successfully tracks the reference model with these conditions, Gaussian type white noise is added to system input channels. Response of the helicopter is shown in Figure 4.32.

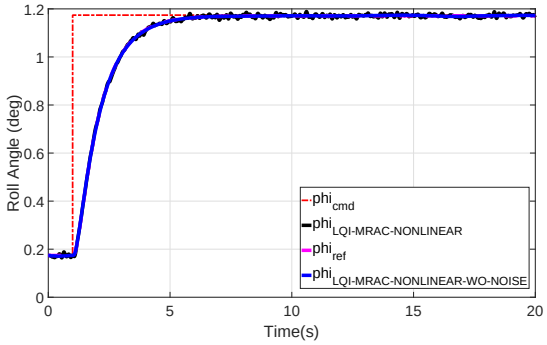

(a) Roll Angle Tracking of LQI-MRAC with Random Dist.

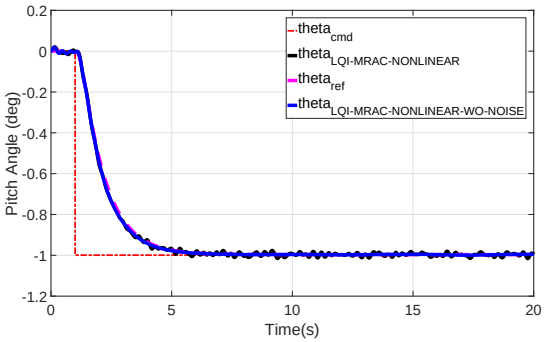

(b) Pitch Angle Tracking of LQI-MRAC with Random Dist.

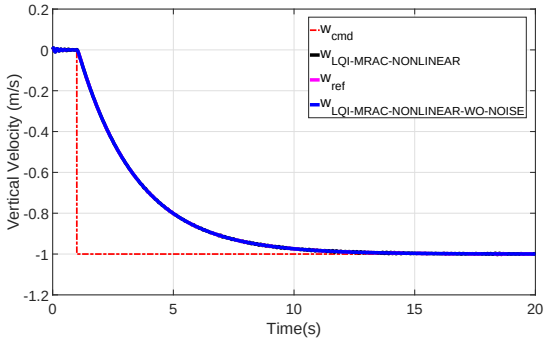

(c) Vertical Velocity Tracking LQI-MRAC with Random Dist.

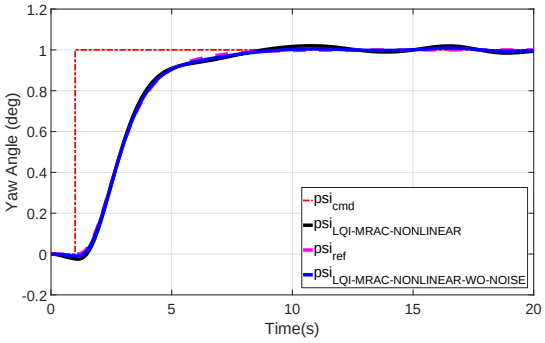

(d) Yaw Angle Tracking of LQI-MRAC with Random Dist.

Figure 4.32: Time Dependent Chebyshev Polynomials Based LQI-MRAC Controller Response with Random Dist. Step Command

It is basically seen that reference model is tracked under random external disturbance with the help of Time Dependent Chebyshev Polynomials Based LQI-MRAC controller. Parametrizing uncertainty in time based approximates the uncertainty successfully and this can be seen in Figure 4.33 for without noise case.

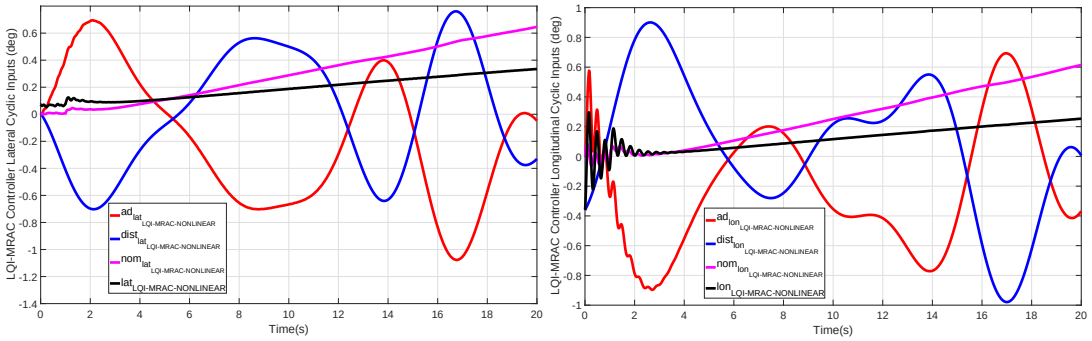

(a) Lateral Cyclic Inputs

(b) Longitudinal Cyclic Inputs

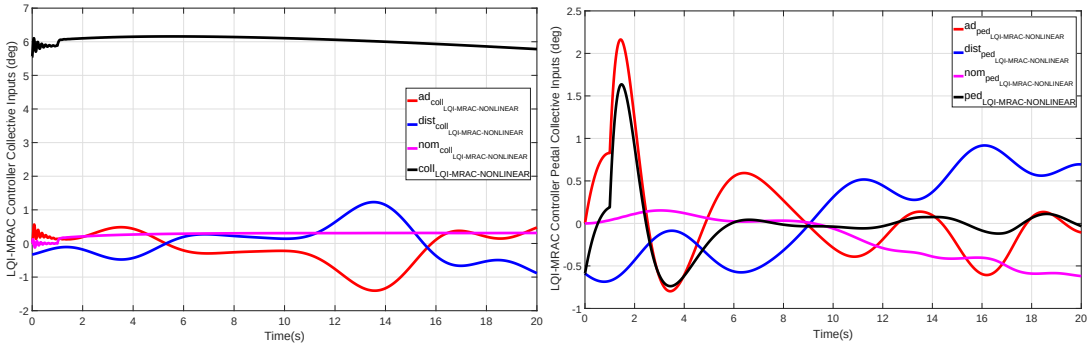

(c) Collective Inputs

(d) Pedal Collective Inputs

Figure 4.33: Inputs of Time Dependent Chebyshev Polynomials Based LQI-MRAC Controller with Random Dist. to Step Command

Lastly, Figure 4.34 shows adaptive weights of MRAC controller where Time Based Chebyshev Polynomials are used in uncertainty parametrization. Again, e-modification, Projection Operator and sinusoidal structure of polynomials guarantees that adaptive inputs are bounded.

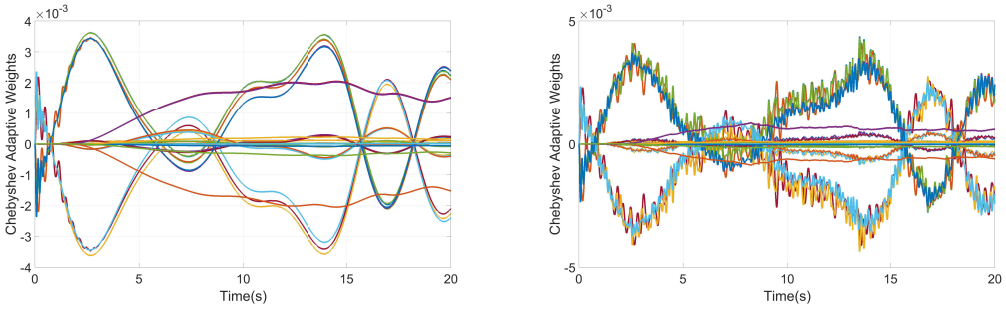

(a) Without Noise Case

(b) With Noise Case

Figure 4.34: Adaptive Weights of Time Dependent Chebyshev Polynomials Based LQI-MRAC with Random External Disturbance

4.2.4 Case Studies

In this section, for random external disturbance case, which is the most complex form in three disturbance types, is applied to the system and more complex flight tasks are commanded to the helicopter. Effect of adaptive controller is also shown in plots obtained by simulations and compared with the non-adaptive case.

4.2.4.1 Sequential Step Commands

In this part, different sequential step commands is given to all channels and response of the helicopter is investigated. Projection operator, e-modification are used in adaptive law in MRAC. Time dependent Chebyshev Polynomials is chosen as the uncertainty parametrization method because of its simplicity of design and good tracking performance.

Outputs of the helicopter model is shown in the following figures when random external uncertainty exists on all input channels.

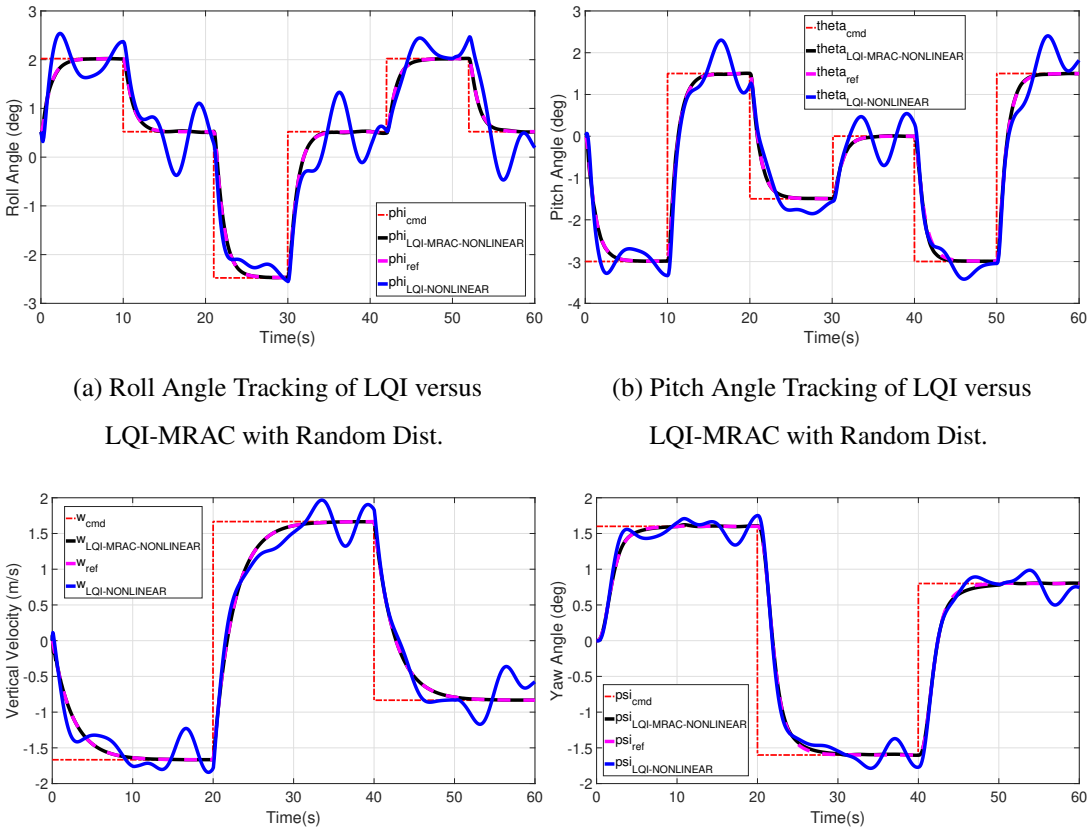

(a) Roll Angle Tracking of LQI versus LQI-MRAC with Random Dist.

(b) Pitch Angle Tracking of LQI versus LQI-MRAC with Random Dist.

(c) Vertical Velocity Tracking of LQI versus LQI-MRAC with Random Dist.

(d) Yaw Angle Tracking of LQI versus LQI-MRAC with Random Dist.

Figure 4.35: Sequential Step Command Tracking Comparison of LQI and LQI-MRAC with Random Dist.

In Figure 4.35, blue line represents the response of the helicopter when adaptive controller is not active on the system, that is only Linear Quadratic Regulator with Integral exists. Although LQI controller do not track reference model shown by magenta color and are not robust to external disturbances, adding MRAC controller to LQI baseline controller solves the tracking problem. MRAC controller adapts the disturbance and cancel out its effect within about five seconds after new step is commanded to the system. By looking closer to Figure 4.35,

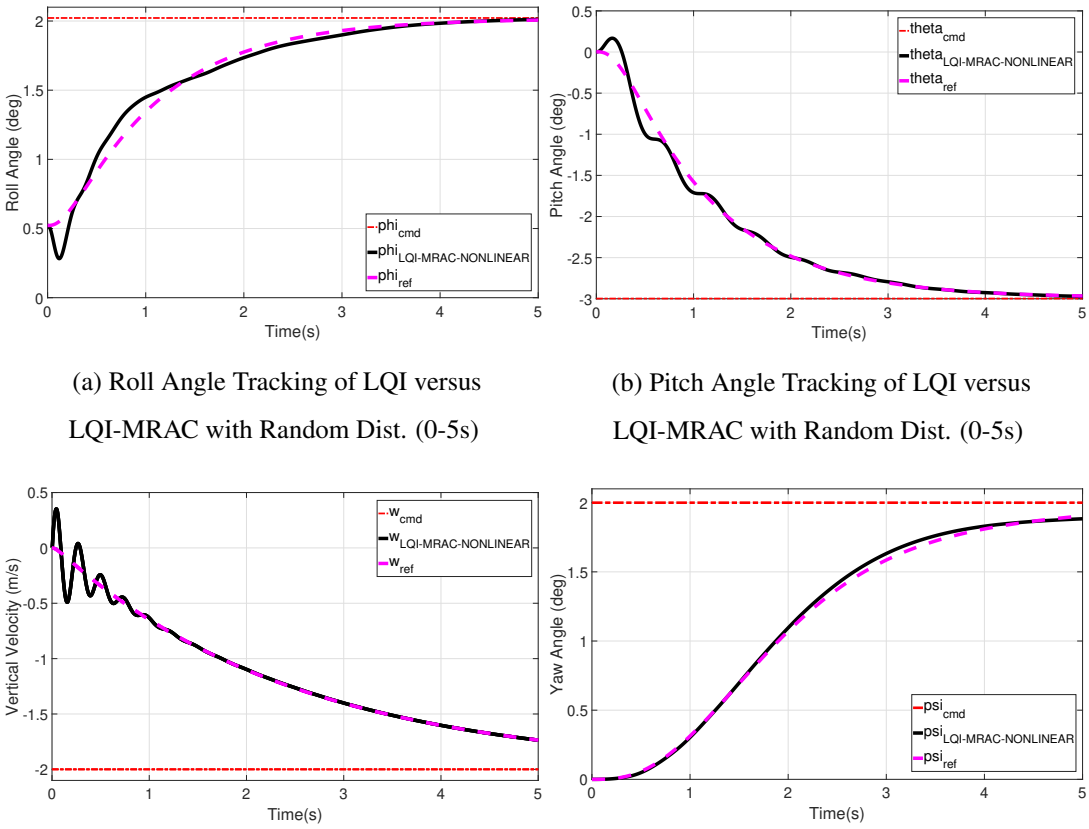

(a) Roll Angle Tracking of LQI versus LQI-MRAC with Random Dist. (0-5s)

(b) Pitch Angle Tracking of LQI versus LQI-MRAC with Random Dist. (0-5s)

(c) Vertical Velocity Tracking of LQI versus LQI-MRAC with Random Dist. (0-5s)

(d) Yaw Angle Tracking of LQI versus LQI-MRAC with Random Dist. (0-5s)

Figure 4.36: Sequential Step Command Tracking Comparison of LQI and LQI-MRAC with Random Dist. (0-5s)

Next, inputs given to the helicopter to track the reference model are shown.

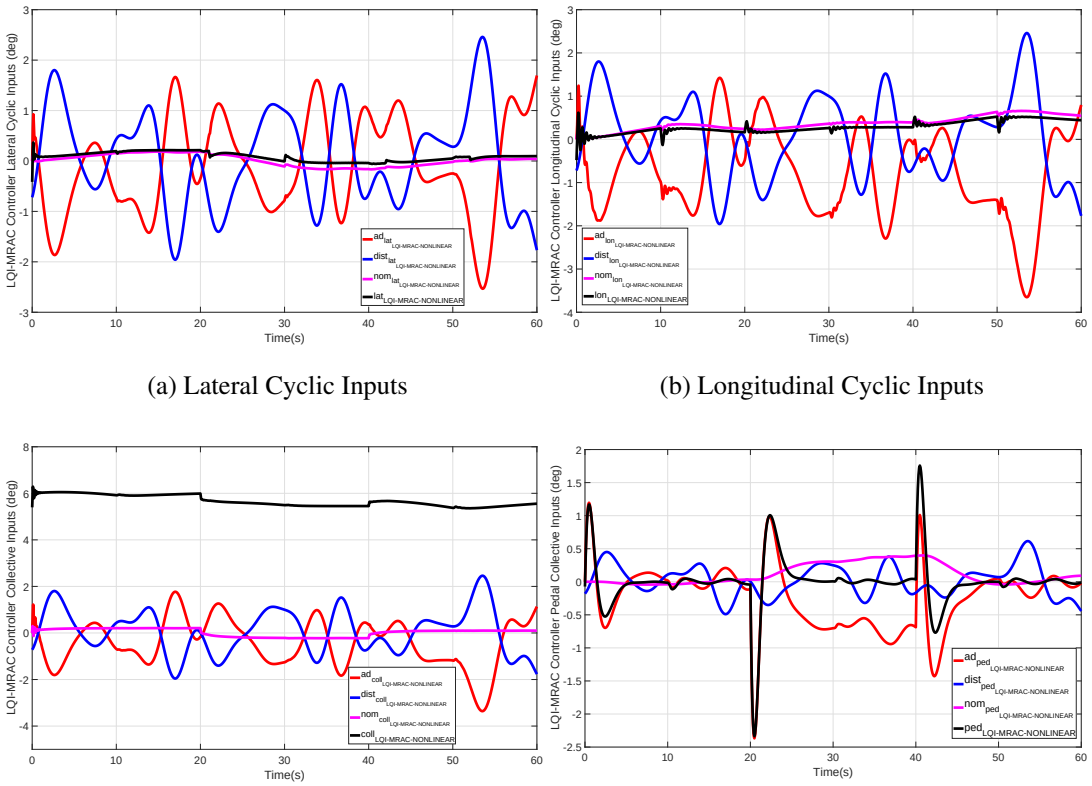

(a) Lateral Cyclic Inputs

(b) Longitudinal Cyclic Inputs

(c) Collective Inputs

(d) Pedal Collective Inputs

Figure 4.37: Inputs of Time Dependent Chebyshev Polynomials Based LQI-MRAC Controller with Random Dist. to Step Command

MRAC controller performance can be seen better in input plots Figure 4.37. Adaptive inputs generated by MRAC controller are almost in same magnitude with the disturbance on the system in opposite direction. This implies that closed loop system acts like that there is not any external disturbance on the system and nonlinear model outputs track the reference model with baseline controller.

By the nature of Chebyshev Polynomials, it is known that they are bounded in [-1,1]. Thus, adaptive weights calculated by using Chebyshev Polynomials in uncertainty parametrization needs to be bounded. They are plotted and shown in Figure 4.38.

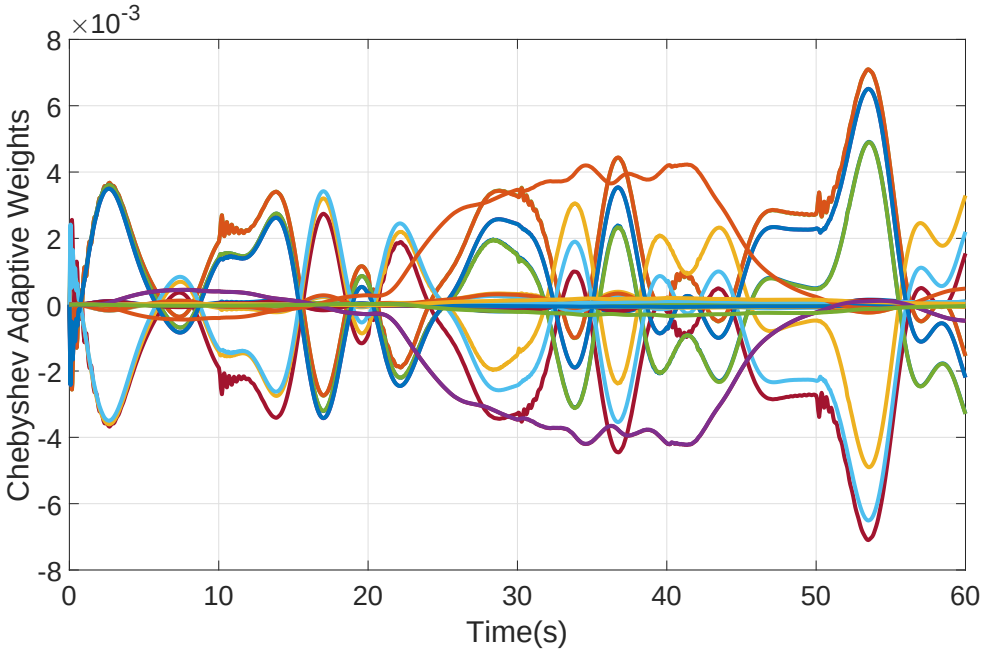

Figure 4.38: Adaptive Weights of LQI-MRAC with Random External Disturbance

Since different commands are given to the helicopter one after another, helicopter model states need to be showed as well as helicopter model outputs.

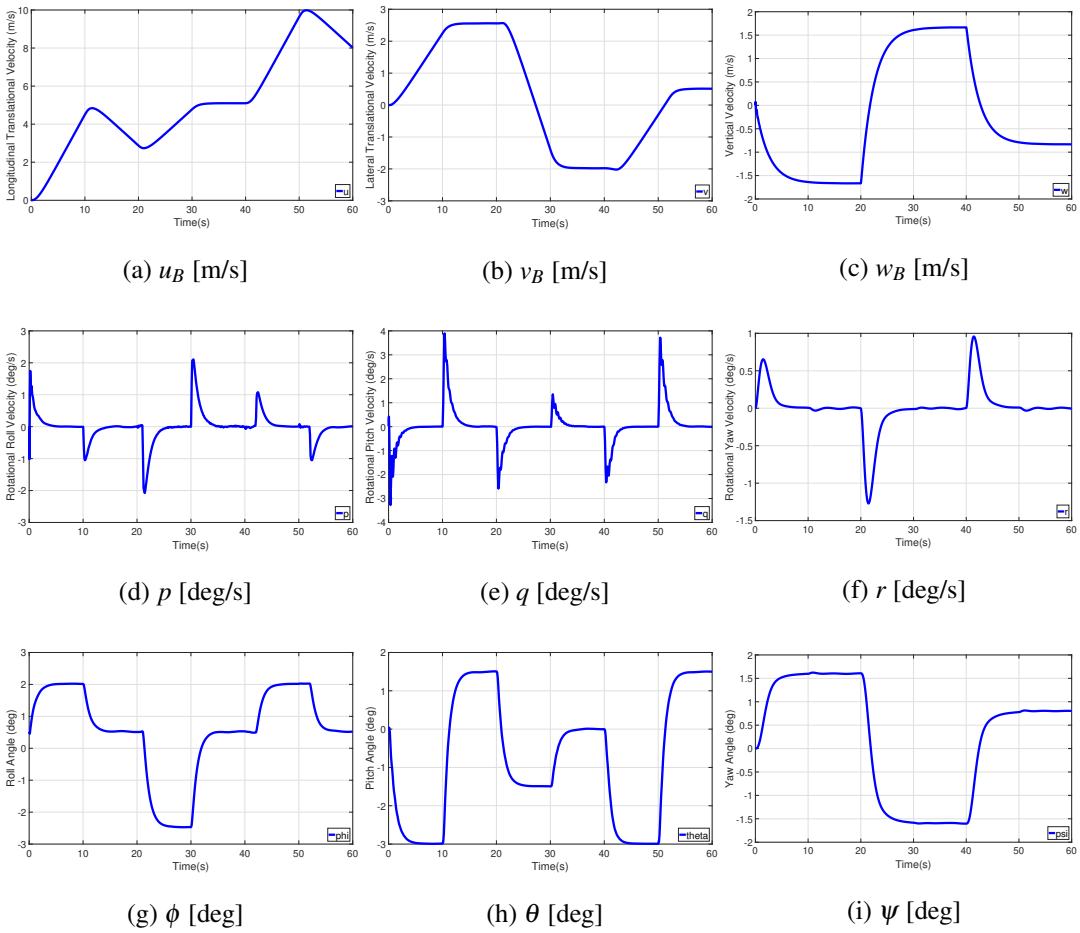

(a) u_B [m/s] (b) v_B [m/s] (c) w_B [m/s]

(d) p [deg/s] (e) q [deg/s] (f) r [deg/s]

(g) ϕ [deg] (h) θ [deg] (i) ψ [deg]

Figure 4.39: Helicopter States when Sequential Step is Commanded with LQI-MRAC and Random Dist.

In Figure 4.39, reduced order helicopter model states are shown. Note that helicopter initial trim point is hovering condition where all translational and rotational velocities are zero. After, reference Euler angles are commanded in pitch, roll and yaw axis. Vertical velocity is commanded in collective axis. Consequently, helicopter velocity is increasing and decreasing in all axis. Since moment of inertia of the relevant axis is small relative to other axis, roll channel has some oscillatory response while tracking reference model. After ten seconds of the simulation, it can be said that helicopter is in forward flight and its speed reaches to 8-10 m/s in 50s. It should be noted that getting far away from the initial condition brings extra uncertainties on the system since reference model and baseline controller is designed considering hovering case.

4.2.4.2 Robustness Analysis

In this section, robustness of the proposed controller is analyzed. Since sample helicopter is chosen a model helicopter, its parameter may not be known exactly. For example, although helicopter mass is assumed constant, it may be increased with payloads and decreased by remove of the some equipment on the helicopter. Its aerodynamics parameters may differ from the values assumed in model parameters. To make sure that designed controller still works with altering physical and aerodynamic parameters of the helicopter, robustness of the helicopter in tracking of the reference model is investigated by changing mass, inertia and some aerodynamics parameters of the helicopter.

Mass and Inertia Differences Firstly, mass and second moment of inertias of all axis are changed in order to examine controller performance. It should be noted that classical adaptive theory defined in Chapter 3 does not guarantee the stability of the system when uncertainty exist on the system matrix. That is, uncertainty cannot be removed completely by the input channel. However, these parameters are the most varying parameters considering the mathematical model and the model helicopter in real world applications. Therefore, it is preferred that the controller still shows reasonable performance and does not create a catastrophic problem. Reference model tracking performance are presented in Figure 4.40-4.43.

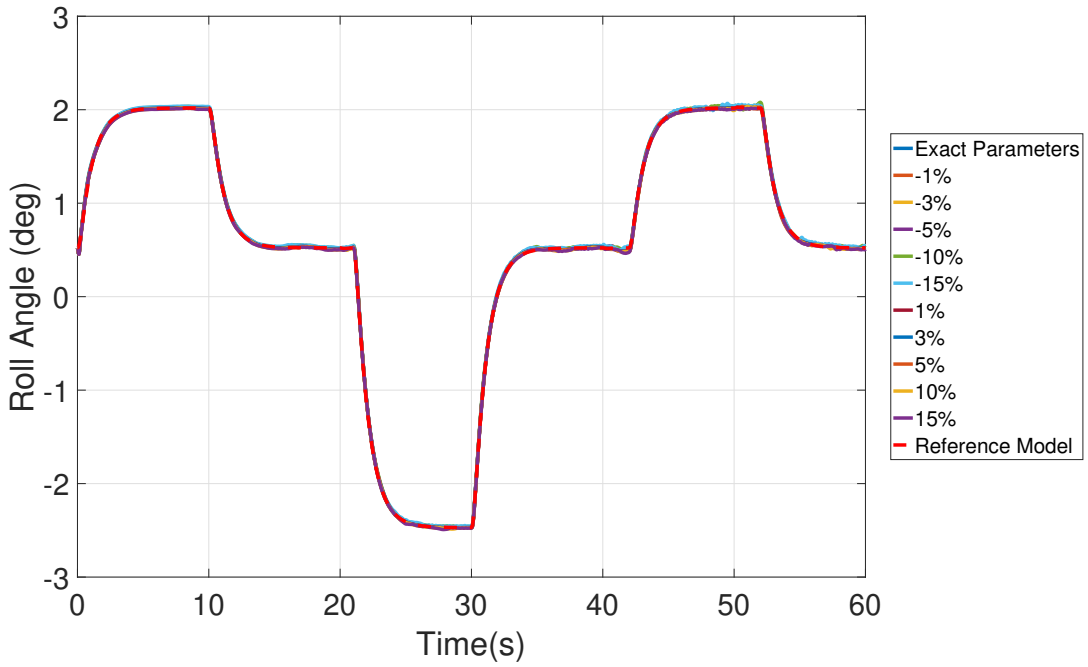

Figure 4.40: Effect of Mass and Inertia Change in Roll Angle Tracking Performance with Random External Dist.

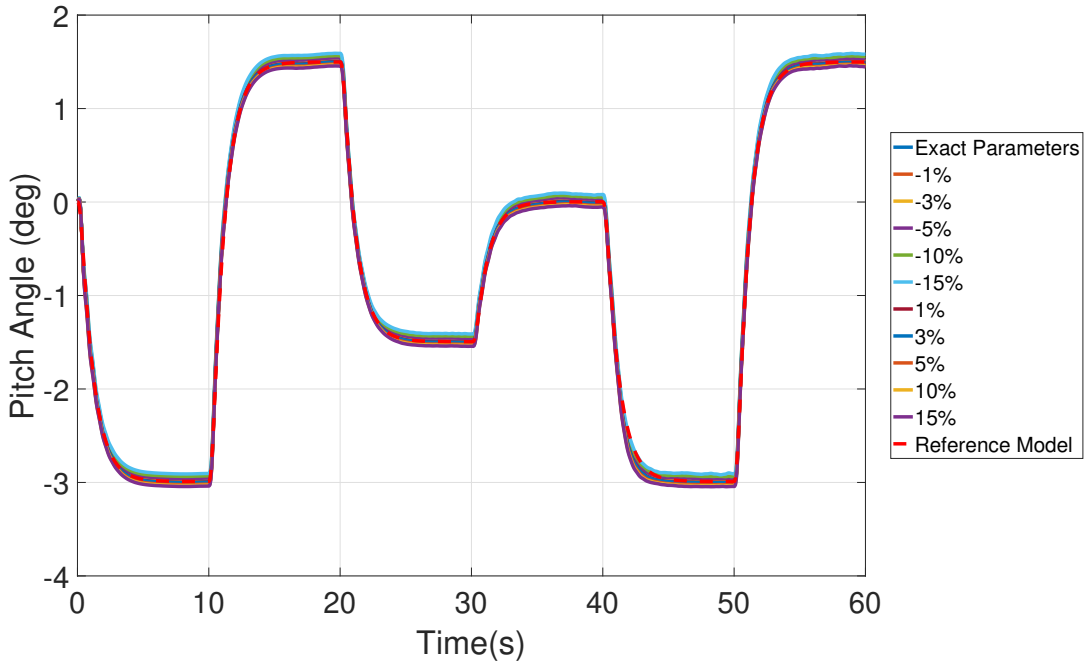

Figure 4.41: Effect of Mass and Inertia Change in Pitch Angle Tracking Performance with Random External Dist.

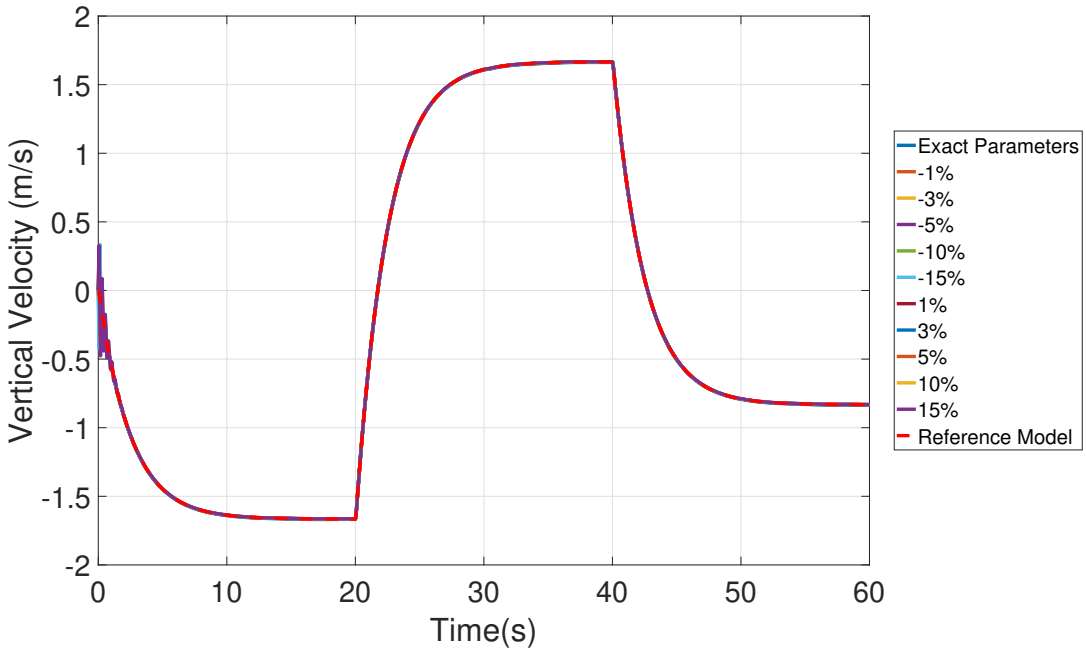

Figure 4.42: Effect of Mass and Inertia Change in Vertical Velocity Tracking Performance with Random External Dist.

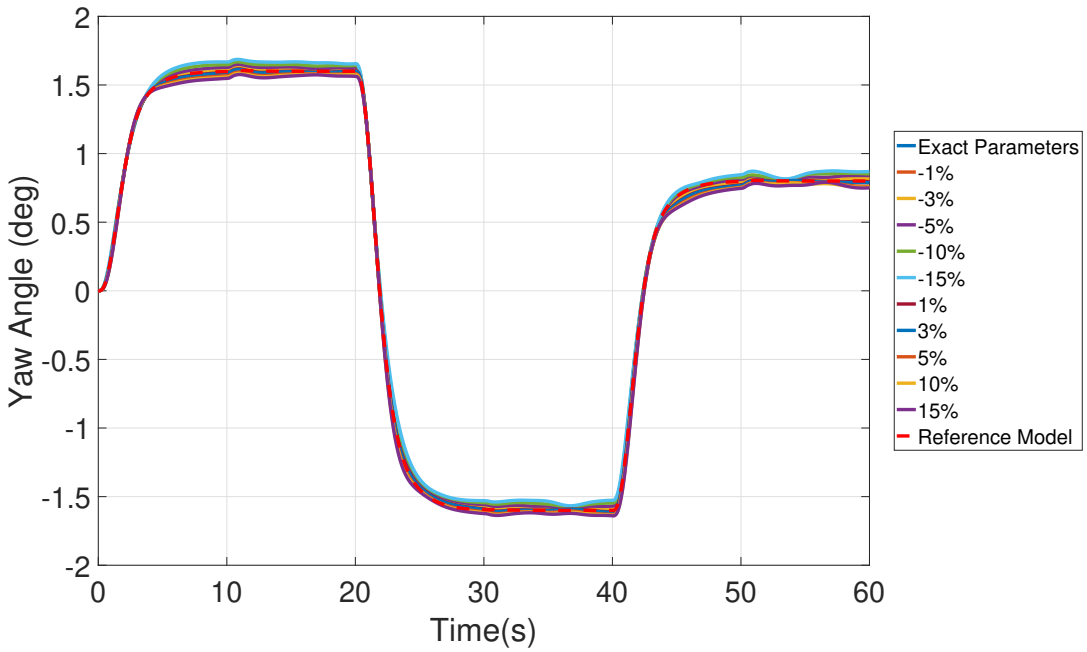

Figure 4.43: Effect of Mass and Inertia Change in Yaw Angle Tracking Performance with Random External Dist.

As seen in Figure 4.40-4.43, mass and inertias are changed up to $\pm 15\%$. It can be said that system uncertainties caused by mass and inertia differences do not create a big

problem and tracking of the system is kept with small errors. It also seems that high frequency oscillations start especially in the collective channel when the difference is around $\pm 10\% - \pm 15\%$. By a close look to first five seconds after simulation start in order to investigate the adaptation process clearly,

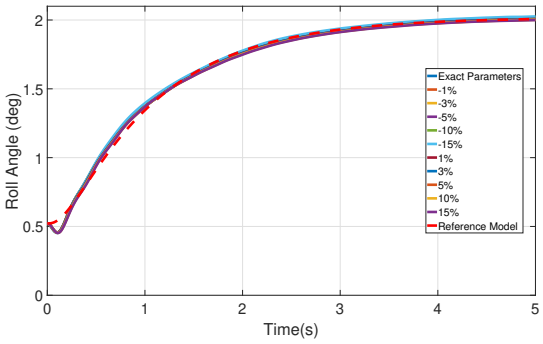

(a) Effect of Mass and Inertia Change in Roll Angle Tracking Performance with Random External Dist. (0-5s)

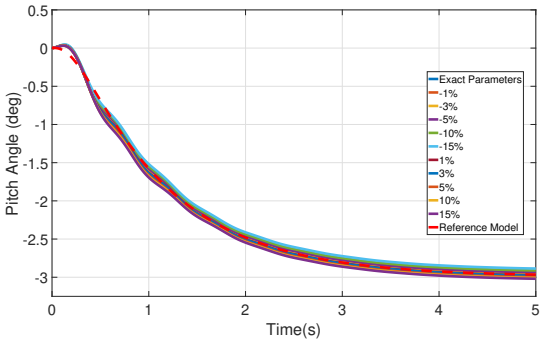

(b) Effect of Mass and Inertia Change in Pitch Angle Tracking Performance with Random External Dist. (0-5s)

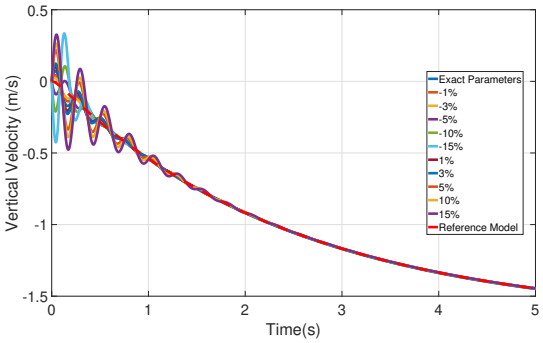

(c) Effect of Mass and Inertia Change in Vertical Velocity Tracking Performance with Random External Dist. (0-5s)

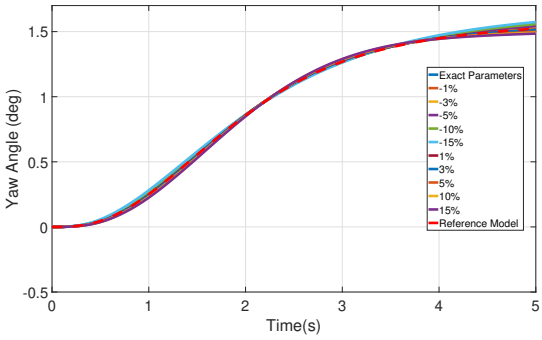

(d) Effect of Mass and Inertia Change in Yaw Angle Tracking Performance with Random External Dist. (0-5s)

Figure 4.44: Effect of Mass and Inertia Change of LQI-MRAC with Random External Dist. (0-5s)

Next, total inputs acting on the four different input channels are shown in Figure 4.45-4.48.

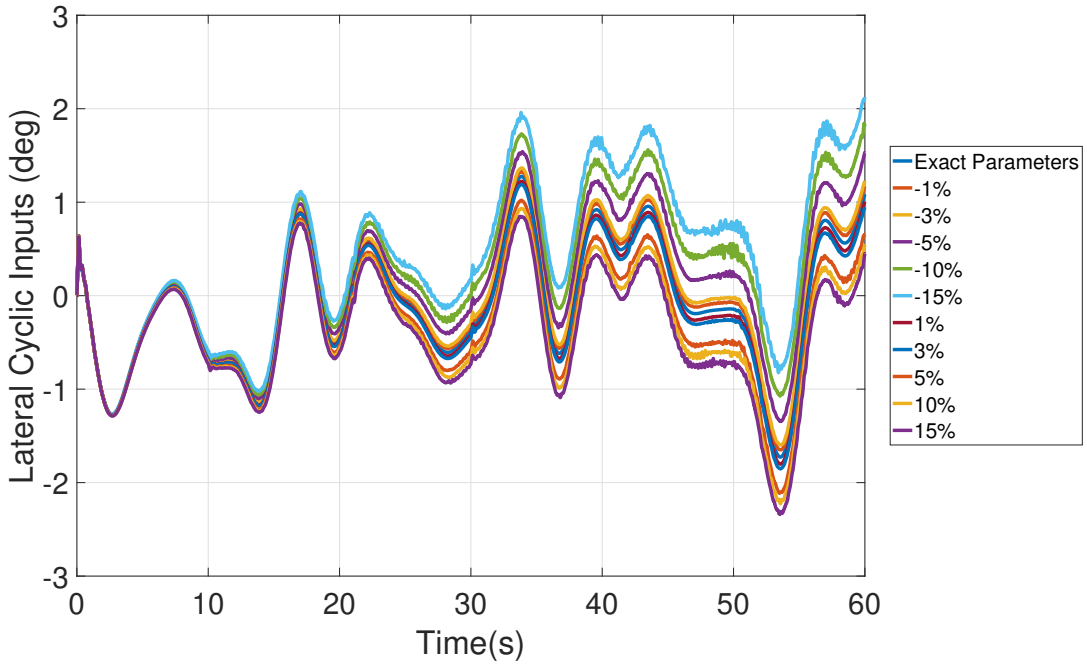

Figure 4.45: Lateral Cyclic Inputs

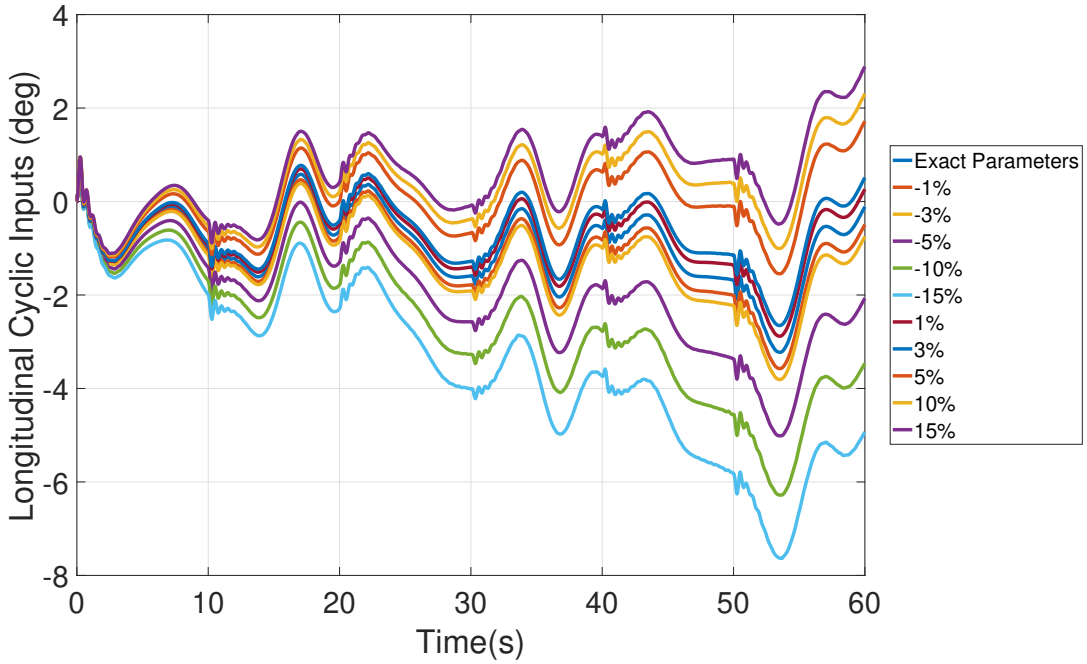

Figure 4.46: Longitudinal Cyclic Inputs

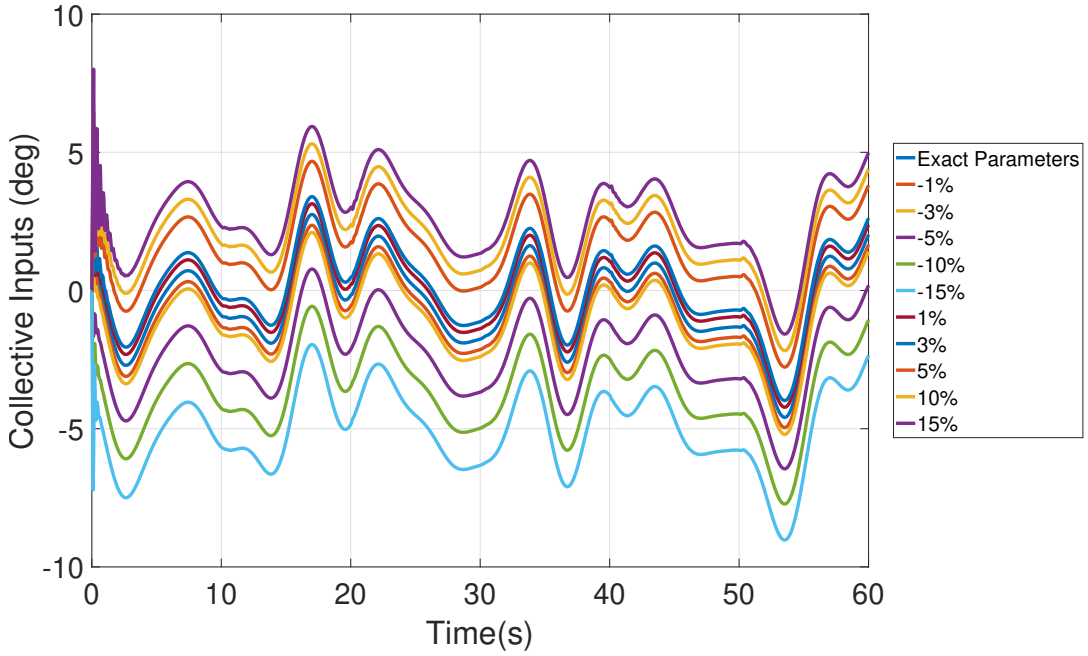

Figure 4.47: Collective Inputs

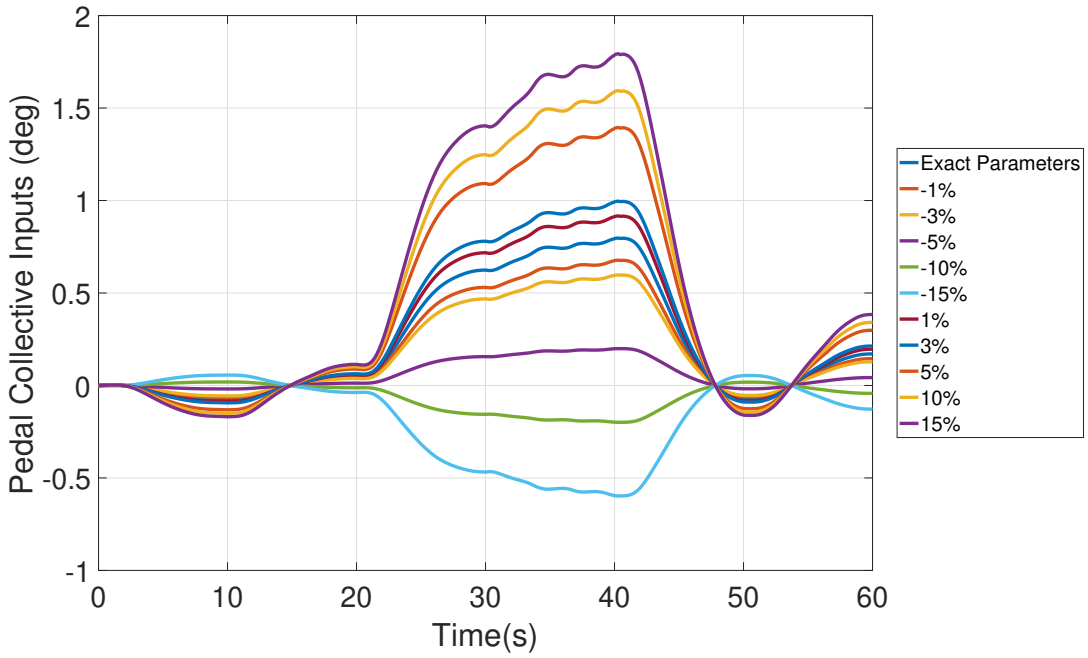

Figure 4.48: Pedal Collective Inputs

By looking total inputs, it can be said that there will not be a serious problem up to %10 percent mass and inertia difference between measured and model parameters. The problem for $10+\%$ is seen in especially collective input in Figure 4.47.

Aerodynamics Parameter Differences: Secondly, aerodynamics parameters variation is examined. Lift curve slope and main rotor rotation speed are the selected parameters to be changed. Reference model tracking performance are presented in Figure 4.49-4.52.

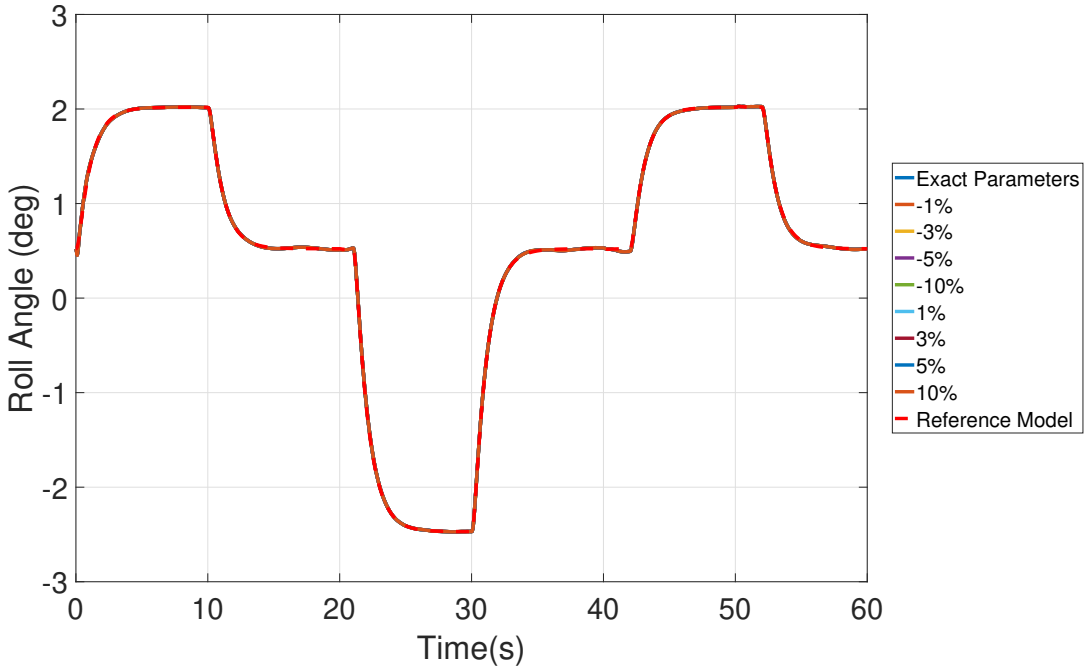

Figure 4.49: Effect of Main Rotor RPM and Lift Curve Slope Change in Roll Angle Tracking Performance with Random External Dist.

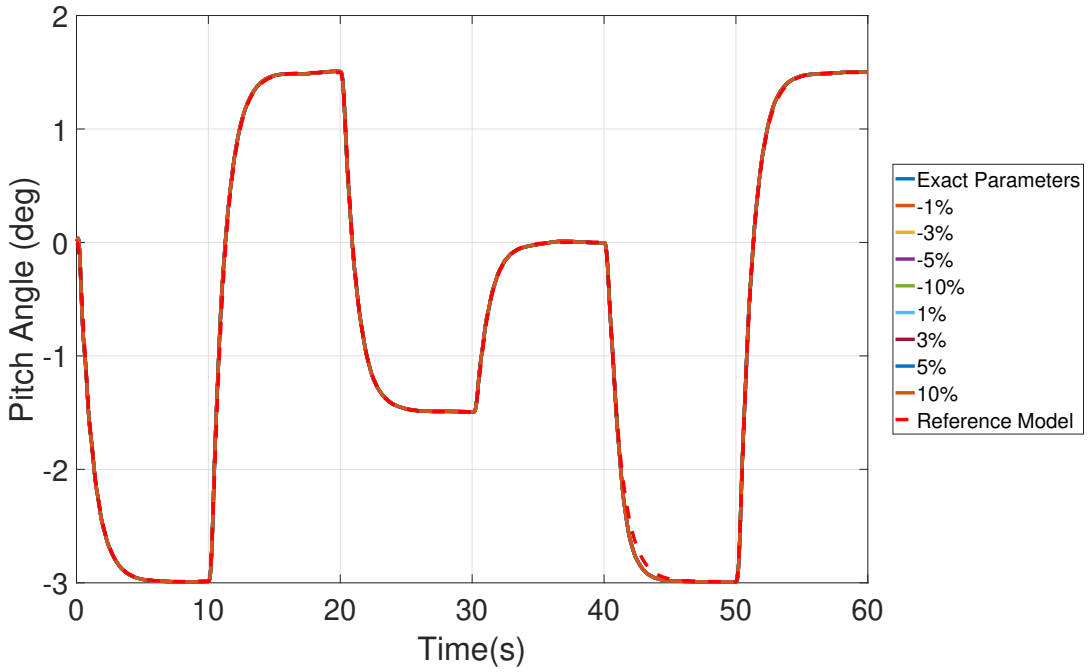

Figure 4.50: Effect of Main Rotor RPM and Lift Curve Slope Change in Pitch Angle Tracking Performance with Random External Dist.

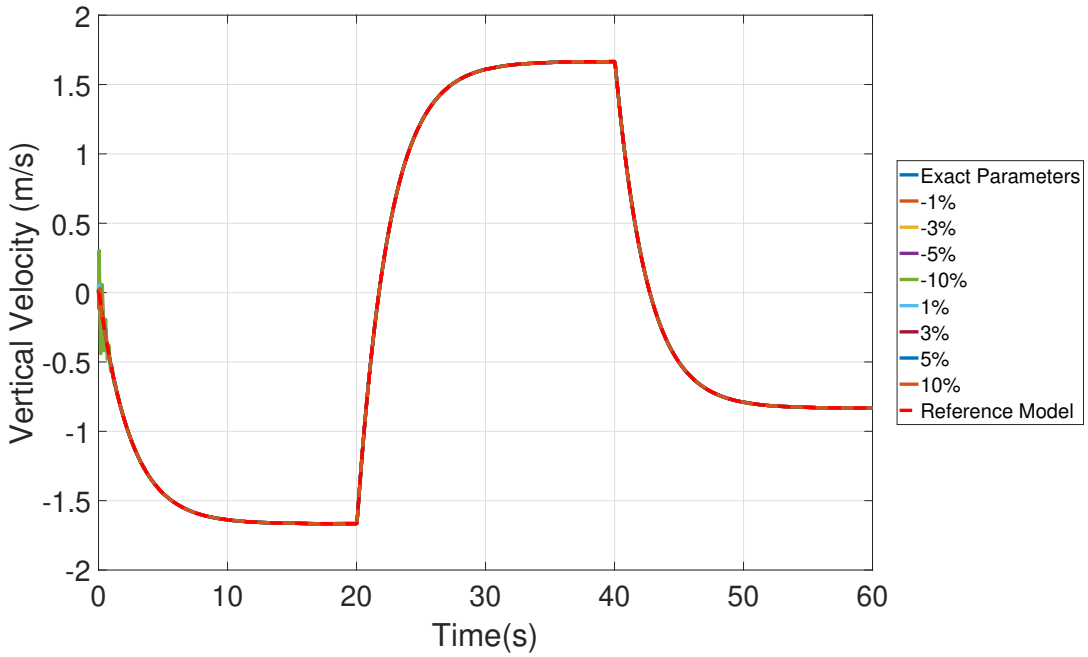

Figure 4.51: Effect of Main Rotor RPM and Lift Curve Slope Change in Vertical Velocity Tracking Performance with Random External Dist.

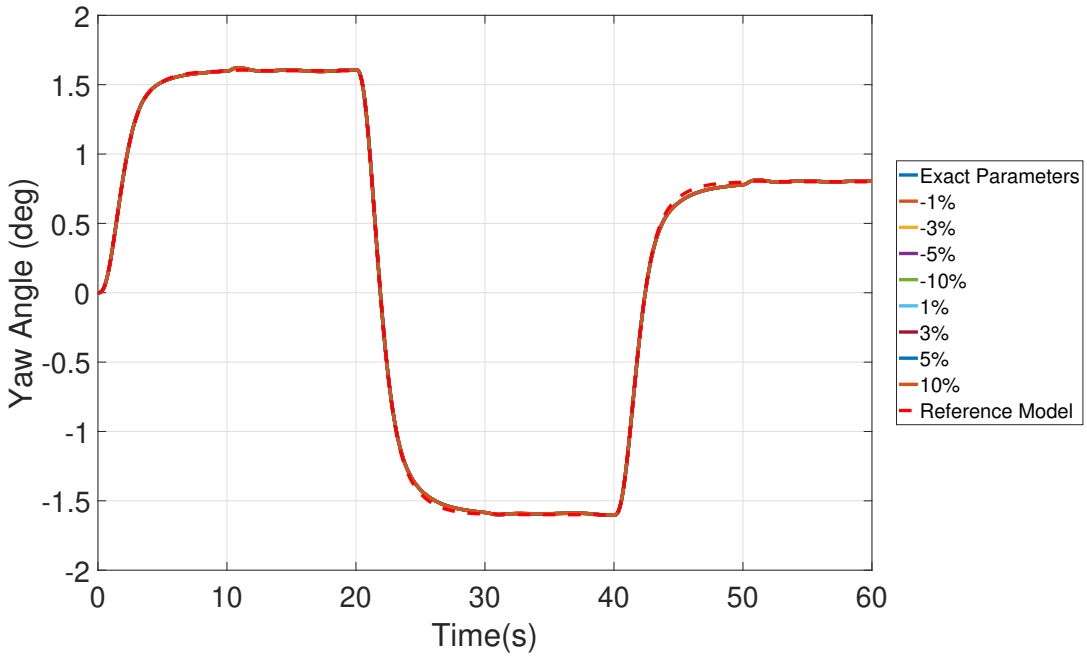

Figure 4.52: Effect of Main Rotor RPM and Lift Curve Slope Change in Yaw Angle Tracking Performance with Random External Dist.

As seen in Figure 4.49–4.52, lift curve slope and main rotor rotation speed are changed up to $\pm 10\%$. Again, aerodynamics parameters does not affect the closed loop system significantly in tracking of reference model manner. It also seems that high frequency oscillations start especially in the collective channel when the difference is around $\pm 10\% - \pm 15\%$. By a close look to first five seconds after simulation start in order to investigate the adaptation process clearly,

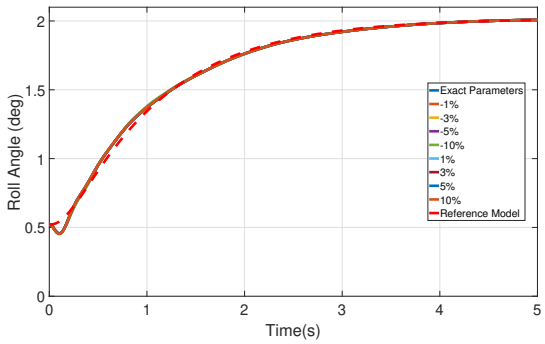

(a) Effect of Main Rotor RPM and Lift Curve Slope Change in Roll Angle Tracking Performance with Random External Dist. (0-5s)

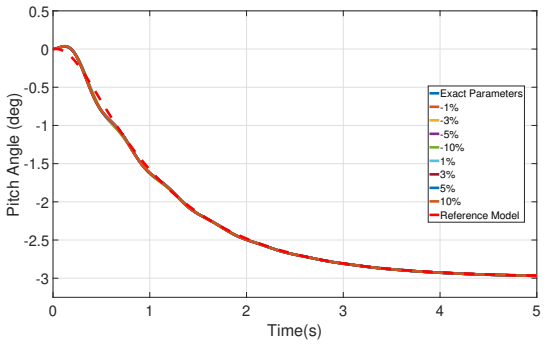

(b) Effect of Main Rotor RPM and Lift Curve Slope Change in Pitch Angle Tracking Performance with Random External Dist. (0-5s)

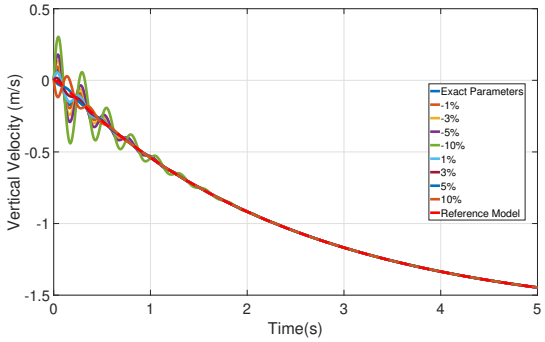

(c) Effect of Main Rotor RPM and Lift Curve Slope Change in Vertical Velocity Tracking Performance with Random External Dist. (0-5s)

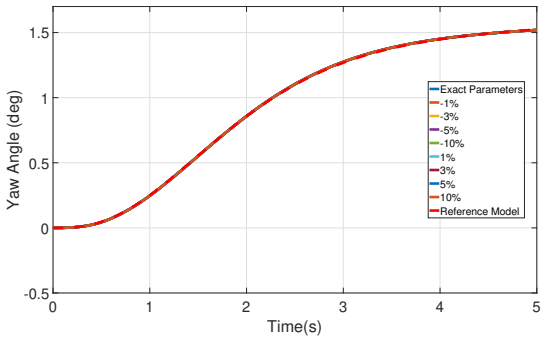

(d) Effect of Main Rotor RPM and Lift Curve Slope Change in Yaw Angle Tracking Performance with Random External Dist. (0-5s)

Figure 4.53: Effect of Mass and Inertia Change of LQI-MRAC with Random External Dist. (0-5s)

As seen in Figure 4.53, in collective channel, system is more sensitive to decrease in selected aerodynamics parameters than increase in these parameters. That is, although tracking performance are not changed significantly when the parameters are increase by 10%, oscillation in first part of the adaptation affects the tracking reference model.

Next, total inputs acting on the four different input channels are shown in Figure 4.54–4.57.

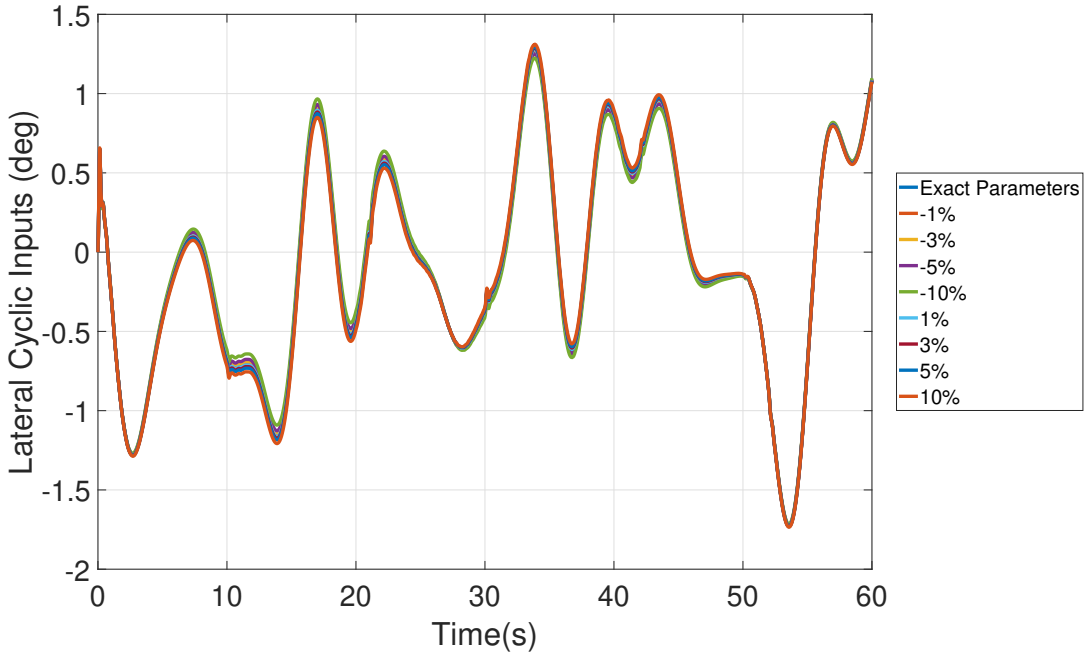

Figure 4.54: Lateral Cyclic Inputs

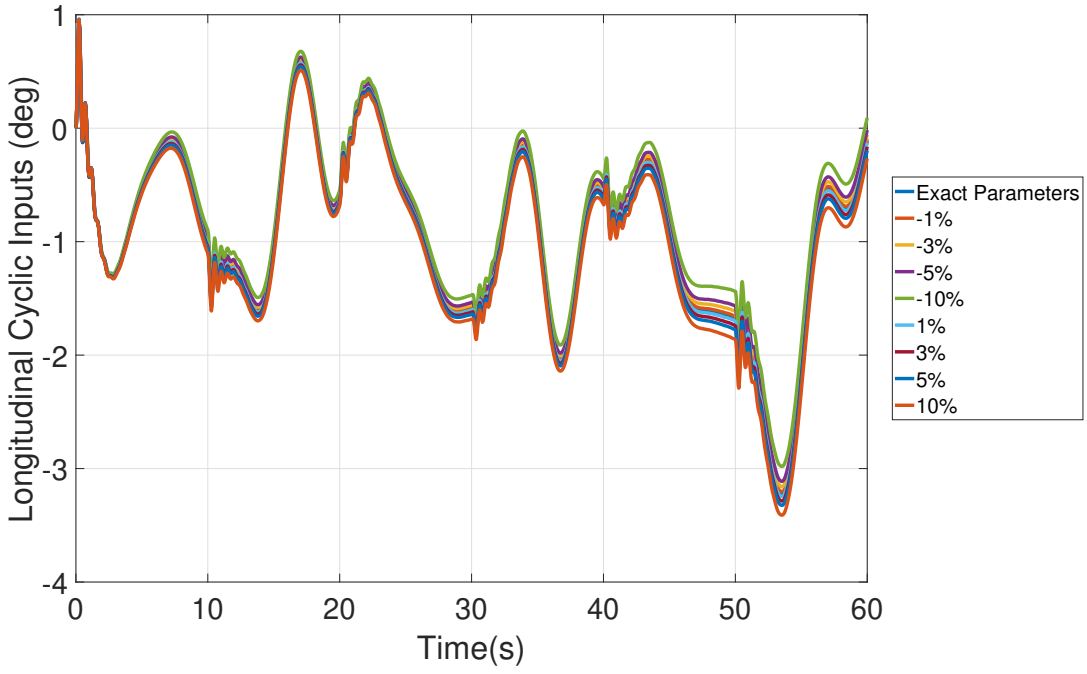

Figure 4.55: Longitudinal Cyclic Inputs

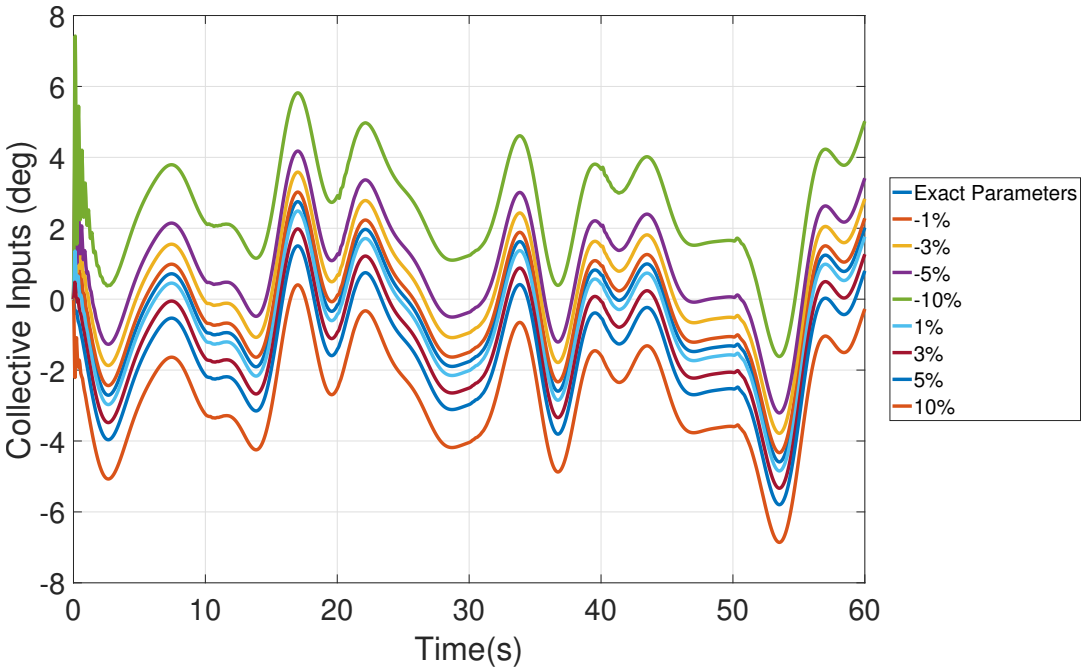

Figure 4.56: Collective Inputs

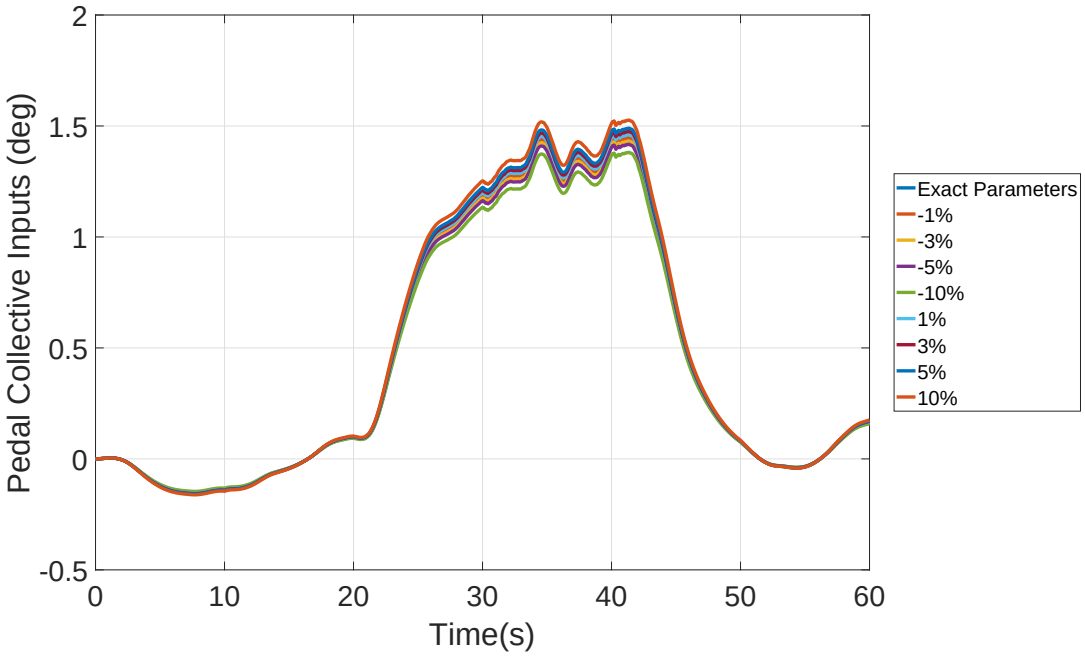

Figure 4.57: Pedal Collective Inputs

By looking total inputs, it can be said that there will not be a serious problem up to 10% percent selected aerodynamic parameters difference between measured and model parameters. The chattering problem for $\pm 10 + \%$ is seen in especially collective input in Figure 4.56.

4.3 Discussions

In this section, LQI and MRAC controllers are implemented on the nonlinear helicopter model. Response of the helicopter, model inputs and adaptive weight are shown and compared under three different types of disturbance in input channels. As the first step of the design and implementation part, reference model is chosen. Considering ideal conditions, that is there is not any uncertainty on the system, ideal response of the helicopter is chosen by LQI controller and the ideal response is plotted in Figure 4.1. Since internal and external uncertainties are not considered in LQI design for the open loop linear helicopter model, it is expected that reference model has exactly the same response with the closed loop helicopter model with the baseline LQI controller (See Figure 4.2). Unlike linear case, some uncertainties exist in the nonlinear helicopter model such as mathematical calculation errors during linearization and model order reduction. Therefore, response of the nonlinear helicopter model with LQI controller are not exactly same with the reference model. Secondly, MRAC controller is designed and implemented to cancel out the internal uncertainties on the system. Consequently, it is provided that closed loop nonlinear helicopter model with baseline LQI controller and MRAC follows the reference model without any transient and steady state error (See Figure 4.3). MRAC controller is designed by using reduced order linear model and reference model and it is testes on both linear and nonlinear helicopter models. In order to realize the effect of MRAC controller, it is a good way to show adaptive inputs of the closed loop systems. In Figure 4.4, it is clearly seen that adaptive inputs are commanded to the nonlinear helicopter model by MRAC controller against the internal uncertainties. Unlike nonlinear case, there is not any uncertainty on the linear helicopter model and adaptive inputs are zero in all input channels as expected (See Figure 4.4). Thirdly, disturbance rejection performance of MRAC augmented LQI controller is analyzed. In this manner, three

different types of disturbance are applied to the input channels (See Figure 4.5–4.7). Response of the nonlinear helicopter models are plotted and tracking performances, oscillations in inputs and boundedness of adaptive weights are evaluated. In the first MRAC design and implementation, projection operator and e-modification are used as modification and sigmoid functions are used in uncertainty parametrization. To examine the effectiveness of modifications, response of the helicopter is plotted with and without MRAC modifications (See Figure 4.8 and Figure 4.11). It is seen that modifications in adaptive law decreases the transient error in tracking the reference model and bounds the adaptive weights. However, tracking performance is still not as desired and the need of modification on uncertainty parametrization arises. Fourthly, Fourier Series are implemented on the uncertainty parametrization element in MRAC controller. In design process, it is noticed that series period and length are effective especially in tracking the reference model. Tuning period and series length, nonlinear helicopter response is plotted and it is seen that a remarkable tracking improvement occurs and high frequency input problems in first MRAC design attempt with sigmoid functions are solved (See Figure 4.18, 4.21 and 4.24). Fifthly, Chebyshev Polynomials are used in the uncertainty parametrization of MRAC. The only one effective design parameter is polynomials length. After tuning polynomials length, simulations are performed with the nonlinear helicopter model controller by MRAC augmented LQI controller. Simulation is stopped about in 5s. Chebyshev Polynomials do not succeed in approximating the uncertainty on the system and the response of the helicopter diverges as seen in Figure 4.26 and 4.27. After analyzing the approximation method and the unknown numbers to be calculated, it is concluded that 4x82 elements are almost impossible to calculate considering the simulation and calculations performance (See Equation 4.11–4.12). Sixthly, a modification on the Chebyshev Polynomials is considered. Although the original polynomials are in terms of system states, they are converted to time based polynomials as in Equation 4.14 by keeping the orthogonal property of the Chebyshev Polynomials. Modified version of polynomials only depend of time and the unknown numbers to be calculated are less than the original one. Then, nonlinear helicopter model response is plotted in Figure 4.29 and 4.32. It is seen that tracking performance is very close to Fourier Series and they are shown in the same plot as in Figure 4.29. It is concluded that using larger series period in Fourier Series approximates the response to Time Based Chebyshev Polynomials

(See Figure 4.31). This completes the design and implementation process. As the last step of the design and implementation part, it is decided that using Time Based Chebyshev Polynomials and Fourier Series in uncertainty parametrization with appropriate design parameters do not differ from each other. However, considering the ease of design and less design parameter encourage to use Chebyshev Polynomials. Moreover, e-modification and projection operator are still effective in decreasing the transient tracking error and boundedness of the adaptive weights. Lastly, some case studies are done to examine the controller performance better. First, sequential step commands are given to the system and it is expected that the nonlinear helicopter model tracks the predefined reference model. Response of the helicopter model is given in Figure 4.35 and it is compared with the non-adaptive case to see the effect of MRAC controller better. Next, robustness analysis is done. Although proposed controller scheme and technique are not assertive with system uncertainties, it is wondered that whether system uncertainties create a catastrophic results or not. The effect of the difference in mass and inertia of real values and model parameters are aimed. Tracking performance and total inputs commanded to the nonlinear helicopter model is analyzed and plotted in Figure 4.40–4.48. Then, difference in main rotor rotation speed and lift curve slope of real values and model parameters are analyzed. Again, tracking performance and total inputs commanded to the nonlinear helicopter model is analyzed and plotted in Figure 4.49–4.57. Consequently, it is concluded that up to about 10%-15% difference with ideal values of main rotor rotation speed and lift curve slope, helicopter tracking performance and total inputs commanded to the nonlinear helicopter model is reasonable.

CHAPTER 5

CONCLUSION

In this thesis, derivation of the nonlinear mathematical model for a small scale helicopter is presented. All equations used in modeling are written in terms of helicopter parameters; however, derived mathematical model is appropriate for small size helicopters satisfying assumptions stated in Section 2.1.1. After constructing the nonlinear helicopter model, it is linearized around hover condition at 100 ft and order of the linear model is reduced for controller design purpose.

Design and modifications of the model reference adaptive control is the other focus of this thesis. First, classical MRAC controller for a MIMO system is designed. Reference model is designed with optimal tracking control by LQR method. Classical MRAC controller is designed without any modifications and Sigmoid Functions are used in its uncertainty parametrization component. Baseline LQR controller and MRAC controller tracking performance is examined under different types of disturbances given to all input channels of the helicopter along the simulation. From the simulations, it is verified that non-adaptive baseline controller could not succeed tracking of the reference model with existence of external disturbances on the system. Classical MRAC performs satisfactory tracking performance and it cancels out the external disturbances; however, it is considered that transient response is not good enough and some oscillations exist in the inputs. Using e-modification and projection operator provides better performance and adaptive law is modified accordingly.

After modifying adaptive law, some modifications are considered on the other key element of MRAC, uncertainty parametrization. Since the helicopter system and designed classical MRAC controller are both MIMO systems, estimating all adaptive weights are not straightforward. Sigmoid Functions require state information of

the helicopter and this may be problematic when state number of the MIMO system is high. At this point, use of time based universal approximators in uncertainty parametrization is proposed. Previously, Fourier Series and Chebyshev Polynomials have been used in wing-rock problem [[13],[34]]. Both approximators are tried to estimate and suppress the uncertainty on the system. While use of Fourier Series performs better transient response and tracking performance than classical MRAC controller, state dependent Chebyshev Polynomials could not estimate the adaptive weights and cause the helicopter response diverges. The source of the problem is again related with the high number of system states and it is proposed to write Chebyshev Polynomials with only time dependent instead of state dependent. Use of time based Chebyshev Polynomials in uncertainty parametrization provides the best performance in terms of reference model tracking and low frequency control input command. Finally, classical MRAC controller is formed to the final configuration in such a manner that e-modification and projection operator are used in its adaptive weight update law and uncertainty is parametrized with time based Chebyshev Polynomials written in the form of Equation 4.14. As the last step, case studies are performed for observing the tracking performance of the MRAC controller in the proposed structure.

5.1 Findings

- Generic mathematical model for model helicopters is derived and implicit equations are given in terms of helicopter parameters. This provides that presented mathematical model can be used for different helicopters satisfying the given assumptions.

- From the simulations performed, it is deduced that the system is more sensitive in roll channel than other channels. This is probably because of the low moment of inertia in the relevant axis. This problem may not be seen with the choice of more robust sample helicopter in roll channel.

- In the controller design and implementation process, control channels are not separated from each other. That is, multidimensional controller gains and weight matrices are used in the design. Adaptive weights calculation does not seem easy with this controller structure, however, it provides the ease of design and

better coupling effects suppression.

- Adaptive law modifications like σ-modification and e-modification improves the adaptation process and tracking performance, however, they are not effective as using them in less complex systems such as wing-rock problem. For more complex systems, uncertainty parametrization plays the key role.

- It may be concluded that using time based Chebyshev Polynomials in uncertainty parametrization provides better tracking performance than using Fourier Series. However, this is related with the tuning of controller gains and learning rates. The only one advantage of using Chebyshev Polynomials is that it requires less design parameter than using Fourier Series. The common property of the both universal approximators is parametrizing uncertainty on the system using time data instead of states of the system.

5.2 Future Search and Recommendations

Future works of this thesis can include the verification of the presented mathematical model with using flight test data. Detailed comparison of the Fourier Series and Chebyshev Polynomials can be performed in terms of adaptation property. Baseline controller can be substituted with a robust controller to handle system uncertainties. Moreover, experimental verification of the proposed controller structure may be the main focus of the future works and robustness of the controller can be examined under real world limitations like input delays of the selected hardwares.

REFERENCES

[1] U. D. o. T. F. A. Administration. *Helicopter Flying Handbook*, volume 5. 2012.

[2] AIAA. American National Standard Guide to Reference and Standard Atmosphere Models. 2010(BSR/AIAA G-003C-2010 (Revision of G-003B-2004)):1–153, 2010.

[3] F. M. Al-Sunni and F. L. Lewis. Gain scheduling simplification by simultaneous control design. *Journal of Guidance, Control, and Dynamics*, 16(3):602–603, 1993.

[4] Astrom, K.J. and Wittenmark, B. *Adaptive Control*. Dover Books on Electrical Engineering. Dover Publications, 2008.

[5] M. Bisgaard. *Modeling , Estimation, and Control of Helicopter Slung Load System*. PhD thesis, Aalborg University, 2007.

[6] R. Chen. *A simplified rotor system mathematical model for piloted flight dynamics simulation*. 1979.

[7] G. Chowdhary and E. Johnson. Adaptive neural network flight control using both current and recorded data. 08 2007.

[8] M. L. Civita, W. Messner, and T. Kanade. Modeling of small-scale helicopters with integrated first-principles and system-identification techniques. In *Proceedings of the 58th Forum of the American Helicopter Society*, pages 2505 – 2516, June 2002.

[9] D. Costarelli. *Sigmoidal Functions Approximation and Applications*. PhD thesis, Roma Tre University, 2013.

[10] J.-J. E. Slotine and J. A. Coetsee. Adaptive sliding controller synthesis for non-linear systems. 43:1631–1651, June 1986.

[11] L. Eugene and K. A. Wise. *Robust and Adaptive Control with Aerospace Applications*. 2013.

[12] V. Gavrilets. *Autonomous Aerobatic Maneuvering of Miniature Helicopters*. PhD thesis, Massachusetts Institute of Technology, 2003.

[13] R. B. Gezer. Fourier Series Based Model Reference Adaptive Control. Master's thesis, METU, 2014.

[14] R. Hibbeler. *Engineering Mechanics: Dynamics*. MasteringEngineering Series. Prentice Hall, 2010.

[15] P. A. Ioannou and P. V. Kokotovic. *Adaptive Systems with Reduced Models*. Springer-Verlag, Berlin, Heidelberg, 1983.

[16] R. K. Heffley and M. A. Mnich. Minimum-complexity helicopter simulation math model. May 1988.

[17] R. E. Kalman. Design of a self-optimizing control system. *Trans. ASME*, 80:468–478, February 1958.

[18] K. Kim, T. Yucelen, and A. Calise. K- modification in adaptive control. April 2010.

[19] E. Lavretsky, R. Gadient, and I. Gregory. Predictor-based model reference adaptive control. 33:1195–1201, 07 2010.

[20] E. Lavretsky and T. E. Gibson. Projection Operator in Adaptive Systems. 2011.

[21] L. Ljung. *System Identification: Theory for the User*. Prentice Hall PTR, 1999.

[22] L. Ljung and I. Landau. Model reference adaptive systems and self-tuning regulators - some connections. *IFAC Proceedings Volumes*, 11(1):1973 – 1979, 1978. 7th Triennial World Congress of the IFAC on A Link Between Science and Applications of Automatic Control, Helsinki, Finland, 12-16 June.

[23] J. Luo and C. Lan. Control of wing-rock motion of slender delta wings. 16:225–231, 03 1993.

[24] R. Mahony, T. Hamel, and A. Dzul. Hover control via lyapunov control for an autonomous model helicopter. 4:3490–3495 vol.4, 1999.

[25] B. Mettler, M. Tischler, and T. Kanade. System identification modeling of a small-scale unmanned rotorcraft for flight control design. *Journal of the American Helicopter Society*, 47(1):50–63, January 2002.

[26] J. C. Morris, M. van Nieuwstadt, and P. Bendotti. Identification and control of a model helicopter in hover. 2:1238–1242 vol.2, June 1994.

[27] J. F. Muller. Systematic Determination of Simplified Gain Scheduling Programs. 152(i), 1967.

[28] C. Munzinger. *Development of a Real-Time Flight Simulator for an Experimental Model Helicopter*. PhD thesis, Georgia Institute of Technology, 1998.

[29] K. Narendra and A. Annaswamy. A new adaptive law for robust adaptive control without persistent excitation. 32:134 – 145, March 1987.

[30] K. Narendra and A. Annaswamy. *Stable Adaptive Systems*. Dover Books on Electrical Engineering. Dover Publications, 2012.

[31] N. Nguyen. Multi-objective optimal control modification adaptive control method for systems with input and unmatched uncertainties. January 2014.

[32] N. Nguyen. *Model-Reference Adaptive Control: A Primer*. Advanced Textbooks in Control and Signal Processing. Springer International Publishing, 2018.

[33] N. Nguyen, K. Krishnakumar, and J. Boskovic. An optimal control modification to model-reference adaptive control for fast adaptation. August 2008.

[34] N. T. Nguyen, J. Burken, and A. Ishihara. Least-Squares Adaptive Control Using Chebyshev Orthogonal Polynomials. *AIAA Infotech Conference*, (March):1–21, 2011.

[35] K. Ogata. *Modern Control Engineering*. 1990.

[36] G. Padfield. *Helicopter Flight Dynamics: The Theory and Application of Flying Qualities and Simulation Modelling*. AIAA education series. Wiley, 2008.

[37] P. Parks. Liapunov redesign of model reference adaptive control systems. *IEEE Transactions on Automatic Control*, 11(3):362–367, Jul 1966.

[38] B. Peterson and K. Narendra. Bounded error adaptive control. *IEEE Transactions on Automatic Control*, 27(6):1161–1168, December 1982.

[39] R. Pettersen, E. Mustafic, and M. Fogh. Nonlinear Control Approach to Helicopter Autonomy. Master's thesis, 2005.

[40] R. Prouty. *Helicopter Performance, Stability, and Control*. R.E. Krieger Publishing Company, 1995.

[41] B. Ren, S. S. Ge, C. Chen, C. H. Fua, and T. H. Lee. *Modeling, control and coordination of helicopter systems*, volume 9781461415633. 2012.

[42] T. Richardson, P. Davison, M. Lowenberg, and M. di Bernardo. Control of Nonlinear Aircraft Models Using Dynamic State-Feedback Gain Scheduling. *AIAA Guidance, Navigation, and Control Conference and Exhibit*, (August):5503, 2003.

[43] J. Roskam. *Airplane Flight Dynamics and Automatic Flight Controls*. Number 1. böl. in Airplane Flight Dynamics and Automatic Flight Controls. Roskam Aviation and Engineering Corporation, 1998.

[44] B. Shackcloth and R. L. Butchart. Synthesis of Model Reference Adaptive Systems by Liapunov's Second Method. *Theory of Self-adaptive Control Systems*, -1:145, 1966.

[45] L. S. Shieh, J. W. Sunkel, Z. Z. Yuan, and X. M. Zhao. Self-tuning control of attitude and momentum management for the Space Station. *Journal of Guidance Control and Dynamics*, 11(1):19–25, 1992.

[46] H. Shim, T. J. Koo, F. Hoffmann, and S. Sastry. A comprehensive study of control design for an autonomous helicopter. 4:3653–3658 vol.4, December 1998.

[47] G. Shumsky. Wing rock on a delta wing. pages 110–111, October 2006.

[48] S. Singh, W. R. Wells, and W. Yirn. Direct adaptive and neural control of wing-rock motion of slender delta wings. 18:25–30, 01 1995.

[49] G. Stein, G. Hartmann, and R. Hendrick. Adaptive control laws for f-8 flight test. *IEEE Transactions on Automatic Control*, 22(5):758–767, October 1977.

[50] P. Talbot and L. D. Corliss. *A mathematical force and moment model of a UH-1H helicopter for flight dynamics simulations*. 1977.

[51] P. D. Talbot, B. E. Tinling, W. a. Decker, and R. T. N. Chen. A mathematical model of a single main rotor helicopter for piloted simulation. *Nasa Technical Memorandum*, 84281(September):46, 1982.

[52] G. Tao. *Adaptive Control Design and Analysis*. Adaptive and Cognitive Dynamic Systems: Signal Processing, Learning, Communications and Control. Wiley, 2003.

[53] K. Y. Volyanskyy, A. J. Calise, and B.-J. Yang. A novel q-modification term for adaptive control. June 2006.

[54] H. Whitaker, J. Yamron, A. Kezer, and M. I. of Technology. Instrumentation Laboratory. *Design of Model-reference Adaptive Control Systems for Aircraft*. Report Massachusetts Institute of Technology Instrumentation Laboratory R. M.I.T. Instrumentation Laboratory, 1958.

[55] T. Yucelen and A. J. Calise. Kalman Filter Modification in Adaptive Control. *Journal of Guidance, Control, and Dynamics*, 33(2):426–439, 2010.

APPENDIX A

EQUATIONS OF THE MAIN ROTOR DYNAMICS

Main Rotor Flappings:

$$\ddot{\beta}_0 = -(24K_s\beta_0 + 24I_{b_{mr}}\beta_0\Omega_{mr}^2 - 12I_{b_{mr}}\beta_0 p^2 - 12I_{b_{mr}}\beta_0 q^2 + 24I_{b_{mr}}\beta_0 r^2$$
$$+ 48I_{b_{mr}}\beta_0\Omega_{mr}r - 24I_{b_{mr}}\beta_0\beta_{1c}\Omega_{mr}p + 24I_{b_{mr}}\beta_0\beta_{1s}\Omega_{mr}q - 24I_{b_{mr}}\beta_0\beta_{1c}pr$$
$$+ 24I_{b_{mr}}\beta_0\beta_{1s}qr + 24X_{cg}\beta_0 e_{mr}m_b\Omega_{mr}^2 + 12X_{cg}\beta_0 e_{mr}m_b p^2 + 12X_{cg}\beta_0 e_{mr}m_b q^2$$
$$+ 24X_{cg}\beta_0 e_{mr}m_b r^2 + 3R_{mr}^4 C_{l_{\alpha_{mr}}}\dot{\beta}_0 c_{mr}\Omega_{mr}\rho + 2R_{mr}^3 C_{l_{\alpha_{mr}}}\dot{\beta}_{1s}c_{mr}\rho u$$
$$+ 2R_{mr}^3 C_{l_{\alpha_{mr}}}\dot{\beta}_{1c}c_{mr}\rho v - C_{l_{\alpha_{mr}}}\dot{\beta}_0 c_{mr}e_{mr}^4\Omega_{mr}\rho + 2R_{mr}^3 C_{l_{\alpha_{mr}}}c_{mr}p\rho u$$
$$+ 4R_{mr}^3 C_{l_{\alpha_{mr}}}c_{mr}\Omega_{mr}\rho v_i - 4R_{mr}^3 C_{l_{\alpha_{mr}}}c_{mr}\Omega_{mr}\rho w + 2R_{mr}^3 C_{l_{\alpha_{mr}}}c_{mr}q\rho v$$
$$- 2C_{l_{\alpha_{mr}}}\dot{\beta}_{1s}c_{mr}e_{mr}^3\rho u - 2C_{l_{\alpha_{mr}}}\dot{\beta}_{1c}c_{mr}e_{mr}^3\rho v + C_{l_{\alpha_{mr}}}c_{mr}e_{mr}^3 p\rho u + 2C_{l_{\alpha_{mr}}}c_{mr}e_{mr}^3\Omega_{mr}\rho v_i$$
$$- 2C_{l_{\alpha_{mr}}}c_{mr}e_{mr}^3\Omega_{mr}\rho w + C_{l_{\alpha_{mr}}}c_{mr}e_{mr}^3 q\rho v - 3R_{mr}^4 C_{l_{\alpha_{mr}}}c_{mr}\Omega_{mr}^2\rho\theta_0 - 3R_{mr}^2 C_{l_{\alpha_{mr}}}c_{mr}\rho\theta_0 u^2$$
$$- 3R_{mr}^2 C_{l_{\alpha_{mr}}}c_{mr}\rho\theta_0 v^2 - C_{l_{\alpha_{mr}}}c_{mr}e_{mr}^4\Omega_{mr}^2\rho\theta_0 - 3C_{l_{\alpha_{mr}}}c_{mr}e_{mr}^2\rho\theta_0 u^2 - 3C_{l_{\alpha_{mr}}}c_{mr}e_{mr}^2\rho\theta_0 v^2$$
$$+ 48X_{cg}\beta_0 e_{mr}m_b\Omega_{mr}r - 8R_{mr}^3 C_{l_{\alpha_{mr}}}\dot{\beta}_0 c_{mr}e_{mr}\Omega_{mr}\rho + 6R_{mr}C_{l_{\alpha_{mr}}}\dot{\beta}_{1s}c_{mr}e_{mr}^2\rho u$$
$$- 6R_{mr}^2 C_{l_{\alpha_{mr}}}\dot{\beta}_{1s}c_{mr}e_{mr}\rho u + 6R_{mr}C_{l_{\alpha_{mr}}}\dot{\beta}_{1c}c_{mr}e_{mr}^2\rho v - 6R_{mr}^2 C_{l_{\alpha_{mr}}}\dot{\beta}_{1c}c_{mr}e_{mr}\rho v$$
$$- 3R_{mr}^2 C_{l_{\alpha_{mr}}}c_{mr}e_{mr}p\rho u - 6R_{mr}^2 C_{l_{\alpha_{mr}}}c_{mr}e_{mr}\Omega_{mr}\rho v_i + 6R_{mr}^2 C_{l_{\alpha_{mr}}}c_{mr}e_{mr}\Omega_{mr}\rho w$$
$$- 3R_{mr}^2 C_{l_{\alpha_{mr}}}c_{mr}e_{mr}q\rho v + 6R_{mr}C_{l_{\alpha_{mr}}}c_{mr}e_{mr}\rho\theta_0 u^2 + 6R_{mr}C_{l_{\alpha_{mr}}}c_{mr}e_{mr}\rho\theta_0 v^2$$
$$+ 4R_{mr}^3 C_{l_{\alpha_{mr}}}c_{mr}\Omega_{mr}\rho\theta_{1s}u - 3C_{l_{\alpha_{mr}}}\beta_{1c}c_{mr}e_{mr}^3\Omega_{mr}\rho u + 4R_{mr}^3 C_{l_{\alpha_{mr}}}c_{mr}\Omega_{mr}\rho\theta_{1c}v$$
$$+ 3C_{l_{\alpha_{mr}}}\beta_{1s}c_{mr}e_{mr}^3\Omega_{mr}\rho v + 2C_{l_{\alpha_{mr}}}c_{mr}e_{mr}^3\Omega_{mr}\rho\theta_{1s}u + 2C_{l_{\alpha_{mr}}}c_{mr}e_{mr}^3\Omega_{mr}\rho\theta_{1c}v$$
$$+ 6R_{mr}^2 C_{l_{\alpha_{mr}}}\dot{\beta}_0 c_{mr}e_{mr}^2\Omega_{mr}\rho + 4R_{mr}^3 C_{l_{\alpha_{mr}}}c_{mr}e_{mr}\Omega_{mr}^2\rho\theta_0 - 6R_{mr}^2 C_{l_{\alpha_{mr}}}c_{mr}e_{mr}\Omega_{mr}\rho\theta_{1s}u$$
$$- 6R_{mr}^2 C_{l_{\alpha_{mr}}}c_{mr}e_{mr}\Omega_{mr}\rho\theta_{1c}v + 6R_{mr}C_{l_{\alpha_{mr}}}\beta_{1c}c_{mr}e_{mr}^2\Omega_{mr}\rho u - 3R_{mr}^2 C_{l_{\alpha_{mr}}}\beta_{1c}c_{mr}e_{mr}\Omega_{mr}\rho u$$
$$- 6R_{mr}C_{l_{\alpha_{mr}}}\beta_{1s}c_{mr}e_{mr}^2\Omega_{mr}\rho v + 3R_{mr}^2 C_{l_{\alpha_{mr}}}\beta_{1s}c_{mr}e_{mr}\Omega_{mr}\rho v)/(24Ib_{mr})$$

$$\ddot{\beta}_{1s} = -(48K_s\beta_{1s} + 96I_{b_{mr}}\dot{\beta}_{1c}\Omega_{mr} - 96I_{b_{mr}}\Omega_{mr}q - 48I_{b_{mr}}qr - 36I_{b_{mr}}\beta_{1s}q^2 + 48I_{b_{mr}}\beta_{1s}r^2$$
$$+ 48I_{b_{mr}}\beta_0^2\Omega_{mr}q + 36I_{b_{mr}}\beta_{1s}^2\Omega_{mr}q + 48I_{b_{mr}}\beta_0^2 qr + 36I_{b_{mr}}\beta_{1s}^2 qr + 96I_{b_{mr}}\beta_{1s}\Omega_{mr}r$$
$$- 96X_{cg}e_{mr}m_b\Omega_{mr}q - 48X_{cg}e_{mr}m_b qr + 48X_{cg}\beta_{1s}e_{mr}m_b\Omega_{mr}^2 + 36X_{cg}\beta_{1s}e_{mr}m_b p^2$$
$$+ 48X_{cg}\beta_{1s}e_{mr}m_b r^2 + 6R_{mr}^4 C_{l_{\alpha_{mr}}}\dot{\beta}_{1s}c_{mr}\Omega_{mr}\rho + 8R_{mr}^3 C_{l_{\alpha_{mr}}}\dot{\beta}_0 c_{mr}\rho u$$

$$+6R_{mr}^4 C_{l_{\alpha_{mr}}} c_{mr} \Omega_{mr} p\rho - 2C_{l_{\alpha_{mr}}} \dot{\beta}_{1s} c_{mr} e_{mr}^4 \Omega_{mr} \rho - 8C_{l_{\alpha_{mr}}} \dot{\beta}_0 c_{mr} e_{mr}^3 \rho u + 12R_{mr}^2 C_{l_{\alpha_{mr}}} c_{mr} \rho u v_i$$
$$-12R_{mr}^2 C_{l_{\alpha_{mr}}} c_{mr} \rho uw + 2C_{l_{\alpha_{mr}}} c_{mr} e_{mr}^4 \Omega_{mr} p\rho + 12C_{l_{\alpha_{mr}}} c_{mr} e_{mr}^2 \rho u v_i - 12C_{l_{\alpha_{mr}}} c_{mr} e_{mr}^2 \rho uw$$
$$+6R_{mr}^4 C_{l_{\alpha_{mr}}} \beta_{1c} c_{mr} \Omega_{mr}^2 \rho + 6R_{mr}^4 C_{l_{\alpha_{mr}}} c_{mr} \Omega_{mr}^2 \rho \theta_{1s} - 2C_{l_{\alpha_{mr}}} \beta_{1c} c_{mr} e_{mr}^4 \Omega_{mr}^2 \rho + 9R_{mr}^2 C_{l_{\alpha_{mr}}} c_{mr} \rho \theta_{1s} u^2$$
$$+2C_{l_{\alpha_{mr}}} c_{mr} e_{mr}^4 \Omega_{mr}^2 \rho \theta_{1s} + 9C_{l_{\alpha_{mr}}} c_{mr} e_{mr}^2 \rho \theta_{1s} u^2 + 96X_{cg} \beta_{1s} e_{mr} m_b \Omega_{mr} r - 24R_{mr} C_{l_{\alpha_{mr}}} c_{mr} e_{mr} \rho u v_i$$
$$+24R_{mr} C_{l_{\alpha_{mr}}} c_{mr} e_{mr} \rho uw + 12R_{mr}^2 C_{l_{\alpha_{mr}}} \beta_{1c} c_{mr} e_{mr}^2 \Omega_{mr}^2 \rho - 16R_{mr}^3 C_{l_{\alpha_{mr}}} \dot{\beta}_{1s} c_{mr} e_{mr} \Omega_{mr} \rho$$
$$+24R_{mr} C_{l_{\alpha_{mr}}} \dot{\beta}_0 c_{mr} e_{mr}^2 \rho u - 24R_{mr}^2 C_{l_{\alpha_{mr}}} \dot{\beta}_0 c_{mr} e_{mr} \rho u - 8R_{mr}^3 C_{l_{\alpha_{mr}}} c_{mr} e_{mr} \Omega_{mr} p\rho$$
$$+8R_{mr}^3 C_{l_{\alpha_{mr}}} \beta_0 c_{mr} \Omega_{mr} \rho v + 9R_{mr}^2 C_{l_{\alpha_{mr}}} \beta_{1s} c_{mr} \rho uv - 18R_{mr} C_{l_{\alpha_{mr}}} c_{mr} e_{mr} \rho \theta_{1s} u^2$$
$$-16R_{mr}^3 C_{l_{\alpha_{mr}}} c_{mr} \Omega_{mr} \rho \theta_0 u + 4C_{l_{\alpha_{mr}}} \beta_0 c_{mr} e_{mr}^3 \Omega_{mr} \rho v + 9C_{l_{\alpha_{mr}}} \beta_{1s} c_{mr} e_{mr}^2 \rho uv$$
$$-8C_{l_{\alpha_{mr}}} c_{mr} e_{mr}^3 \Omega_{mr} \rho \theta_0 u - 16R_{mr}^3 C_{l_{\alpha_{mr}}} \beta_{1c} c_{mr} e_{mr} \Omega_{mr}^2 \rho + 12R_{mr}^2 C_{l_{\alpha_{mr}}} \dot{\beta}_{1s} c_{mr} e_{mr}^2 \Omega_{mr} \rho$$
$$-8R_{mr}^3 C_{l_{\alpha_{mr}}} c_{mr} e_{mr} \Omega_{mr}^2 \rho \theta_{1s} + 24R_{mr}^2 C_{l_{\alpha_{mr}}} c_{mr} e_{mr} \Omega_{mr} \rho \theta_0 u - 18R_{mr} C_{l_{\alpha_{mr}}} \beta_{1s} c_{mr} e_{mr} \rho uv$$
$$-12R_{mr}^2 C_{l_{\alpha_{mr}}} \beta_0 c_{mr} e_{mr} \Omega_{mr} \rho v)/(48 I b_{mr})$$

$$\ddot{\beta}_{1c} = -(48K_s \beta_{1c} - 96I_{b_{mr}} \dot{\beta}_{1s} \Omega_{mr} + 96I_{b_{mr}} \Omega_{mr} p + 48I_{b_{mr}} pr - 36I_{b_{mr}} \beta_{1c} p^2 + 48I_{b_{mr}} \beta_{1c} r^2$$
$$-48I_{b_{mr}} \beta_0^2 \Omega_{mr} p - 36I_{b_{mr}} \beta_{1c}^2 \Omega_{mr} p - 48I_{b_{mr}} \beta_0^2 pr - 36I_{b_{mr}} \beta_{1c}^2 pr + 96I_{b_{mr}} \beta_{1c} \Omega_{mr} r$$
$$+96X_{cg} e_{mr} m_b \Omega_{mr} p + 48X_{cg} e_{mr} m_b pr + 48X_{cg} \beta_{1c} e_{mr} m_b \Omega_{mr}^2 + 36X_{cg} \beta_{1c} e_{mr} m_b q^2$$
$$+48X_{cg} \beta_{1c} e_{mr} m_b r^2 + 6R_{mr}^4 C_{l_{\alpha_{mr}}} \dot{\beta}_{1c} c_{mr} \Omega_{mr} \rho + 8R_{mr}^3 C_{l_{\alpha_{mr}}} \dot{\beta}_0 c_{mr} \rho v + 6R_{mr}^4 C_{l_{\alpha_{mr}}} c_{mr} \Omega_{mr} q\rho$$
$$-2C_{l_{\alpha_{mr}}} \dot{\beta}_{1c} c_{mr} e_{mr}^4 \Omega_{mr} \rho - 8C_{l_{\alpha_{mr}}} \dot{\beta}_0 c_{mr} e_{mr}^3 \rho v + 12R_{mr}^2 C_{l_{\alpha_{mr}}} c_{mr} \rho v v_i - 12R_{mr}^2 C_{l_{\alpha_{mr}}} c_{mr} \rho vw$$
$$+2C_{l_{\alpha_{mr}}} c_{mr} e_{mr}^4 \Omega_{mr} q\rho + 12C_{l_{\alpha_{mr}}} c_{mr} e_{mr}^2 \rho v v_i - 12C_{l_{\alpha_{mr}}} c_{mr} e_{mr}^2 \rho vw - 6R_{mr}^4 C_{l_{\alpha_{mr}}} \beta_{1s} c_{mr} \Omega_{mr}^2 \rho$$
$$+6R_{mr}^4 C_{l_{\alpha_{mr}}} c_{mr} \Omega_{mr}^2 \rho \theta_{1c} + 2C_{l_{\alpha_{mr}}} \beta_{1s} c_{mr} e_{mr}^4 \Omega_{mr}^2 \rho + 9R_{mr}^2 C_{l_{\alpha_{mr}}} c_{mr} \rho \theta_{1c} v^2 + 2C_{l_{\alpha_{mr}}} c_{mr} e_{mr}^4 \Omega_{mr}^2 \rho \theta_{1c}$$
$$+9C_{l_{\alpha_{mr}}} c_{mr} e_{mr}^2 \rho \theta_{1c} v^2 + 96X_{cg} \beta_{1c} e_{mr} m_b \Omega_{mr} r - 24R_{mr} C_{l_{\alpha_{mr}}} c_{mr} e_{mr} \rho v v_i + 24R_{mr} C_{l_{\alpha_{mr}}} c_{mr} e_{mr} \rho vw$$
$$-12R_{mr}^2 C_{l_{\alpha_{mr}}} \beta_{1s} c_{mr} e_{mr}^2 \Omega_{mr}^2 \rho - 16R_{mr}^3 C_{l_{\alpha_{mr}}} \dot{\beta}_{1c} c_{mr} e_{mr} \Omega_{mr} \rho + 24R_{mr} C_{l_{\alpha_{mr}}} \dot{\beta}_0 c_{mr} e_{mr}^2 \rho v$$
$$-24R_{mr}^2 C_{l_{\alpha_{mr}}} \dot{\beta}_0 c_{mr} e_{mr} \rho v - 8R_{mr}^3 C_{l_{\alpha_{mr}}} c_{mr} e_{mr} \Omega_{mr} q\rho - 8R_{mr}^3 C_{l_{\alpha_{mr}}} \beta_0 c_{mr} \Omega_{mr} \rho u$$
$$-9R_{mr}^2 C_{l_{\alpha_{mr}}} \beta_{1c} c_{mr} \rho uv - 18R_{mr} C_{l_{\alpha_{mr}}} c_{mr} e_{mr} \rho \theta_{1c} v^2 - 4C_{l_{\alpha_{mr}}} \beta_0 c_{mr} e_{mr}^3 \Omega_{mr} \rho u$$
$$-16R_{mr}^3 C_{l_{\alpha_{mr}}} c_{mr} \Omega_{mr} \rho \theta_0 v - 9C_{l_{\alpha_{mr}}} \beta_{1c} c_{mr} e_{mr}^2 \rho uv - 8C_{l_{\alpha_{mr}}} c_{mr} e_{mr}^3 \Omega_{mr} \rho \theta_0 v$$
$$+16R_{mr}^3 C_{l_{\alpha_{mr}}} \beta_{1s} c_{mr} e_{mr} \Omega_{mr}^2 \rho + 12R_{mr}^2 C_{l_{\alpha_{mr}}} \dot{\beta}_{1c} c_{mr} e_{mr}^2 \Omega_{mr} \rho - 8R_{mr}^3 C_{l_{\alpha_{mr}}} c_{mr} e_{mr} \Omega_{mr}^2 \rho \theta_{1c}$$
$$+24R_{mr}^2 C_{l_{\alpha_{mr}}} c_{mr} e_{mr} \Omega_{mr} \rho \theta_0 v + 18R_{mr} C_{l_{\alpha_{mr}}} \beta_{1c} c_{mr} e_{mr} \rho uv + 12R_{mr}^2 C_{l_{\alpha_{mr}}} \beta_0 c_{mr} e_{mr} \Omega_{mr} \rho u)/(48 I b_{mr})$$

Main Rotor Forces:

$$T_{mr} = (N_{mr} C_{l_{\alpha_{mr}}} c_{mr} \rho (R_{mr} - e_{mr})(3R_{mr} \dot{\beta}_{1s} u - 6\theta_0 v^2 - 4R_{mr}^2 \Omega_{mr}^2 \theta_0 - 4e_{mr}^2 \Omega_{mr}^2 \theta_0 - 6\theta_0 u^2$$
$$+3R_{mr} \dot{\beta}_{1c} v + 3R_{mr} pu + 6R_{mr} \Omega_{mr} v_i - 6R_{mr} \Omega_{mr} w + 3R_{mr} qv - 3\dot{\beta}_{1s} e_{mr} u - 3\dot{\beta}_{1c} e_{mr} v$$
$$+3e_{mr} pu + 6e_{mr} \Omega_{mr} v_i - 6e_{mr} \Omega_{mr} w + 3e_{mr} qv + 4R_{mr}^2 \dot{\beta}_0 \Omega_{mr} - 2\dot{\beta}_0 e_{mr}^2 \Omega_{mr} + 6R_{mr} \Omega_{mr} \theta_{1s} u$$
$$-6\beta_{1c} e_{mr} \Omega_{mr} u + 6R_{mr} \Omega_{mr} \theta_{1c} v + 6\beta_{1s} e_{mr} \Omega_{mr} v + 6e_{mr} \Omega_{mr} \theta_{1s} u + 6e_{mr} \Omega_{mr} \theta_{1c} v$$
$$-4R_{mr} e_{mr} \Omega_{mr}^2 \theta_0 - 2R_{mr} \dot{\beta}_0 e_{mr} \Omega_{mr}))/24$$

$$
\begin{aligned}
H_{mr} = {} & (N_{mr}c_{mr}\rho(R_{mr}-e_{mr})(24C_{l_{\alpha_{mr}}}e_{mr}pv_i - 24C_{l_{\alpha_{mr}}}e_{mr}pw + 72C_{l_{\alpha_{mr}}}\beta_0 vv_i \\
& - 72C_{l_{\alpha_{mr}}}\beta_0 vw - 24C_{l_{\alpha_{mr}}}\theta_0 uv_i + 24C_{l_{\alpha_{mr}}}\theta_0 uw + 16R_{mr}^2 C_{l_{\alpha_{mr}}}\dot{\beta}_0\dot{\beta}_{1s} + 16R_{mr}^2 C_{l_{\alpha_{mr}}}\dot{\beta}_0 p \\
& + 16C_{l_{\alpha_{mr}}}\dot{\beta}_0\dot{\beta}_{1s}e_{mr}^2 - 8C_{l_{\alpha_{mr}}}\dot{\beta}_0 e_{mr}^2 p + 48C_{l_{\alpha_{mr}}}\beta_0\beta_{1s}v^2 + 24C_{l_{\alpha_{mr}}}\beta_0\theta_{1c}v^2 - 24C_{l_{\alpha_{mr}}}\beta_{1c}\theta_0 v^2 \\
& - 24C_d R_{mr}\Omega_{mr}u + 24R_{mr}C_{l_{\alpha_{mr}}}\dot{\beta}_{1s}v_i - 24R_{mr}C_{l_{\alpha_{mr}}}\dot{\beta}_{1s}w - 24C_d e_{mr}\Omega_{mr}u + 24R_{mr}C_{l_{\alpha_{mr}}}pv_i \\
& - 24R_{mr}C_{l_{\alpha_{mr}}}pw - 24C_{l_{\alpha_{mr}}}\dot{\beta}_{1s}e_{mr}v_i + 24C_{l_{\alpha_{mr}}}\dot{\beta}_{1s}e_{mr}w - 8R_{mr}^2 C_{l_{\alpha_{mr}}}\beta_0\beta_{1s}\Omega_{mr}^2 \\
& + 8R_{mr}^2 C_{l_{\alpha_{mr}}}\beta_0\Omega_{mr}^2\theta_{1c} - 16R_{mr}^2 C_{l_{\alpha_{mr}}}\beta_{1c}\Omega_{mr}^2\theta_0 + 4C_{l_{\alpha_{mr}}}\beta_0\beta_{1s}e_{mr}^2\Omega_{mr}^2 + 8C_{l_{\alpha_{mr}}}\beta_0 e_{mr}^2\Omega_{mr}^2\theta_{1c} \\
& - 4C_{l_{\alpha_{mr}}}\beta_{1c}e_{mr}^2\Omega_{mr}^2\theta_0 - 32R_{mr}C_{l_{\alpha_{mr}}}\dot{\beta}_0\dot{\beta}_{1s}e_{mr} - 8R_{mr}C_{l_{\alpha_{mr}}}\dot{\beta}_0 e_{mr}p - 3R_{mr}C_{l_{\alpha_{mr}}}\beta_{1c}\dot{\beta}_{1s}u \\
& - 3R_{mr}C_{l_{\alpha_{mr}}}\beta_{1s}\dot{\beta}_{1c}u + 36R_{mr}C_{l_{\alpha_{mr}}}\beta_0\dot{\beta}_0 v + 15R_{mr}C_{l_{\alpha_{mr}}}\beta_{1c}\dot{\beta}_{1c}v + 21R_{mr}C_{l_{\alpha_{mr}}}\beta_{1s}\dot{\beta}_{1s}v \\
& - 3R_{mr}C_{l_{\alpha_{mr}}}\beta_{1c}pu + 36R_{mr}C_{l_{\alpha_{mr}}}\beta_{1c}\Omega_{mr}v_i + 21R_{mr}C_{l_{\alpha_{mr}}}\beta_{1s}pv - 3R_{mr}C_{l_{\alpha_{mr}}}\beta_{1s}qu \\
& - 36R_{mr}C_{l_{\alpha_{mr}}}\beta_{1c}\Omega_{mr}w + 15R_{mr}C_{l_{\alpha_{mr}}}\beta_{1c}qv - 12R_{mr}C_{l_{\alpha_{mr}}}\dot{\beta}_0\theta_0 u + 3R_{mr}C_{l_{\alpha_{mr}}}\dot{\beta}_{1c}\theta_{1c}u \\
& + 9R_{mr}C_{l_{\alpha_{mr}}}\dot{\beta}_{1s}\theta_{1s}u + 3C_{l_{\alpha_{mr}}}\beta_{1c}\dot{\beta}_{1s}e_{mr}u + 3C_{l_{\alpha_{mr}}}\beta_{1s}\dot{\beta}_{1c}e_{mr}u + 3R_{mr}C_{l_{\alpha_{mr}}}\dot{\beta}_{1c}\theta_{1s}v \\
& + 3R_{mr}C_{l_{\alpha_{mr}}}\dot{\beta}_{1s}\theta_{1c}v - 36C_{l_{\alpha_{mr}}}\beta_0\dot{\beta}_0 e_{mr}v - 15C_{l_{\alpha_{mr}}}\beta_{1c}\dot{\beta}_{1c}e_{mr}v - 21C_{l_{\alpha_{mr}}}\beta_{1s}\dot{\beta}_{1s}e_{mr}v \\
& + 9R_{mr}C_{l_{\alpha_{mr}}}p\theta_{1s}u + 12R_{mr}C_{l_{\alpha_{mr}}}\Omega_{mr}\theta_{1s}v_i - 3C_{l_{\alpha_{mr}}}\beta_{1c}e_{mr}pu + 3R_{mr}C_{l_{\alpha_{mr}}}p\theta_{1c}v \\
& + 3R_{mr}C_{l_{\alpha_{mr}}}q\theta_{1c}u - 12R_{mr}C_{l_{\alpha_{mr}}}\Omega_{mr}\theta_{1s}w - 12C_{l_{\alpha_{mr}}}\beta_{1c}e_{mr}\Omega_{mr}v_i + 21C_{l_{\alpha_{mr}}}\beta_{1s}e_{mr}pv \\
& - 3C_{l_{\alpha_{mr}}}\beta_{1s}e_{mr}qu + 3R_{mr}C_{l_{\alpha_{mr}}}q\theta_{1s}v + 12C_{l_{\alpha_{mr}}}\beta_{1c}e_{mr}\Omega_{mr}w + 15C_{l_{\alpha_{mr}}}\beta_{1c}e_{mr}qv \\
& - 48C_{l_{\alpha_{mr}}}\beta_0\beta_{1c}uv + 12C_{l_{\alpha_{mr}}}\dot{\beta}_0 e_{mr}\theta_0 u - 3C_{l_{\alpha_{mr}}}\dot{\beta}_{1c}e_{mr}\theta_{1c}u - 9C_{l_{\alpha_{mr}}}\dot{\beta}_{1s}e_{mr}\theta_{1s}u \\
& - 3C_{l_{\alpha_{mr}}}\dot{\beta}_{1c}e_{mr}\theta_{1s}v - 3C_{l_{\alpha_{mr}}}\dot{\beta}_{1s}e_{mr}\theta_{1c}v + 9C_{l_{\alpha_{mr}}}e_{mr}p\theta_{1s}u + 12C_{l_{\alpha_{mr}}}e_{mr}\Omega_{mr}\theta_{1s}v_i \\
& + 3C_{l_{\alpha_{mr}}}e_{mr}p\theta_{1c}v + 3C_{l_{\alpha_{mr}}}e_{mr}q\theta_{1c}u - 12C_{l_{\alpha_{mr}}}e_{mr}\Omega_{mr}\theta_{1s}w + 3C_{l_{\alpha_{mr}}}e_{mr}q\theta_{1s}v + 24C_{l_{\alpha_{mr}}}\beta_0\theta_{1s}uv \\
& - 24C_{l_{\alpha_{mr}}}\beta_{1s}\theta_0 uv + 8R_{mr}^2 C_{l_{\alpha_{mr}}}\beta_0\dot{\beta}_{1c}\Omega_{mr} + 24R_{mr}^2 C_{l_{\alpha_{mr}}}\beta_{1c}\dot{\beta}_0\Omega_{mr} + 8R_{mr}^2 C_{l_{\alpha_{mr}}}\beta_0\Omega_{mr}q \\
& + 8R_{mr}^2 C_{l_{\alpha_{mr}}}\dot{\beta}_0\Omega_{mr}\theta_{1s} - 8R_{mr}^2 C_{l_{\alpha_{mr}}}\dot{\beta}_{1s}\Omega_{mr}\theta_0 - 12R_{mr}C_{l_{\alpha_{mr}}}\beta_0^2\Omega_{mr}u - 12R_{mr}C_{l_{\alpha_{mr}}}\beta_{1c}^2\Omega_{mr}u \\
& - 4C_{l_{\alpha_{mr}}}\beta_0\dot{\beta}_{1c}e_{mr}^2\Omega_{mr} + 12C_{l_{\alpha_{mr}}}\beta_{1c}\dot{\beta}_0 e_{mr}^2\Omega_{mr} - 8R_{mr}^2 C_{l_{\alpha_{mr}}}\Omega_{mr}p\theta_0 + 8C_{l_{\alpha_{mr}}}\beta_0 e_{mr}^2\Omega_{mr}q \\
& - 4C_{l_{\alpha_{mr}}}\dot{\beta}_0 e_{mr}^2\Omega_{mr}\theta_{1s} + 4C_{l_{\alpha_{mr}}}\dot{\beta}_{1s}e_{mr}^2\Omega_{mr}\theta_0 - 12C_{l_{\alpha_{mr}}}\beta_0^2 e_{mr}\Omega_{mr}u - 6C_{l_{\alpha_{mr}}}\beta_{1c}^2 e_{mr}\Omega_{mr}u \\
& - 6C_{l_{\alpha_{mr}}}\beta_{1s}^2 e_{mr}\Omega_{mr}u - 8C_{l_{\alpha_{mr}}}e_{mr}^2\Omega_{mr}p\theta_0 + 4R_{mr}C_{l_{\alpha_{mr}}}\beta_0\beta_{1s}e_{mr}\Omega_{mr}^2 + 8R_{mr}C_{l_{\alpha_{mr}}}\beta_0 e_{mr}\Omega_{mr}^2\theta_{1c} \\
& - 4R_{mr}C_{l_{\alpha_{mr}}}\beta_{1c}e_{mr}\Omega_{mr}^2\theta_0 - 4R_{mr}C_{l_{\alpha_{mr}}}\beta_0\dot{\beta}_{1c}e_{mr}\Omega_{mr} - 36R_{mr}C_{l_{\alpha_{mr}}}\beta_{1c}\dot{\beta}_0 e_{mr}\Omega_{mr} \\
& + 8R_{mr}C_{l_{\alpha_{mr}}}\beta_0 e_{mr}\Omega_{mr}q + 12R_{mr}C_{l_{\alpha_{mr}}}\beta_{1c}\beta_{1s}\Omega_{mr}v - 4R_{mr}C_{l_{\alpha_{mr}}}\dot{\beta}_0 e_{mr}\Omega_{mr}\theta_{1s} \\
& + 4R_{mr}C_{l_{\alpha_{mr}}}\dot{\beta}_{1s}e_{mr}\Omega_{mr}\theta_0 - 8R_{mr}C_{l_{\alpha_{mr}}}e_{mr}\Omega_{mr}p\theta_0 + 12R_{mr}C_{l_{\alpha_{mr}}}\beta_{1c}\Omega_{mr}\theta_{1s}u \\
& - 36R_{mr}C_{l_{\alpha_{mr}}}\beta_0\Omega_{mr}\theta_0 v + 24R_{mr}C_{l_{\alpha_{mr}}}\beta_{1c}\Omega_{mr}\theta_{1c}v + 12R_{mr}C_{l_{\alpha_{mr}}}\beta_{1s}\Omega_{mr}\theta_{1s}v \\
& - 6C_{l_{\alpha_{mr}}}\beta_{1c}e_{mr}\Omega_{mr}\theta_{1s}u + 6C_{l_{\alpha_{mr}}}\beta_{1s}e_{mr}\Omega_{mr}\theta_{1c}u - 36C_{l_{\alpha_{mr}}}\beta_0 e_{mr}\Omega_{mr}\theta_0 v \\
& + 18C_{l_{\alpha_{mr}}}\beta_{1c}e_{mr}\Omega_{mr}\theta_{1c}v + 18C_{l_{\alpha_{mr}}}\beta_{1s}e_{mr}\Omega_{mr}\theta_{1s}v))/96
\end{aligned}
$$

$$
\begin{aligned}
Y_{mr} = {} & -(N_{mr}c_{mr}\rho(R_{mr}-e_{mr})(24C_{l_{\alpha_{mr}}}e_{mr}qw - 24C_{l_{\alpha_{mr}}}e_{mr}qv_i + 72C_{l_{\alpha_{mr}}}\beta_0 uv_i - 72C_{l_{\alpha_{mr}}}\beta_0 uw \\
& + 24C_{l_{\alpha_{mr}}}\theta_0 vv_i - 24C_{l_{\alpha_{mr}}}\theta_0 vw - 16R_{mr}^2 C_{l_{\alpha_{mr}}}\dot{\beta}_0\dot{\beta}_{1c} - 16R_{mr}^2 C_{l_{\alpha_{mr}}}\dot{\beta}_0 q - 16C_{l_{\alpha_{mr}}}\dot{\beta}_0\dot{\beta}_{1c}e_{mr}^2 \\
& + 8C_{l_{\alpha_{mr}}}\dot{\beta}_0 e_{mr}^2 q - 48C_{l_{\alpha_{mr}}}\beta_0\beta_{1c}u^2 + 24C_{l_{\alpha_{mr}}}\beta_0\theta_{1s}u^2 - 24C_{l_{\alpha_{mr}}}\beta_{1s}\theta_0 u^2
\end{aligned}
$$

$$+24C_dR_{mr}\Omega_{mr}v-24R_{mr}C_{l_{\alpha_{mr}}}\dot{\beta}_{1c}v_i+24R_{mr}C_{l_{\alpha_{mr}}}\dot{\beta}_{1c}w+24C_de_{mr}\Omega_{mr}v$$
$$-24R_{mr}C_{l_{\alpha_{mr}}}qv_i+24R_{mr}C_{l_{\alpha_{mr}}}qw+24C_{l_{\alpha_{mr}}}\dot{\beta}_{1c}e_{mr}v_i-24C_{l_{\alpha_{mr}}}\dot{\beta}_{1c}e_{mr}w+8R_{mr}^2C_{l_{\alpha_{mr}}}\beta_0\beta_{1c}\Omega_{mr}^2$$
$$+8R_{mr}^2C_{l_{\alpha_{mr}}}\beta_0\Omega_{mr}^2\theta_{1s}-16R_{mr}^2C_{l_{\alpha_{mr}}}\beta_{1s}\Omega_{mr}^2\theta_0-4C_{l_{\alpha_{mr}}}\beta_0\beta_{1c}e_{mr}^2\Omega_{mr}^2+8C_{l_{\alpha_{mr}}}\beta_0e_{mr}^2\Omega_{mr}^2\theta_{1s}$$
$$-4C_{l_{\alpha_{mr}}}\beta_{1s}e_{mr}^2\Omega_{mr}^2\theta_0+32R_{mr}C_{l_{\alpha_{mr}}}\dot{\beta}_0\dot{\beta}_{1c}e_{mr}+8R_{mr}C_{l_{\alpha_{mr}}}\dot{\beta}_0e_{mr}q+36R_{mr}C_{l_{\alpha_{mr}}}\beta_0\dot{\beta}_0u$$
$$+21R_{mr}C_{l_{\alpha_{mr}}}\beta_{1c}\dot{\beta}_{1c}u+15R_{mr}C_{l_{\alpha_{mr}}}\beta_{1s}\dot{\beta}_{1s}u-3R_{mr}C_{l_{\alpha_{mr}}}\beta_{1c}\dot{\beta}_{1s}v-3R_{mr}C_{l_{\alpha_{mr}}}\beta_{1s}\dot{\beta}_{1c}v$$
$$+15R_{mr}C_{l_{\alpha_{mr}}}\beta_{1s}pu+36R_{mr}C_{l_{\alpha_{mr}}}\beta_{1s}\Omega_{mr}v_i-3R_{mr}C_{l_{\alpha_{mr}}}\beta_{1c}pv+21R_{mr}C_{l_{\alpha_{mr}}}\beta_{1c}qu$$
$$-36R_{mr}C_{l_{\alpha_{mr}}}\beta_{1s}\Omega_{mr}w-3R_{mr}C_{l_{\alpha_{mr}}}\beta_{1s}qv-3R_{mr}C_{l_{\alpha_{mr}}}\dot{\beta}_{1c}\theta_{1s}u-3R_{mr}C_{l_{\alpha_{mr}}}\dot{\beta}_{1s}\theta_{1c}u$$
$$-36C_{l_{\alpha_{mr}}}\beta_0\dot{\beta}_0e_{mr}u-21C_{l_{\alpha_{mr}}}\beta_{1c}\dot{\beta}_{1c}e_{mr}u-15C_{l_{\alpha_{mr}}}\beta_{1s}\dot{\beta}_{1s}e_{mr}u+12R_{mr}C_{l_{\alpha_{mr}}}\dot{\beta}_0\theta_0v$$
$$-9R_{mr}C_{l_{\alpha_{mr}}}\dot{\beta}_{1c}\theta_{1c}v-3R_{mr}C_{l_{\alpha_{mr}}}\dot{\beta}_{1s}\theta_{1s}v+3C_{l_{\alpha_{mr}}}\beta_{1c}\dot{\beta}_{1s}e_{mr}v+3C_{l_{\alpha_{mr}}}\beta_{1s}\dot{\beta}_{1c}e_{mr}v-3R_{mr}C_{l_{\alpha_{mr}}}p\theta_{1c}u$$
$$-12R_{mr}C_{l_{\alpha_{mr}}}\Omega_{mr}\theta_{1c}v_i+15C_{l_{\alpha_{mr}}}\beta_{1s}e_{mr}pu-3R_{mr}C_{l_{\alpha_{mr}}}p\theta_{1s}v-3R_{mr}C_{l_{\alpha_{mr}}}q\theta_{1s}u$$
$$+12R_{mr}C_{l_{\alpha_{mr}}}\Omega_{mr}\theta_{1c}w-12C_{l_{\alpha_{mr}}}\beta_{1s}e_{mr}\Omega_{mr}v_i-3C_{l_{\alpha_{mr}}}\beta_{1c}e_{mr}pv+21C_{l_{\alpha_{mr}}}\beta_{1c}e_{mr}qu$$
$$-9R_{mr}C_{l_{\alpha_{mr}}}q\theta_{1c}v+12C_{l_{\alpha_{mr}}}\beta_{1s}e_{mr}\Omega_{mr}w-3C_{l_{\alpha_{mr}}}\beta_{1s}e_{mr}qv+48C_{l_{\alpha_{mr}}}\beta_0\beta_{1s}uv+3C_{l_{\alpha_{mr}}}\dot{\beta}_{1c}e_{mr}\theta_{1s}u$$
$$+3C_{l_{\alpha_{mr}}}\dot{\beta}_{1s}e_{mr}\theta_{1c}u-12C_{l_{\alpha_{mr}}}\dot{\beta}_0e_{mr}\theta_0v+9C_{l_{\alpha_{mr}}}\dot{\beta}_{1c}e_{mr}\theta_{1c}v+3C_{l_{\alpha_{mr}}}\dot{\beta}_{1s}e_{mr}\theta_{1s}v-3C_{l_{\alpha_{mr}}}e_{mr}p\theta_{1c}u$$
$$-12C_{l_{\alpha_{mr}}}e_{mr}\Omega_{mr}\theta_{1c}v_i-3C_{l_{\alpha_{mr}}}e_{mr}p\theta_{1s}v-3C_{l_{\alpha_{mr}}}e_{mr}q\theta_{1s}u+12C_{l_{\alpha_{mr}}}e_{mr}\Omega_{mr}\theta_{1c}w$$
$$-9C_{l_{\alpha_{mr}}}e_{mr}q\theta_{1c}v+24C_{l_{\alpha_{mr}}}\beta_0\theta_{1c}uv-24C_{l_{\alpha_{mr}}}\beta_{1c}\theta_0uv+8R_{mr}^2C_{l_{\alpha_{mr}}}\beta_0\dot{\beta}_{1s}\Omega_{mr}$$
$$+24R_{mr}^2C_{l_{\alpha_{mr}}}\beta_{1s}\dot{\beta}_0\Omega_{mr}+8R_{mr}^2C_{l_{\alpha_{mr}}}\beta_0\Omega_{mr}p-8R_{mr}^2C_{l_{\alpha_{mr}}}\dot{\beta}_0\Omega_{mr}\theta_{1c}+8R_{mr}^2C_{l_{\alpha_{mr}}}\dot{\beta}_{1c}\Omega_{mr}\theta_0$$
$$-4C_{l_{\alpha_{mr}}}\beta_0\dot{\beta}_{1s}e_{mr}^2\Omega_{mr}+12C_{l_{\alpha_{mr}}}\beta_{1s}\dot{\beta}_0e_{mr}^2\Omega_{mr}+12R_{mr}C_{l_{\alpha_{mr}}}\beta_0^2\Omega_{mr}v+12R_{mr}C_{l_{\alpha_{mr}}}\beta_{1s}^2\Omega_{mr}v$$
$$+8C_{l_{\alpha_{mr}}}\beta_0e_{mr}^2\Omega_{mr}p+8R_{mr}^2C_{l_{\alpha_{mr}}}\Omega_{mr}q\theta_0+4C_{l_{\alpha_{mr}}}\dot{\beta}_0e_{mr}^2\Omega_{mr}\theta_{1c}-4C_{l_{\alpha_{mr}}}\dot{\beta}_{1c}e_{mr}^2\Omega_{mr}\theta_0$$
$$+12C_{l_{\alpha_{mr}}}\beta_0^2e_{mr}\Omega_{mr}v+6C_{l_{\alpha_{mr}}}\beta_{1c}^2e_{mr}\Omega_{mr}v+6C_{l_{\alpha_{mr}}}\beta_{1s}^2e_{mr}\Omega_{mr}v+8C_{l_{\alpha_{mr}}}e_{mr}^2\Omega_{mr}q\theta_0$$
$$-4R_{mr}C_{l_{\alpha_{mr}}}\beta_0\beta_{1c}e_{mr}\Omega_{mr}^2+8R_{mr}C_{l_{\alpha_{mr}}}\beta_0e_{mr}\Omega_{mr}^2\theta_{1s}-4R_{mr}C_{l_{\alpha_{mr}}}\beta_{1s}e_{mr}\Omega_{mr}^2\theta_0$$
$$-4R_{mr}C_{l_{\alpha_{mr}}}\beta_0\dot{\beta}_{1s}e_{mr}\Omega_{mr}-36R_{mr}C_{l_{\alpha_{mr}}}\beta_{1s}\dot{\beta}_0e_{mr}\Omega_{mr}+8R_{mr}C_{l_{\alpha_{mr}}}\beta_0e_{mr}\Omega_{mr}p$$
$$-12R_{mr}C_{l_{\alpha_{mr}}}\beta_{1c}\beta_{1s}\Omega_{mr}u+4R_{mr}C_{l_{\alpha_{mr}}}\dot{\beta}_0e_{mr}\Omega_{mr}\theta_{1c}-4R_{mr}C_{l_{\alpha_{mr}}}\dot{\beta}_{1c}e_{mr}\Omega_{mr}\theta_0$$
$$+8R_{mr}C_{l_{\alpha_{mr}}}e_{mr}\Omega_{mr}q\theta_0-36R_{mr}C_{l_{\alpha_{mr}}}\beta_0\Omega_{mr}\theta_0u+12R_{mr}C_{l_{\alpha_{mr}}}\beta_{1c}\Omega_{mr}\theta_{1c}u$$
$$+24R_{mr}C_{l_{\alpha_{mr}}}\beta_{1s}\Omega_{mr}\theta_{1s}u+12R_{mr}C_{l_{\alpha_{mr}}}\beta_{1s}\Omega_{mr}\theta_{1c}v-36C_{l_{\alpha_{mr}}}\beta_0e_{mr}\Omega_{mr}\theta_0u$$
$$+18C_{l_{\alpha_{mr}}}\beta_{1c}e_{mr}\Omega_{mr}\theta_{1c}u+18C_{l_{\alpha_{mr}}}\beta_{1s}e_{mr}\Omega_{mr}\theta_{1s}u$$
$$+6C_{l_{\alpha_{mr}}}\beta_{1c}e_{mr}\Omega_{mr}\theta_{1s}v-6C_{l_{\alpha_{mr}}}\beta_{1s}e_{mr}\Omega_{mr}\theta_{1c}v))/96$$

Main Rotor Moments:

$$Q_{mr}=(N_{mr}c_{mr}\rho(R_{mr}-e_{mr})(12R_{mr}^3C_{l_{\alpha_{mr}}}\dot{\beta}_0^2-12C_dR_{mr}^3\Omega_{mr}^2+6R_{mr}^3C_{l_{\alpha_{mr}}}\dot{\beta}_{1c}^2+6R_{mr}^3C_{l_{\alpha_{mr}}}\dot{\beta}_{1s}^2$$
$$-12C_de_{mr}^3\Omega_{mr}^2+6R_{mr}^3C_{l_{\alpha_{mr}}}p^2+6R_{mr}^3C_{l_{\alpha_{mr}}}q^2+4C_{l_{\alpha_{mr}}}\dot{\beta}_0^2e_{mr}^3+2C_{l_{\alpha_{mr}}}\dot{\beta}_{1c}^2e_{mr}^3+2C_{l_{\alpha_{mr}}}\dot{\beta}_{1s}^2e_{mr}^3$$
$$+6C_{l_{\alpha_{mr}}}e_{mr}^3p^2+6C_{l_{\alpha_{mr}}}e_{mr}^3q^2-12C_dR_{mr}u^2-12C_dR_{mr}v^2-12C_de_{mr}u^2-12C_de_{mr}v^2$$
$$+24R_{mr}C_{l_{\alpha_{mr}}}v_i^2+24R_{mr}C_{l_{\alpha_{mr}}}w^2+24C_{l_{\alpha_{mr}}}e_{mr}v_i^2+24C_{l_{\alpha_{mr}}}e_{mr}w^2-48R_{mr}C_{l_{\alpha_{mr}}}v_iw$$
$$+6R_{mr}^3C_{l_{\alpha_{mr}}}\beta_{1c}^2\Omega_{mr}^2+6R_{mr}^3C_{l_{\alpha_{mr}}}\beta_{1s}^2\Omega_{mr}^2-48C_{l_{\alpha_{mr}}}e_{mr}v_iw+2C_{l_{\alpha_{mr}}}\beta_{1c}^2e_{mr}^3\Omega_{mr}^2$$

$$
\begin{aligned}
&+2C_{l_{\alpha_{mr}}}\beta_{1s}^2 e_{mr}^3\Omega_{mr}^2+12R_{mr}^3C_{l_{\alpha_{mr}}}\dot{\beta}_{1s}p+12R_{mr}^3C_{l_{\alpha_{mr}}}\dot{\beta}_{1c}q+32R_{mr}^2C_{l_{\alpha_{mr}}}\dot{\beta}_0 v_i\\
&-32R_{mr}^2C_{l_{\alpha_{mr}}}\dot{\beta}_0 w-4C_{l_{\alpha_{mr}}}\dot{\beta}_{1s}e_{mr}^3p-4C_{l_{\alpha_{mr}}}\dot{\beta}_{1c}e_{mr}^3q-16C_{l_{\alpha_{mr}}}\dot{\beta}_0 e_{mr}^2v_i\\
&+16C_{l_{\alpha_{mr}}}\dot{\beta}_0 e_{mr}^2w-12C_dR_{mr}e_{mr}^2\Omega_{mr}^2-12C_dR_{mr}^2e_{mr}\Omega_{mr}^2+4R_{mr}C_{l_{\alpha_{mr}}}\dot{\beta}_0^2e_{mr}^2\\
&-20R_{mr}^2C_{l_{\alpha_{mr}}}\dot{\beta}_0^2e_{mr}+2R_{mr}C_{l_{\alpha_{mr}}}\dot{\beta}_{1c}^2e_{mr}^2-10R_{mr}^2C_{l_{\alpha_{mr}}}\dot{\beta}_{1c}^2e_{mr}+2R_{mr}C_{l_{\alpha_{mr}}}\dot{\beta}_{1s}^2e_{mr}^2\\
&-10R_{mr}^2C_{l_{\alpha_{mr}}}\dot{\beta}_{1s}^2e_{mr}+6R_{mr}C_{l_{\alpha_{mr}}}e_{mr}^2p^2+6R_{mr}^2C_{l_{\alpha_{mr}}}e_{mr}p^2+6R_{mr}C_{l_{\alpha_{mr}}}e_{mr}^2q^2\\
&+6R_{mr}^2C_{l_{\alpha_{mr}}}e_{mr}q^2+12R_{mr}C_{l_{\alpha_{mr}}}\beta_0^2u^2+9R_{mr}C_{l_{\alpha_{mr}}}\beta_{1c}^2u^2+3R_{mr}C_{l_{\alpha_{mr}}}\beta_{1s}^2u^2\\
&+12R_{mr}C_{l_{\alpha_{mr}}}\beta_0^2v^2+3R_{mr}C_{l_{\alpha_{mr}}}\beta_{1c}^2v^2+9R_{mr}C_{l_{\alpha_{mr}}}\beta_{1s}^2v^2+12C_{l_{\alpha_{mr}}}\beta_0^2e_{mr}u^2\\
&+9C_{l_{\alpha_{mr}}}\beta_{1c}^2e_{mr}u^2+3C_{l_{\alpha_{mr}}}\beta_{1s}^2e_{mr}u^2+12C_{l_{\alpha_{mr}}}\beta_0^2e_{mr}v^2+3C_{l_{\alpha_{mr}}}\beta_{1c}^2e_{mr}v^2+9C_{l_{\alpha_{mr}}}\beta_{1s}^2e_{mr}v^2\\
&+6R_{mr}^3C_{l_{\alpha_{mr}}}\beta_{1c}\Omega_{mr}^2\theta_{1s}-6R_{mr}^3C_{l_{\alpha_{mr}}}\beta_{1s}\Omega_{mr}^2\theta_{1c}-2C_{l_{\alpha_{mr}}}\beta_{1c}e_{mr}^3\Omega_{mr}^2\theta_{1s}+2C_{l_{\alpha_{mr}}}\beta_{1s}e_{mr}^3\Omega_{mr}^2\theta_{1c}\\
&-16R_{mr}C_{l_{\alpha_{mr}}}\dot{\beta}_0e_{mr}v_i+16R_{mr}C_{l_{\alpha_{mr}}}\dot{\beta}_0e_{mr}w-24R_{mr}C_{l_{\alpha_{mr}}}\beta_{1c}uv_i+24R_{mr}C_{l_{\alpha_{mr}}}\beta_{1c}uw\\
&+24R_{mr}C_{l_{\alpha_{mr}}}\beta_{1s}vv_i-24R_{mr}C_{l_{\alpha_{mr}}}\beta_{1s}vw+2R_{mr}C_{l_{\alpha_{mr}}}\beta_{1c}^2e_{mr}^2\Omega_{mr}^2-10R_{mr}^2C_{l_{\alpha_{mr}}}\beta_{1c}^2e_{mr}\Omega_{mr}^2\\
&+2R_{mr}C_{l_{\alpha_{mr}}}\beta_{1s}^2e_{mr}^2\Omega_{mr}^2-10R_{mr}^2C_{l_{\alpha_{mr}}}\beta_{1s}^2e_{mr}\Omega_{mr}^2+12R_{mr}C_{l_{\alpha_{mr}}}\theta_{1s}uv_i-12R_{mr}C_{l_{\alpha_{mr}}}\theta_{1s}uw\\
&-24C_{l_{\alpha_{mr}}}\beta_{1c}e_{mr}uv_i+12R_{mr}C_{l_{\alpha_{mr}}}\theta_{1c}vv_i+24C_{l_{\alpha_{mr}}}\beta_{1c}e_{mr}uw-12R_{mr}C_{l_{\alpha_{mr}}}\theta_{1c}vw\\
&+24C_{l_{\alpha_{mr}}}\beta_{1s}e_{mr}vv_i-24C_{l_{\alpha_{mr}}}\beta_{1s}e_{mr}vw+12C_{l_{\alpha_{mr}}}e_{mr}\theta_{1s}uv_i-12C_{l_{\alpha_{mr}}}e_{mr}\theta_{1s}uw\\
&+12C_{l_{\alpha_{mr}}}e_{mr}\theta_{1c}vv_i-12C_{l_{\alpha_{mr}}}e_{mr}\theta_{1c}vw+12R_{mr}^3C_{l_{\alpha_{mr}}}\beta_{1c}\dot{\beta}_{1s}\Omega_{mr}-12R_{mr}^3C_{l_{\alpha_{mr}}}\beta_{1s}\dot{\beta}_{1c}\Omega_{mr}\\
&-4R_{mr}C_{l_{\alpha_{mr}}}\dot{\beta}_{1s}e_{mr}^2p-4R_{mr}^2C_{l_{\alpha_{mr}}}\dot{\beta}_{1s}e_{mr}p-4R_{mr}C_{l_{\alpha_{mr}}}\dot{\beta}_{1c}e_{mr}^2q-4R_{mr}^2C_{l_{\alpha_{mr}}}\dot{\beta}_{1c}e_{mr}q\\
&-16R_{mr}^2C_{l_{\alpha_{mr}}}\beta_0\dot{\beta}_{1c}u-16R_{mr}^2C_{l_{\alpha_{mr}}}\beta_{1c}\dot{\beta}_0u+16R_{mr}^2C_{l_{\alpha_{mr}}}\beta_0\dot{\beta}_{1s}v+16R_{mr}^2C_{l_{\alpha_{mr}}}\beta_{1s}\dot{\beta}_0v\\
&+12R_{mr}^3C_{l_{\alpha_{mr}}}\beta_{1c}\Omega_{mr}p-12R_{mr}^3C_{l_{\alpha_{mr}}}\beta_{1s}\Omega_{mr}q-12R_{mr}^3C_{l_{\alpha_{mr}}}\dot{\beta}_0\Omega_{mr}\theta_0\\
&+6R_{mr}^3C_{l_{\alpha_{mr}}}\dot{\beta}_{1c}\Omega_{mr}\theta_{1c}+6R_{mr}^3C_{l_{\alpha_{mr}}}\dot{\beta}_{1s}\Omega_{mr}\theta_{1s}+4C_{l_{\alpha_{mr}}}\beta_{1c}\dot{\beta}_{1s}e_{mr}^3\Omega_{mr}-4C_{l_{\alpha_{mr}}}\beta_{1s}\dot{\beta}_{1c}e_{mr}^3\Omega_{mr}\\
&+16R_{mr}^2C_{l_{\alpha_{mr}}}\beta_0pv-16R_{mr}^2C_{l_{\alpha_{mr}}}\beta_0qu-3R_{mr}C_{l_{\alpha_{mr}}}\beta_{1c}\theta_{1s}u^2-3R_{mr}C_{l_{\alpha_{mr}}}\beta_{1s}\theta_{1c}u^2\\
&+8R_{mr}^2C_{l_{\alpha_{mr}}}\dot{\beta}_0\theta_{1s}u-8R_{mr}^2C_{l_{\alpha_{mr}}}\dot{\beta}_{1s}\theta_0u+8C_{l_{\alpha_{mr}}}\beta_0\dot{\beta}_{1c}e_{mr}^2u+8C_{l_{\alpha_{mr}}}\beta_{1c}\dot{\beta}_0e_{mr}^2u\\
&+3R_{mr}C_{l_{\alpha_{mr}}}\beta_{1c}\theta_{1s}v^2+3R_{mr}C_{l_{\alpha_{mr}}}\beta_{1s}\theta_{1c}v^2+8R_{mr}^2C_{l_{\alpha_{mr}}}\dot{\beta}_0\theta_{1c}v-8R_{mr}^2C_{l_{\alpha_{mr}}}\dot{\beta}_{1c}\theta_0v\\
&-8C_{l_{\alpha_{mr}}}\beta_0\dot{\beta}_{1s}e_{mr}^2v-8C_{l_{\alpha_{mr}}}\beta_{1s}\dot{\beta}_0e_{mr}^2v+6R_{mr}^3C_{l_{\alpha_{mr}}}\Omega_{mr}p\theta_{1s}-4C_{l_{\alpha_{mr}}}\beta_{1c}e_{mr}^3\Omega_{mr}p\\
&+6R_{mr}^3C_{l_{\alpha_{mr}}}\Omega_{mr}q\theta_{1c}+4C_{l_{\alpha_{mr}}}\beta_{1s}e_{mr}^3\Omega_{mr}q+4C_{l_{\alpha_{mr}}}\dot{\beta}_0e_{mr}^3\Omega_{mr}\theta_0\\
&-2C_{l_{\alpha_{mr}}}\dot{\beta}_{1c}e_{mr}^3\Omega_{mr}\theta_{1c}-2C_{l_{\alpha_{mr}}}\dot{\beta}_{1s}e_{mr}^3\Omega_{mr}\theta_{1s}-8R_{mr}^2C_{l_{\alpha_{mr}}}p\theta_0u-16R_{mr}^2C_{l_{\alpha_{mr}}}\Omega_{mr}\theta_0v_i\\
&+16R_{mr}^2C_{l_{\alpha_{mr}}}\Omega_{mr}\theta_0w+16C_{l_{\alpha_{mr}}}\beta_0e_{mr}^2pv-16C_{l_{\alpha_{mr}}}\beta_0e_{mr}^2qu-8R_{mr}^2C_{l_{\alpha_{mr}}}q\theta_0v\\
&-3C_{l_{\alpha_{mr}}}\beta_{1c}e_{mr}\theta_{1s}u^2-3C_{l_{\alpha_{mr}}}\beta_{1s}e_{mr}\theta_{1c}u^2-4C_{l_{\alpha_{mr}}}\dot{\beta}_0e_{mr}^2\theta_{1s}u+4C_{l_{\alpha_{mr}}}\dot{\beta}_{1s}e_{mr}^2\theta_0u\\
&+3C_{l_{\alpha_{mr}}}\beta_{1c}e_{mr}\theta_{1s}v^2+3C_{l_{\alpha_{mr}}}\beta_{1s}e_{mr}\theta_{1c}v^2-4C_{l_{\alpha_{mr}}}\dot{\beta}_0e_{mr}^2\theta_{1c}v+4C_{l_{\alpha_{mr}}}\dot{\beta}_{1c}e_{mr}^2\theta_0v\\
&+6C_{l_{\alpha_{mr}}}e_{mr}^3\Omega_{mr}p\theta_{1s}+6C_{l_{\alpha_{mr}}}e_{mr}^3\Omega_{mr}q\theta_{1c}-8C_{l_{\alpha_{mr}}}e_{mr}^2p\theta_0u-16C_{l_{\alpha_{mr}}}e_{mr}^2\Omega_{mr}\theta_0v_i\\
&+16C_{l_{\alpha_{mr}}}e_{mr}^2\Omega_{mr}\theta_0w-8C_{l_{\alpha_{mr}}}e_{mr}^2q\theta_0v+4R_{mr}C_{l_{\alpha_{mr}}}\beta_{1c}\dot{\beta}_{1s}e_{mr}^2\Omega_{mr}-4R_{mr}C_{l_{\alpha_{mr}}}\beta_{1s}\dot{\beta}_{1c}e_{mr}^2\Omega_{mr}\\
&-20R_{mr}^2C_{l_{\alpha_{mr}}}\beta_{1c}\dot{\beta}_{1s}e_{mr}\Omega_{mr}+20R_{mr}^2C_{l_{\alpha_{mr}}}\beta_{1s}\dot{\beta}_{1c}e_{mr}\Omega_{mr}-4R_{mr}C_{l_{\alpha_{mr}}}\beta_{1c}e_{mr}^2\Omega_{mr}p\\
&-4R_{mr}^2C_{l_{\alpha_{mr}}}\beta_{1c}e_{mr}\Omega_{mr}p+4R_{mr}C_{l_{\alpha_{mr}}}\beta_{1s}e_{mr}^2\Omega_{mr}q+4R_{mr}^2C_{l_{\alpha_{mr}}}\beta_{1s}e_{mr}\Omega_{mr}q\\
&+16R_{mr}^2C_{l_{\alpha_{mr}}}\beta_0\beta_{1s}\Omega_{mr}u+16R_{mr}^2C_{l_{\alpha_{mr}}}\beta_0\beta_{1c}\Omega_{mr}v+4R_{mr}C_{l_{\alpha_{mr}}}\dot{\beta}_0e_{mr}^2\Omega_{mr}\theta_0
\end{aligned}
$$

$$+4R_{mr}^2C_{l_{\alpha_{mr}}}\dot{\beta}_0e_{mr}\Omega_{mr}\theta_0-2R_{mr}C_{l_{\alpha_{mr}}}\dot{\beta}_{1c}e_{mr}^2\Omega_{mr}\theta_{1c}-2R_{mr}^2C_{l_{\alpha_{mr}}}\dot{\beta}_{1c}e_{mr}\Omega_{mr}\theta_{1c}$$
$$-2R_{mr}C_{l_{\alpha_{mr}}}\dot{\beta}_{1s}e_{mr}^2\Omega_{mr}\theta_{1s}-2R_{mr}^2C_{l_{\alpha_{mr}}}\dot{\beta}_{1s}e_{mr}\Omega_{mr}\theta_{1s}+6R_{mr}C_{l_{\alpha_{mr}}}e_{mr}^2\Omega_{mr}p\theta_{1s}$$
$$+6R_{mr}^2C_{l_{\alpha_{mr}}}e_{mr}\Omega_{mr}p\theta_{1s}+6R_{mr}C_{l_{\alpha_{mr}}}e_{mr}^2\Omega_{mr}q\theta_{1c}+6R_{mr}^2C_{l_{\alpha_{mr}}}e_{mr}\Omega_{mr}q\theta_{1c}$$
$$-8R_{mr}^2C_{l_{\alpha_{mr}}}\beta_0\Omega_{mr}\theta_{1c}u-8C_{l_{\alpha_{mr}}}\beta_0\beta_{1s}e_{mr}^2\Omega_{mr}u+8R_{mr}^2C_{l_{\alpha_{mr}}}\beta_0\Omega_{mr}\theta_{1s}v-8C_{l_{\alpha_{mr}}}\beta_0\beta_{1c}e_{mr}^2\Omega_{mr}v$$
$$-8C_{l_{\alpha_{mr}}}\beta_0e_{mr}^2\Omega_{mr}\theta_{1c}u+12C_{l_{\alpha_{mr}}}\beta_{1c}e_{mr}^2\Omega_{mr}\theta_0u+8C_{l_{\alpha_{mr}}}\beta_0e_{mr}^2\Omega_{mr}\theta_{1s}v-12C_{l_{\alpha_{mr}}}\beta_{1s}e_{mr}^2\Omega_{mr}\theta_0v$$
$$-2R_{mr}C_{l_{\alpha_{mr}}}\beta_{1c}e_{mr}^2\Omega_{mr}^2\theta_{1s}+2R_{mr}C_{l_{\alpha_{mr}}}\beta_{1s}e_{mr}^2\Omega_{mr}^2\theta_{1c}-2R_{mr}^2C_{l_{\alpha_{mr}}}\beta_{1c}e_{mr}\Omega_{mr}^2\theta_{1s}$$
$$+2R_{mr}^2C_{l_{\alpha_{mr}}}\beta_{1s}e_{mr}\Omega_{mr}^2\theta_{1c}+8R_{mr}C_{l_{\alpha_{mr}}}\beta_0\dot{\beta}_{1c}e_{mr}u+8R_{mr}C_{l_{\alpha_{mr}}}\beta_{1c}\dot{\beta}_0e_{mr}u$$
$$-8R_{mr}C_{l_{\alpha_{mr}}}\beta_0\dot{\beta}_{1s}e_{mr}v-8R_{mr}C_{l_{\alpha_{mr}}}\beta_{1s}\dot{\beta}_0e_{mr}v+16R_{mr}C_{l_{\alpha_{mr}}}\beta_0e_{mr}pv-16R_{mr}C_{l_{\alpha_{mr}}}\beta_0e_{mr}qu$$
$$-12R_{mr}C_{l_{\alpha_{mr}}}\beta_{1c}\beta_{1s}uv-4R_{mr}C_{l_{\alpha_{mr}}}\dot{\beta}_0e_{mr}\theta_{1s}u+4R_{mr}C_{l_{\alpha_{mr}}}\dot{\beta}_{1s}e_{mr}\theta_0u-4R_{mr}C_{l_{\alpha_{mr}}}\dot{\beta}_0e_{mr}\theta_{1c}v$$
$$+4R_{mr}C_{l_{\alpha_{mr}}}\dot{\beta}_{1c}e_{mr}\theta_0v-8R_{mr}C_{l_{\alpha_{mr}}}e_{mr}p\theta_0u-16R_{mr}C_{l_{\alpha_{mr}}}e_{mr}\Omega_{mr}\theta_0v_i$$
$$+16R_{mr}C_{l_{\alpha_{mr}}}e_{mr}\Omega_{mr}\theta_0w-8R_{mr}C_{l_{\alpha_{mr}}}e_{mr}q\theta_0v-6R_{mr}C_{l_{\alpha_{mr}}}\beta_{1c}\theta_{1c}uv$$
$$+6R_{mr}C_{l_{\alpha_{mr}}}\beta_{1s}\theta_{1s}uv-12C_{l_{\alpha_{mr}}}\beta_{1c}\beta_{1s}e_{mr}uv-6C_{l_{\alpha_{mr}}}\beta_{1c}e_{mr}\theta_{1c}uv$$
$$+6C_{l_{\alpha_{mr}}}\beta_{1s}e_{mr}\theta_{1s}uv-8R_{mr}C_{l_{\alpha_{mr}}}\beta_0\beta_{1s}e_{mr}\Omega_{mr}u-8R_{mr}C_{l_{\alpha_{mr}}}\beta_0\beta_{1c}e_{mr}\Omega_{mr}v$$
$$-8R_{mr}C_{l_{\alpha_{mr}}}\beta_0e_{mr}\Omega_{mr}\theta_{1c}u+12R_{mr}C_{l_{\alpha_{mr}}}\beta_{1c}e_{mr}\Omega_{mr}\theta_0u+8R_{mr}C_{l_{\alpha_{mr}}}\beta_0e_{mr}\Omega_{mr}\theta_{1s}v$$
$$-12R_{mr}C_{l_{\alpha_{mr}}}\beta_{1s}e_{mr}\Omega_{mr}\theta_0v))/96$$

$$M_{x_{mr}}=-(N_{mr}(R_{mr}-e_{mr})(3C_{l_{\alpha_{mr}}}\beta_{1c}c_{mr}e_{mr}\rho v^2-2C_{l_{\alpha_{mr}}}\dot{\beta}_{1s}c_{mr}e_{mr}^3\Omega_{mr}\rho-3C_{l_{\alpha_{mr}}}\beta_{1c}c_{mr}e_{mr}\rho u^2$$
$$-6C_{l_{\alpha_{mr}}}\dot{\beta}_0c_{mr}e_{mr}^2\rho u-24K_s\beta_{1s}+4C_{l_{\alpha_{mr}}}c_{mr}e_{mr}^3\Omega_{mr}p\rho+9C_{l_{\alpha_{mr}}}c_{mr}e_{mr}\rho\theta_{1s}u^2+3C_{l_{\alpha_{mr}}}c_{mr}e_{mr}\rho\theta_{1s}v^2$$
$$-2C_{l_{\alpha_{mr}}}\beta_{1c}c_{mr}e_{mr}^3\Omega_{mr}^2\rho+4C_{l_{\alpha_{mr}}}c_{mr}e_{mr}^3\Omega_{mr}^2\rho\theta_{1s}+12C_{l_{\alpha_{mr}}}c_{mr}e_{mr}\rho uv_i-12C_{l_{\alpha_{mr}}}c_{mr}e_{mr}\rho uw$$
$$+6R_{mr}C_{l_{\alpha_{mr}}}\dot{\beta}_0c_{mr}e_{mr}\rho u+6C_{l_{\alpha_{mr}}}\beta_{1s}c_{mr}e_{mr}\rho uv+6C_{l_{\alpha_{mr}}}c_{mr}e_{mr}\rho\theta_{1c}uv-2R_{mr}C_{l_{\alpha_{mr}}}\dot{\beta}_{1s}c_{mr}e_{mr}^2\Omega_{mr}\rho$$
$$+4R_{mr}^2C_{l_{\alpha_{mr}}}\dot{\beta}_{1s}c_{mr}e_{mr}\Omega_{mr}\rho+4R_{mr}C_{l_{\alpha_{mr}}}c_{mr}e_{mr}^2\Omega_{mr}p\rho+4R_{mr}^2C_{l_{\alpha_{mr}}}c_{mr}e_{mr}\Omega_{mr}p\rho$$
$$+6C_{l_{\alpha_{mr}}}\beta_0c_{mr}e_{mr}^2\Omega_{mr}\rho v-12C_{l_{\alpha_{mr}}}c_{mr}e_{mr}^2\Omega_{mr}\rho\theta_0u-2R_{mr}C_{l_{\alpha_{mr}}}\beta_{1c}c_{mr}e_{mr}^2\Omega_{mr}^2\rho$$
$$+4R_{mr}^2C_{l_{\alpha_{mr}}}\beta_{1c}c_{mr}e_{mr}\Omega_{mr}^2\rho+4R_{mr}C_{l_{\alpha_{mr}}}c_{mr}e_{mr}^2\Omega_{mr}^2\rho\theta_{1s}+4R_{mr}^2C_{l_{\alpha_{mr}}}c_{mr}e_{mr}\Omega_{mr}^2\rho\theta_{1s}$$
$$+6R_{mr}C_{l_{\alpha_{mr}}}\beta_0c_{mr}e_{mr}\Omega_{mr}\rho v-12R_{mr}C_{l_{\alpha_{mr}}}c_{mr}e_{mr}\Omega_{mr}\rho\theta_0u))/48$$

$$M_{y_{mr}}=-(N_{mr}(R_{mr}-e_{mr})(24K_s\beta_{1c}-2C_{l_{\alpha_{mr}}}\dot{\beta}_{1c}c_{mr}e_{mr}^3\Omega_{mr}\rho-3C_{l_{\alpha_{mr}}}\beta_{1s}c_{mr}e_{mr}\rho u^2$$
$$+3C_{l_{\alpha_{mr}}}\beta_{1s}c_{mr}e_{mr}\rho v^2-6C_{l_{\alpha_{mr}}}\dot{\beta}_0c_{mr}e_{mr}^2\rho v+4C_{l_{\alpha_{mr}}}c_{mr}e_{mr}^3\Omega_{mr}q\rho+3C_{l_{\alpha_{mr}}}c_{mr}e_{mr}\rho\theta_{1c}u^2$$
$$+9C_{l_{\alpha_{mr}}}c_{mr}e_{mr}\rho\theta_{1c}v^2+2C_{l_{\alpha_{mr}}}\beta_{1s}c_{mr}e_{mr}^3\Omega_{mr}^2\rho+4C_{l_{\alpha_{mr}}}c_{mr}e_{mr}^3\Omega_{mr}^2\rho\theta_{1c}+12C_{l_{\alpha_{mr}}}c_{mr}e_{mr}\rho vv_i$$
$$-12C_{l_{\alpha_{mr}}}c_{mr}e_{mr}\rho vw+6R_{mr}C_{l_{\alpha_{mr}}}\dot{\beta}_0c_{mr}e_{mr}\rho v-6C_{l_{\alpha_{mr}}}\beta_{1c}c_{mr}e_{mr}\rho uv+6C_{l_{\alpha_{mr}}}c_{mr}e_{mr}\rho\theta_{1s}uv$$
$$-2R_{mr}C_{l_{\alpha_{mr}}}\dot{\beta}_{1c}c_{mr}e_{mr}^2\Omega_{mr}\rho+4R_{mr}^2C_{l_{\alpha_{mr}}}\dot{\beta}_{1c}c_{mr}e_{mr}\Omega_{mr}\rho+4R_{mr}C_{l_{\alpha_{mr}}}c_{mr}e_{mr}^2\Omega_{mr}q\rho$$
$$+4R_{mr}^2C_{l_{\alpha_{mr}}}c_{mr}e_{mr}\Omega_{mr}q\rho-6C_{l_{\alpha_{mr}}}\beta_0c_{mr}e_{mr}^2\Omega_{mr}\rho u-12C_{l_{\alpha_{mr}}}c_{mr}e_{mr}^2\Omega_{mr}\rho\theta_0v$$
$$+2R_{mr}C_{l_{\alpha_{mr}}}\beta_{1s}c_{mr}e_{mr}^2\Omega_{mr}^2\rho-4R_{mr}^2C_{l_{\alpha_{mr}}}\beta_{1s}c_{mr}e_{mr}\Omega_{mr}^2\rho+4R_{mr}C_{l_{\alpha_{mr}}}c_{mr}e_{mr}^2\Omega_{mr}^2\rho\theta_{1c}$$
$$+4R_{mr}^2C_{l_{\alpha_{mr}}}c_{mr}e_{mr}\Omega_{mr}^2\rho\theta_{1c}-6R_{mr}C_{l_{\alpha_{mr}}}\beta_0c_{mr}e_{mr}\Omega_{mr}\rho u-12R_{mr}C_{l_{\alpha_{mr}}}c_{mr}e_{mr}\Omega_{mr}\rho\theta_0v))/48$$

Stabilizer Bar Flappings:

$$\dot{\beta}_{1s_{sb}} = -(256I_{b_{sb}}^2\Omega_{mr}p + R_{sb}^8C_{l_{\alpha_{sb}}}^2c_{sb}^2\Omega_{mr}p\rho^2 + R_l^8C_{l_{\alpha_{sb}}}^2c_{sb}^2\Omega_{mr}p\rho^2 + R_{sb}^8C_{l_{\alpha_{sb}}}^2\beta_{1c_{sb}}c_{sb}^2\Omega_{mr}^2\rho^2 + R_l^8C_{l_{\alpha_{sb}}}^2\beta_{1c_{sb}}c_{sb}^2\Omega_{mr}^2\rho^2 + R_{sb}^8C_{l_{\alpha_{sb}}}^2c_{sb}^2\Omega_{mr}^2\rho^2\theta_{1s} + R_l^8C_{l_{\alpha_{sb}}}^2c_{sb}^2\Omega_{mr}^2\rho^2\theta_{1s} - 2R_{sb}^4R_l^4C_{l_{\alpha_{sb}}}^2\beta_{1c_{sb}}c_{sb}^2\Omega_{mr}^2\rho^2 - 2R_{sb}^4R_l^4C_{l_{\alpha_{sb}}}^2c_{sb}^2\Omega_{mr}^2\rho^2\theta_{1s} + 16I_{b_{sb}}R_{sb}^4C_{l_{\alpha_{sb}}}\beta_{1s_{sb}}c_{sb}\Omega_{mr}^2\rho - 16I_{b_{sb}}R_l^4C_{l_{\alpha_{sb}}}\beta_{1s_{sb}}c_{sb}\Omega_{mr}^2\rho - 16I_{b_{sb}}R_{sb}^4C_{l_{\alpha_{sb}}}c_{sb}\Omega_{mr}^2\rho\theta_{1c} + 16I_{b_{sb}}R_l^4C_{l_{\alpha_{sb}}}c_{sb}\Omega_{mr}^2\rho\theta_{1c} - 2R_{sb}^4R_l^4C_{l_{\alpha_{sb}}}^2c_{sb}^2\Omega_{mr}p\rho^2)/(\Omega_{mr}(256I_{b_{sb}}^2 + R_{sb}^8C_{l_{\alpha_{sb}}}^2c_{sb}^2\rho^2 - 2R_{sb}^4R_l^4C_{l_{\alpha_{sb}}}^2c_{sb}^2\rho^2 + R_l^8C_{l_{\alpha_{sb}}}^2c_{sb}^2\rho^2))$$

$$\dot{\beta}_{1c_{sb}} = -(256I_{b_{sb}}^2\Omega_{mr}q + R_{sb}^8C_{l_{\alpha_{sb}}}^2c_{sb}^2\Omega_{mr}q\rho^2 + R_l^8C_{l_{\alpha_{sb}}}^2c_{sb}^2\Omega_{mr}q\rho^2 - R_{sb}^8C_{l_{\alpha_{sb}}}^2\beta_{1s_{sb}}c_{sb}^2\Omega_{mr}^2\rho^2 - R_l^8C_{l_{\alpha_{sb}}}^2\beta_{1s_{sb}}c_{sb}^2\Omega_{mr}^2\rho^2 + R_{sb}^8C_{l_{\alpha_{sb}}}^2c_{sb}^2\Omega_{mr}^2\rho^2\theta_{1c} + R_l^8C_{l_{\alpha_{sb}}}^2c_{sb}^2\Omega_{mr}^2\rho^2\theta_{1c} + 2R_{sb}^4R_l^4C_{l_{\alpha_{sb}}}^2\beta_{1s_{sb}}c_{sb}^2\Omega_{mr}^2\rho^2 - 2R_{sb}^4R_l^4C_{l_{\alpha_{sb}}}^2c_{sb}^2\Omega_{mr}^2\rho^2\theta_{1c} + 16I_{b_{sb}}R_{sb}^4C_{l_{\alpha_{sb}}}\beta_{1c_{sb}}c_{sb}\Omega_{mr}^2\rho - 16I_{b_{sb}}R_l^4C_{l_{\alpha_{sb}}}\beta_{1c_{sb}}c_{sb}\Omega_{mr}^2\rho + 16I_{b_{sb}}R_{sb}^4C_{l_{\alpha_{sb}}}c_{sb}\Omega_{mr}^2\rho\theta_{1s} - 16I_{b_{sb}}R_l^4C_{l_{\alpha_{sb}}}c_{sb}\Omega_{mr}^2\rho\theta_{1s} - 2R_{sb}^4R_l^4C_{l_{\alpha_{sb}}}^2c_{sb}^2\Omega_{mr}q\rho^2)/(256\Omega_{mr}I_{b_{sb}}^2 + \Omega_{mr}R_{sb}^8C_{l_{\alpha_{sb}}}^2c_{sb}^2\rho^2 - 2\Omega_{mr}R_{sb}^4R_l^4C_{l_{\alpha_{sb}}}^2c_{sb}^2\rho^2 + \Omega_{mr}R_l^8C_{l_{\alpha_{sb}}}^2c_{sb}^2\rho^2)$$

APPENDIX B

R-50 MODEL HELICOPTER PARAMETERS

Table B.1: R50 Model Helicopter Parameters [28]

Symbol	Value	Unit	Definition
Main Rotor Parameters			
m_b	0.3	kg	Main rotor blade mass
R_{mr}	1.5392	m	Main rotor blade radius
$C_{l_{\alpha_{mr}}}$	6	$1/rad$	Main rotor lift curve slope
c_{mr}	0.1079	m	Main rotor mean blade chord
e_{mr}	0.030785	m	Main rotor hinge offset
$I_{b_{mr}}$	0.86754	$kg.m^2$	Main rotor blade flapping inertia about flapping hinge
Ω_{mr}	91.106	rad/s	Main rotor angular velocity
θ_{tw}	0	deg	Main rotor blade twist angle
i_s	0	deg	Main rotor shaft tilt angle
N_{mr}	2	-	Number of main rotor blades
C_d	0.010	-	Main rotor blade drag coefficient
σ_{mr}	0.044626	-	Main rotor solidity
A_{mr}	7.4432	m^2	Main rotor disk area
M_b	3.3483	Nm	Main rotor flapping hinge moment
K_{sw}	0.2	-	Swashplate linkage gain
K_1	0	deg	δ_3 angle
C_T	0.00226	-	Main rotor thrust coefficient
X_{cg}	0.77	m	Main rotor blade c.g. location
K_s	0	N/rad	Main rotor spring constant

Table B.1 continued from previous page

Symbol	Value	Unit	Definition
Loading Parameters			
I_{xx}	1.9887	$kg.m^2$	Helicopter moment of inertia in x axis
I_{yy}	6.2051	$kg.m^2$	Helicopter moment of inertia in y axis
I_{zz}	5.9751	$kg.m^2$	Helicopter moment of inertia in z axis
I_{xz}	0	$kg.m^2$	Helicopter product of inertia in xz axis
m_h	44.384	kg	Helicopter mass
Tail Rotor Parameters			
R_{tr}	0.26	m	Tail rotor blade radius
$C_{l_{\alpha_{tr}}}$	3	$1/rad$	Tail rotor lift curve slope
Ω_{tr}	565.49	rad/s	Tail rotor angular velocity
$\theta_{tw_{tr}}$	0	deg	Tail rotor blade twist
N_{tr}	2	-	Number of tail rotor blades
c_{tr}	0.04444	m	Tail rotor mean blade chord
σ_{tr}	0.10881	-	Tail rotor solidity
A_{tr}	0.21236	m^2	Tail rotor disk area
Stabilizer Bar Parameters			
R_{sb}	0.56501	m	Distance from the top center of the rotor hub to the end of the stabilizer bar blades
c_{sb}	0.099974	m	Stabilizer bar mean chord
l_{sb}	0.15	m	Stabilizer bar blade length
R_{sb_p}	0.41501	m	Distance from the top center of the rotor hub to the beginning of the stabilizer bar blades
AR	1.5	-	Stabilizer bar aspect ratio
$C_{l_{\alpha_{sb}}}$	2.6931	$1/rad$	Stabilizer bar lift curve slope
$I_{b_{sb}}$	0.061907	$kg.m^2$	Stabilizer bar blade flapping inertia about flapping hinge
K_{sb}	0.8	-	Stabilizer bar linkage gain
N_{sb}	2	-	Number of stabilizer bar blades

Table B.1 continued from previous page

Symbol	Value	Unit	Definition
Geometric Parameters			
$R_{x_{mr}}$	0	m	Distance from c.g. point to main rotor hub in x_B axis
$R_{y_{mr}}$	0	m	Distance from c.g. point to main rotor hub in y_B axis
$R_{z_{mr}}$	-0.56124	m	Distance from c.g. point to main rotor hub in z_B axis
$R_{x_{tr}}$	-1.8418	m	Distance from c.g. point to tail rotor in x_B axis
$R_{y_{tr}}$	0	m	Distance from c.g. point to tail rotor in y_B axis
$R_{z_{tr}}$	-0.14468	m	Distance from c.g. point to tail rotor in z_B axis
$R_{x_{hs}}$	-1.8418	m	Distance from c.g. point to horizontal stabilizer in x_B axis
$R_{y_{hs}}$	0	m	Distance from c.g. point to horizontal stabilizer in y_B axis
$R_{z_{hs}}$	0	m	Distance from c.g. point to horizontal stabilizer in z_B axis
$R_{x_{vf}}$	-1.8418	m	Distance from c.g. point to vertical stabilizer in x_B axis
$R_{y_{vf}}$	0	m	Distance from c.g. point to vertical stabilizer in y_B axis
$R_{z_{vf}}$	0	m	Distance from c.g. point to vertical stabilizer in z_B axis
Fuselage Parameters			
A_{fus_x}	0.21572	m^2	Fuselage flat plate drag area along x_B axis
A_{fus_y}	0.7292	m^2	Fuselage flat plate drag area along y_B axis

Table B.1 continued from previous page

Symbol	Value	Unit	Definition
A_{fus_z}	0.64661	m^2	Fuselage flat plate drag area along z_B axis
C_{d_x}	0.01	-	Fuselage flat plate drag coefficient along x_B axis
C_{d_y}	0.01	-	Fuselage flat plate drag coefficient along y_B axis
C_{d_z}	0.01	-	Fuselage flat plate drag coefficient along z_B axis
Empennage Parameters			
$C_{l_{\alpha_{hs}}}$	3	$1/rad$	Horizontal stabilizer lift curve slope
$C_{l_{\alpha_{vf}}}$	3	$1/rad$	Vertical stabilizer lift curve slope
A_{hs}	0.075	m^2	Area of horizontal stabilizer
A_{vf}	0.0375	m^2	Area of vertical stabilizer

APPENDIX C

MODEL ANALYSIS

Designed Model				Model from literature				
Re	Im	Damping	Freq.	Re	Im	Damping	Freq.	Mode
0.03585	0.49642	-0.0720	0.4977	0.0309	0.7663	-0.0402	0.7669	Lateral Oscillation
0.03585	-0.49642	-0.0720	0.4977	0.0309	-0.7663	-0.0402	0.7669	
-0.0181	0.3465	0.0522	0.3470	-0.0043	0.6423	0.0067	0.6423	Longitudinal Oscillation
-0.0181	-0.3465	0.0522	0.3470	-0.0043	-0.6423	0.0067	0.6423	
-0.65688	0	1	0.6569	-0.6838	0	1	0.6838	Heave
-2.0707	0	1	2.0707	-1.9241	0	1	1.9241	Yaw
-4.456	2.8063	0.8462	5.2660	-4.0211	7.7222	0.4619	8.7064	Longitudinal Stabilizer Bar
-4.456	-2.8063	0.8462	5.2660	-4.0211	-7.7222	0.4619	8.7064	
-13.582	8.0636	0.8599	15.7953	-10.011	15.3329	0.5467	18.3116	Lateral Stabilizer Bar
-13.582	-8.0636	0.8599	15.7953	-10.011	-15.3329	0.5467	18.3116	
-68.579	27.34	0.9289	73.8279					Flapping
-68.579	-27.34	0.9289	73.8279					
-65.857	63.307	0.7209	91.3505					
-65.857	-63.307	0.7209	91.3505					
-65.324	125.012	0.4631	141.0504					
-65.324	-125.012	0.4631	141.0504					
0	0	0	-					Yaw

Figure C.1: Comparison of eigenvalues [28]